Shock Analysis of On-board Equipment Submitted to Underwater Explosion

Enes TASDELEN

Master Thesis

presented in partial fulfillment
of the requirements for the double degree:
“Advanced Master in Naval Architecture” conferred by University of Liege
"Master of Sciences in Applied Mechanics, specialization in Hydrodynamics, Energetics and Propulsion” conferred by Ecole Centrale de Nantes

developed at L'Institut Catholique d'Arts et Métiers, Carquefou

in the framework of the
“EMSHIP”
Erasmus Mundus Master Course
in “Integrated Advanced Ship Design”

EMJMD 159652 – Grant Agreement 2015-1687

Supervisor: Prof. Hervé Le Sourne, ICAM, Nantes

Reviewer: Prof. Maciej Taczala, ZUT, Szczecin

Nantes, February 2018

This page is intentionally left blank.

DECLARATION OF AUTHORSHIP

I, Enes TASDELEN declare that this thesis and the work presented in it are my own and has been generated by me as the result of my own original research.

Shock Analysis of On-board Equipment Submitted to Underwater Explosion

I confirm that:

1. This work was done wholly or mainly while in candidature for a research degree at Institut Catholique d'Arts et Metiers (ICAM), Nantes

2. Where any part of this thesis has previously been submitted for a degree or any other qualification at this University or any other institution, this has been clearly stated;

3. Where I have consulted the published work of others, this is always clearly attributed;

4. Where I have quoted from the work of others, the source is always given. With the exception of such quotations, this thesis is entirely my own work;

5. I have acknowledged all main sources of help;

6. Where the thesis is based on work done by myself jointly with others, I have made clear exactly what was done by others and what I have contributed myself;

7. Either none of this work has been published before submission;

8. I cede copyright of the thesis in favour of Institut Catholique d'Arts et Metiers (ICAM), Nantes

Signed:

Date:

This page is intentionally left blank.

ABSTRACT

Shock Analysis of On-board Equipment Submitted to Underwater Explosion

By **Enes TASDELEN**

This thesis is dedicated to obtain the structural responses of the particular equipment when a surface ship is submitted to underwater explosion (UNDEX). In the analysis, the influence of first shock wave and first two bubbles pulsations are taken into account. The main purpose of the thesis is to analyze the response of the equipment in case of UNDEX.

Once, the main shock analysis method for the equipment (DDAM) is explained widely for evaluation of the structural response of the equipment. The Dynamic Design Analysis Method (DDAM) is based on shock response spectrum theory. Therefore, shock response spectrum is described in the thesis and generated by two different codes ANSYS and MATLAB for given time-history responses, which are obtained from a finite element transient analysis to simplified ship model. In order to get the response of the vessel's structure, the finite element transient analysis is performed, considering the pressure load of the explosion which is provided by STX Europe. Additionally, the analysis is carried out in an explicit solver LS-DYNA for a simplified ship model (semi-cylinder hull) structure which as much as presents a frigate properties.

The first DDAM analysis is performed with both ANSYS and MSC. NASTRAN for a cantilever beam by using only the specified coefficients from NRL-1396 report. Obtained numerical results are compared with an analytical solution to verify the DDAM process in a finite element solver. Afterwards, the procedure is followed by more complex beam structure analysis such as an antenna.

In the analyses of the antenna, the shock response spectrum is obtained from the acceleration or displacement time-history signals for an equipment on the vessel, where equipment located, also, by specified DDAM coefficients from G.J. O'Hara R.O. Belsheim NRL 1396, which is used by US and British Navies.

Finally, the responses of the equipment such as displacements, stresses are obtained for different calculations and are compared in a manner based on the theory stands.
Keywords: UNDEX, Underwater Explosion, Dynamic Design Analysis Method (DDAM), Shock Response Spectrum (SRS)

This page is intentionally left blank.

CONTENTS

LIST OF FIGURES

LIST OF TABLES

1. INTRODUCTION

As the naval defense industry is considered, it can be noticed that many countries pay attention to develop their naval industries. Nowadays, the investments in defence industry are increased dramatically. In the same time, this situation brings that designs must be safe, ergonomic and economic which requests unavoidable numerical analysis, test, etc. in this field.

The main purpose of this thesis is to assess the responses of embarked equipment when the ship is submitted to underwater explosion (UNDEX) and evaluate the equipment and structure by using different modelling methods. Therefore, the structure of the thesis is carried out respectively explaining the underwater explosion phenomenon, the main important parameters and the main damages on the structure. After a general study on underwater explosion, the study is focused on the analysis of equipment.

Moreover, different shock analysis methods are described and the so-called DDAM analysis is studied deeply. This analysis is based on shock response spectrum, which is a powerful and efficient tool to obtain the response of small scale structures like equipment.

A transient analysis is as well performed to get the response of the equipment itself in the analysis and the time history data is used as an input to generate SRS for DDAM analysis.

Finally, the results that obtained by different approaches and then, they are compared among them to achieve the most convenient method for the shock analysis of an equipment subjected to underwater explosion.

1.1. Background and Motivation

The first study in underwater explosion has been started in the 1860's however the first test was reported by General H. L Abbot in USA (Abbot, 1881). Also, the number of process has been increased until prior to World War I. During the WWI, the naval forces are realized that they needed to interest more about underwater explosions search. Thus, the test and researches were studied intensively at beginning of World War II. The experiences and the attacks force the researchers to improve the ship structural design in WWII. In other words, the battles in the history pushed the navies to invest in that field.

A systematic presentation of physical consequence of the underwater explosion was revealed by (Cole, 1948). Since his book does not have adequate information on damage case, the

comprehensive researches have been continued. After the gas bubble and pulsation effects were explained, Keil studied the ship response and hull damages as a result of different aspect of underwater explosion. Beside the large wave shock, during the expansion and contraction of the explosive gas bubble, the oscillations may cause critical damage to the ship. If the frequency of the bubble pulsation coincides with one of the bending natural frequencies of the hull, the resonance phenomenon may cause large hull beam deformation and but also damage on embarked equipment (such as electronic equipment) because of resulting hull beam high accelerations (Keil, 1961). A typical underwater explosion can be seen in Figure 1.

Figure 1 Typical underwater explosion view

It is very important to evaluate the response of the ship when subjected to dynamic forces which are generated by UNDEX. In order to define the shock loads, some analytic, numerical and empirical solutions were developed. So far, there are many approaches which are obtained from real scaled experiments and these approaches give the approximated results. For the underwater explosion, obviously experimental studies have many difficulties and obstacles. Therefore, the behaviour of the structure is generally simulated using numerical or analytical methods. Further, the validation of the numerical solution is done by comparison with experiments which are performed on the scaled patterns.

(Belsheim&O'Hara, 1963) studied the dynamic design analysis method (DDAM) for the shock analysis of the equipment on board. They performed a dynamic analysis, which is based on modal summation method and shock response spectrum theory. The shock response

of the ship structure was obtained by recording the data in real scale UNDEX experiment by US navy. The high-order damage can be obtained by DDAM using a shock response spectrum calculated considering the maximum responses of the structure at particular natural frequency. DDAM is limited to linear analysis, i.e elastic response of the considered structure as well as small deformations.

(Hurwitz, 1981) applied a DDAM analysis in order to obtain the response of the on-board equipment using NASTRAN finite element solver. (Mark, 1984) programmed the DDAM procedure for the structures discretized with less than 50 degrees of freedom. (Remmers, O'Hara, & Cunniff, 1996) searched out the strong relation between the modal effective mass and shock value. Moreover, (McCarthy, 1995) published NAVSEA 0908-LP-000-3010 report, which includes all derivation DDAM, theory, analytical solution as well as the limitation of the DDAM. This booklet is also known as the "bible" of the DDAM analysis. In research and studies, it is realised that DDAM gives very reliable idea about response of the equipment. In the same time, it is very fast and allows for accurate estimation for shock analysis of the equipment.

In the framework of EMSHIP program, Mauricio Garcia Navarro (Navarro, 2015) studied the structural response of a flat plate which is loaded by an incident pressure that is caused by first UNDEX shock wave. On the other hand, when the first shock wave compared with the oscillation of bubble, it can be seen that bubble oscillation is less effective than the first shock wave. Apart from the first shock wave damage on the vessel, the first and the second bubble oscillations might cause the vessel hull beam to go into resonance. The consequence of this phenomenon was numerically studied by Ssu-Chieh Tsai (Tsai, 2017) who simulated the hull beam whipping response of a surface ship when subjected to underwater explosion.

Indeed, the present master thesis will be extension of Mauricio Garcia Navarro's thesis and Ssu-Chieh Tsai's thesis and will focus on the dynamic design and shock analyses of on-board equipment when the ship is submitted to underwater explosion. Thanks to Mauricio Garcia Navarro's and Ssu-Chieh Tsai's works, STX France is able to get the consequence of an underwater explosion in term of velocity, acceleration and displacements time evolutions on every each point of a pattern ship's structure. DDAM analysis will be carried out by using those data on the foundation of the on-board equipment.

1.2. Objective of the thesis

In order to study the response of an equipment subjected to an underwater explosion, this thesis will carry out three main objectives. The first one is to apply a DDAM (Dynamic

Design Analysis Method) which is based on experimental coefficients. The second one is to perform a transient analysis of the ship's structure with equipment. The third one is to perform a spectrum analysis by using a shock response spectrum which can be obtained from shock transient analysis data. The work can be decomposed into the following main steps.

- Study empirical and analytical calculations dedicated to DDAM analysis.
- Validate a numerical DDAM analysis of a simple cantilever beam by comparing the results with analytical solutions.
- Perform a transient analysis on a stiffened half-cylinder representative of a surface ship, considering the pressure fields generated by the first shock wave and the gas bubble first two pulsations.
- Obtain the time-dependent response of the equipment as result of the transient solution.
- Study the shock response spectrum (SRS) concept, then develop and validate a generator of SRS.
- Generate SRS (shock response spectrum) according to time history responses obtained from the transient analysis of stiffened half-cylinder.
- Perform a spectrum analysis of an antenna structure by using DDAM's coefficients and SRS obtained from the transient analysis.

The structure of the work is visualised in the flowchart presented in Figure 2 for three different objectives, in order to understand all process of the shock analysis of the equipment.

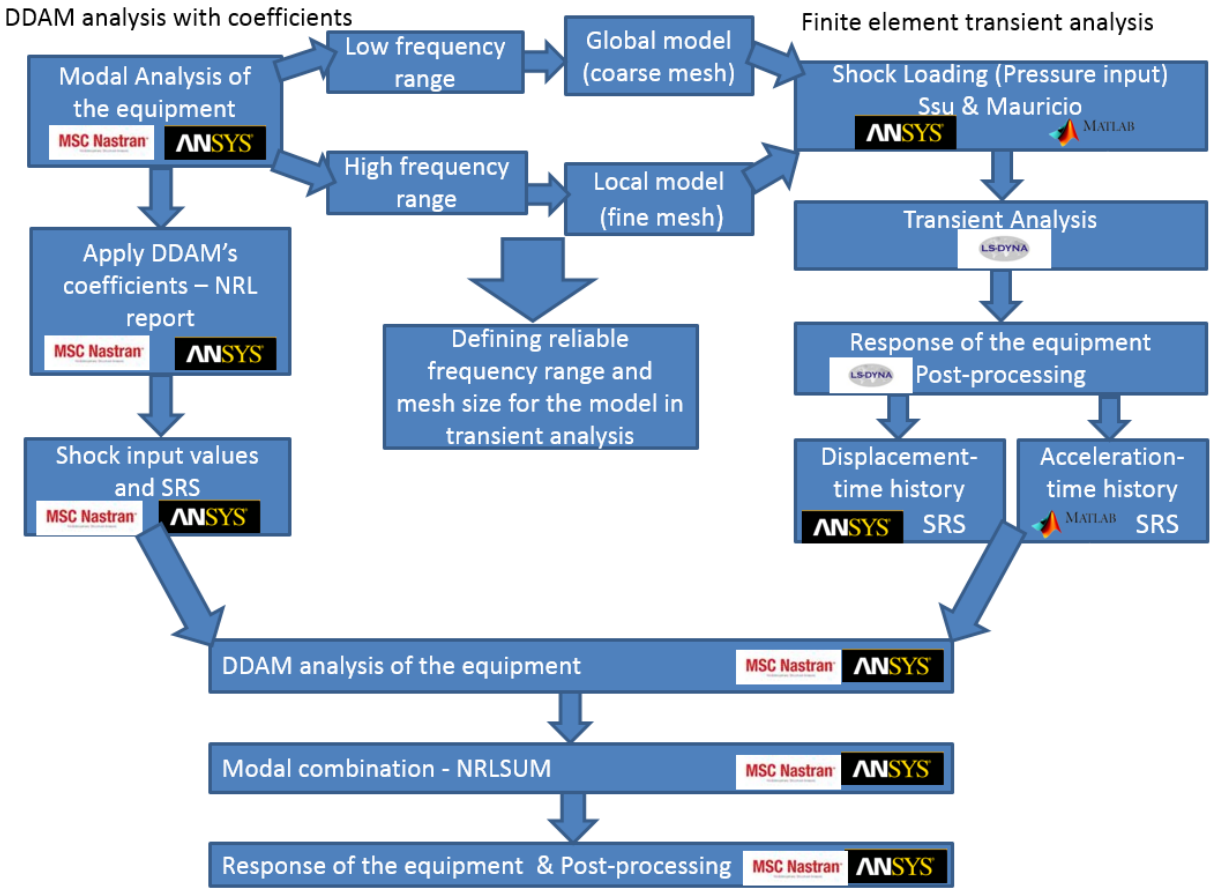

Figure 2 Flowchart to Shock analysis of the on-board equipment

Once, DDAM analysis can be performed independently by using specified coefficient extracted from NRL report. Moreover, the analysis does not need any model of the ship and explosion charge, only the equipment structure is sufficient for this calculation.

On the other hand, DDAM analysis is also performed with a particular SRS obtained from transient analyses, instead of coefficients from NRL report. Thus, this kind of DDAM analysis requires representative shock response spectrum as input for the analysis. In order to get reliable SRS at the dedicated location, a fine element transient analysis is necessary to perform. Whereas a fine element transient analysis is needed, a fine section model was studied. Because globally fine-meshed whole ship structure generates too big file which takes too much computational time to analyse, also, software and computers have limitations to calculate such big simulations.

In the end, all the obtained results are compared in order to rule on the relevance of each method regarding on-board equipment shock analysis.

2. GENERAL REVIEW REGARDING UNDERWATER EXPLOSION

An explosion is occurred as consequence of fast and sudden reactions which generate enormous high heat, noise, energy and pulse. The influence of shock due to explosion causes different threats depending on the environment. In other words, the same amount of explosive at underwater would cause much greater damage than the same amount of explosive at the air. The reason is for that, the physical property of water is incompressible which leads to transmit the influence of the shock effect faster. (Reid, 1996)

2.1. Sequence of Events

In this part, a brief description will be presented about the phenomena of the underwater explosion and bubbles oscillations. The case of explosion releases sudden high energy which causes extreme heat, high compressed gas bubble and shock wave under the water.

In the water, the wave pressure decays exponentially as a spherical. This spherical wave speed in water is much higher than the speed of sound (1500 m/s). Therefore, as a consequence of underwater explosion, the first shock wave is released from the charge with very high energy and pressure and then, the explosive gas bubble pulsations start to take a place after the first shock wave. Regarding the bubble pulsation phenomenon, the form of the gas bubble is widened until the specific point where the hydrostatic pressure equals the pressure inside the bubble. After a maximum radius and a minimum pressure is reached, the bubble starts to contract, slowly at the beginning but a rapid collapse occurs to minimum radius at final stage. Since the radius is minimum, very high pressure is generated inside the bubble then the bubble expansion starts again. These cycles follow each other until the bubble reach the free surface and not reflect by it. The time evolutions of both pressure and gas bubble radius are showed in Figure 3.

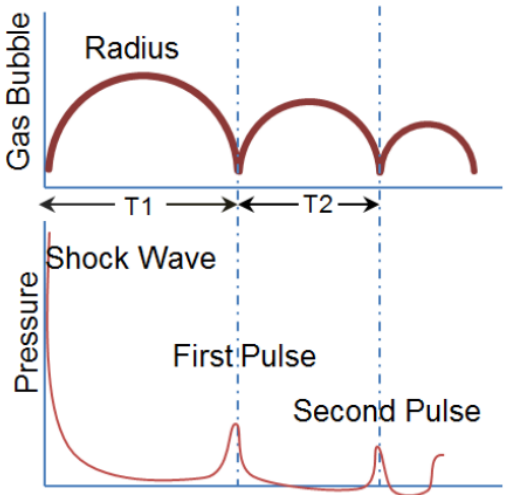

Figure 3 The schematic demonstration of the shock wave over time, (Keil, 1961)

The figure shows the shock wave, first and second bubble pulses. The shock wave has the biggest pressure value and this pressure value decrease on the first and second pulses on passing time. Generally the shock wave, first and second pulses are taken into account for analysis of the ship response since they have most important influence on the structure.

On the other hand, the surface effect was studied by Costanzo (Costanzo, 2010). He carried out some experimental test to observe the underwater explosion surface effects. The shock wave interaction with free surface causes spray dome. As shown in Figure 4, some water particles are ejected vertically above the water but the shock wave propagates back into water like a tensile wave.

After the shock wave effect, the gas bubble starts to pulsate. Resulting from bubble oscillations explained before, a first plume appears on the free surface as shown in Figure 4. The bubble migrates and continues to pulsate and the second pulsation occurs more effective and bigger in surface as indicated in Figure 4.

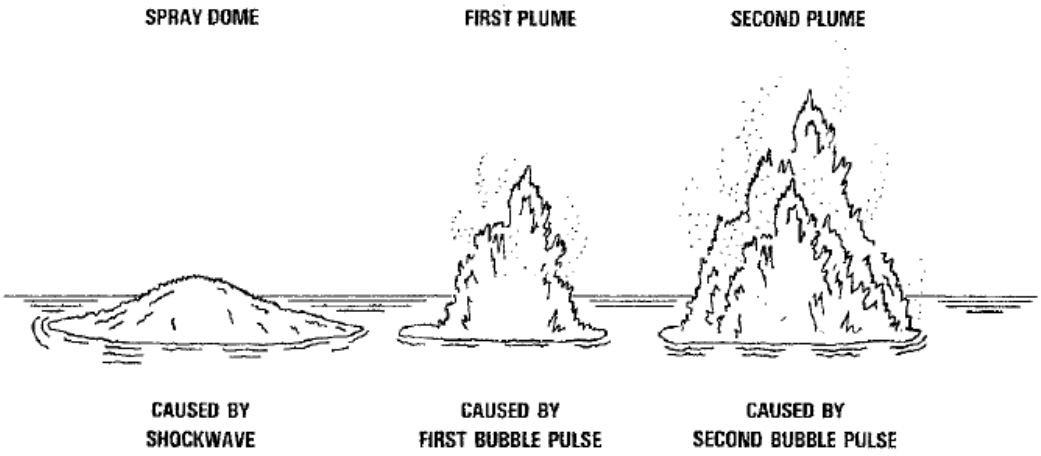

Figure 4 Underwater explosion phenomena on the free surface, (Costanzo, 2010)

In order to see the consequence of UNDEX on the free surface, Costanzo examined the particular photos from real shock test and compared Hydrocode simulation results for same test conditions. Figure 5 below compares simulations results to photos.

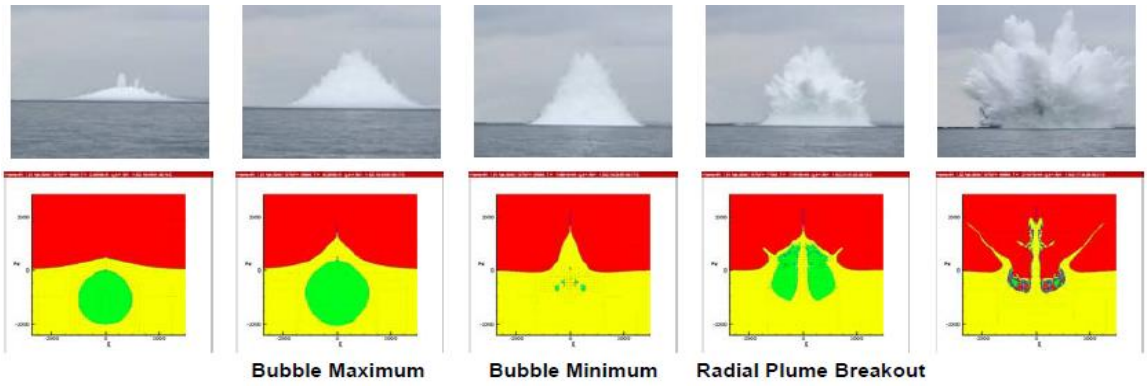

Figure 5 UNDEX Plume Above-Surface Effects (Costanzo, 2010)

From Figure 5, the behaviours of maximum and minimum bubbles can be seen with the integration of the free surface. In addition, the radial plume breaks out and its effect can be observed visually.

Additionally, the free surface and seabed affects the propagation of the shock waves inside the fluid domain. If the assumption (no pressure transmission between water to air) is considered for the free surface, the over pressure at free surface should be equal to 0 and it must not transmit to air. When the incidence wave (compression wave) reaches this free surface, it is reflected. Hollyer presented that the free surface will be similar to a mirror and reflect the shock waves (Hollyer, 1959). This situation is illustrated by Figure 6.

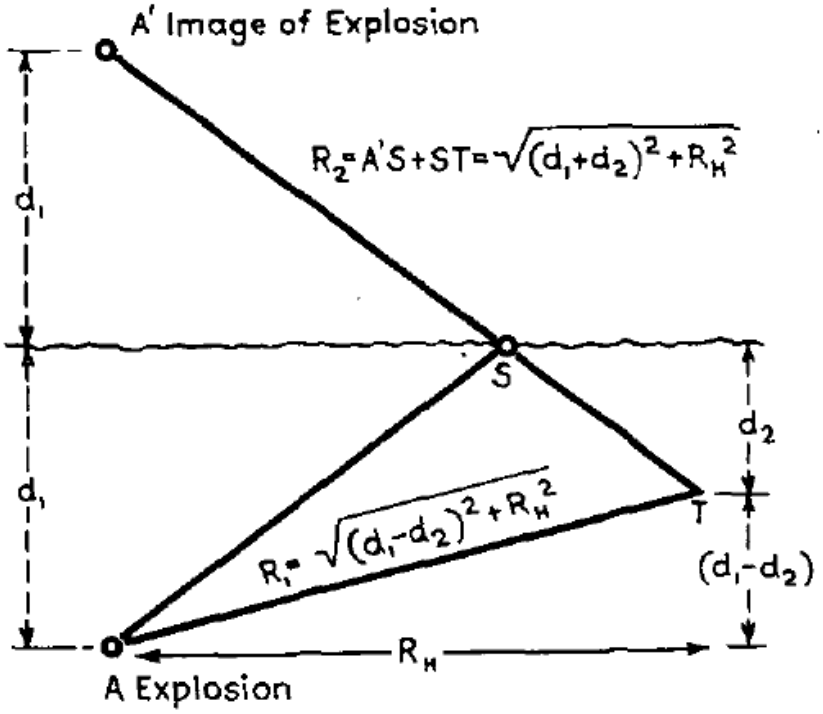

Figure 6 A schematic view for the surface reflection of the shock wave (Hollyer, 1959).

From this figure, it can be observed how shock pressure value and standoff distance at T point can be calculated whereas shock wave is reflected by free surface. The reflection influences the decaying shock pressure and the direction of the pressure (tension-compression) since the cut-off phenomenon occurred on the pressure wave. The following Figure 7 highlights the surface cut-off effect phenomenon.

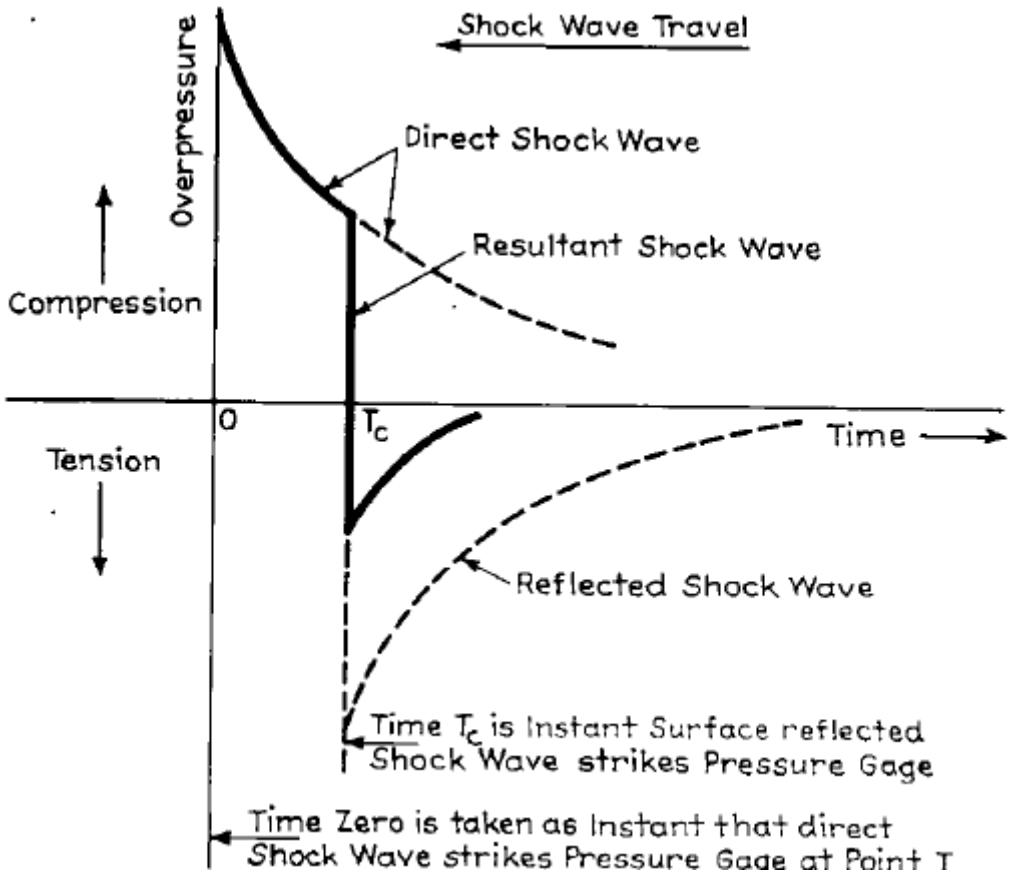

Figure 7 Resultant of reflected and direct shock waves in surface cut-off phenomenon, (Hollyer, 1959)

2.2. Parameters of Underwater Explosion

Reid presented mathematical models to obtain the shock wave pressure in an explosion field, these models are created according to empirical coefficients which depend on the explosion source such as amount, distance and type (Reid, 1996). Also, the earlier definition by (Cole, 1948), gives the maximum peak pressure in underwater explosion as following formulation (Eq. 1)

$$P_0 = f\left(\frac{W}{R}\right) \tag{1}$$

Where;

P_0=Peak pressure

W=The amount of the explosive

R = Standoff distance at the point where measured

f = Coefficient based on the explosive

The other formulation for peak pressure is defined by Reid as shown below (Eq. 2):

$$P_0 = K1\left(\frac{W^{1/3}}{R}\right)^{A1} \tag{2}$$

Where;

P_0=Peak pressure in MPa

W=The weight of TNT in Kg

R= Standoff distance in m

$K1, A1$= Shock wave coefficient, given in Table 1.

The pressure value decreases by following exponential decay. The time evolution of pressure at a point located at a distance R of the explosive is given by (Eq. 3):

$$P_m(t) = K1\left(W^{\frac{1}{3}}/_R\right)^{A1} * e^{\frac{(t-to)}{\theta}} = P_0 * e^{\frac{(t-to)}{\theta}} \tag{3}$$

Where;

$P_m(t)$ = Free field pressure

to= Initial time

P_0= Peak pressure in MPa

t= The passing time on the distance R

θ= Decay time constant

The value θ is taken as a unit of time for the pressure to decay. Exponential decay time constant can be calculated as shown below:

$$\theta = K2\, W^{1/3}\left(\frac{W^{1/3}}{R}\right)^{A2} \tag{4}$$

Moreover, Impulsive function of the blast can be obtained by integration of the pressure over the passing time during the blast.

$$I(t) = \int_0^t P(t)dt \tag{5}$$

(Eq. 5) can be modified as:

$$I(t) = K3W^{1/3}\left(\frac{W^{1/3}}{R}\right)^{A3} \tag{6}$$

The shock wave energy flux density can be described by measuring the work done over the surface, or the energy density per unit area. It can be obtained by the following (Eq. 7):

$$I(t) = \frac{1}{\rho c}\int_0^t P(t)^2 dt \tag{7}$$

Where;

ρ= Water density

c= Speed of sound

The explosion generates the gas bubble which has the form close to spherical. The maximum radius of the bubble can be estimated by following expression:

$$R_{max} = K5\left(\frac{W^{\frac{1}{3}}}{Z_o^{\frac{1}{3}}}\right) \tag{8}$$

R_{max} is the maximum radius in m. The other term Z_0 is the static pressure (hydrostatic + atmospheric pressure) at explosion location at D that is the depth of explosion from free surface and Z_0 can be written as $Z_0 = D + 9{,}8$. The taken time necessary to reach the maximum bubble radius from the first minimum bubble radius can be calculated from (Eq. 9):

$$T = K6\left(\frac{W^{\frac{1}{3}}}{Z_o^{\frac{5}{6}}}\right) \tag{9}$$

The constant coefficients involved in above expressions are related to the explosive type and listed in Table 1 for different explosive materials.

Table 1 Coefficient for Similitude Equations, (Reid, 1996)

	Coefficient	HBX-1	TNT	PENT	NUCLEAR
Shock- wave	K1	53,51	52,12	56,21	1,06E+04
Pressure	A1	1,144	1,18	1,194	1,13
Decay	K2	0,092	0,092	0,086	3,627
Time- Constant	A2	-0,247	-0,185	-0,257	-0,22
Impulsive	K3	7,263	6,52	6,518	4,50E+04
	A3	0,856	0,98	0,903	0,91
Energy Flux	K4	106,8	94,34	103,11	1,15E+07
Density	A4	2,039	2,155	2,9	2,04
Bubble Period	K5	2,302	2,064	2,098	249,1
Bubble Radius	K6	3,775	3,383	3,439	400,5

2.3. Gas Bubble Parameters

By discounting the surface tension and viscosity (perfect fluid), Rayleigh bubble momentum equation can be defined as shown below. (Rayleig, 1917)

$$R_b\ddot{R}_b + 3/2\dot{R}_b{}^2 = \frac{P(R_b) - P_\infty}{\rho_l} \tag{10}$$

Where;

R_b =Radius of the bubble,

P_∞=Pressure in the liquid at infinity

$P(R_b)$ = Pressure at bubble boundary

ρ_l= Liquid density

(Plesset&Prosperetti, 1977) took into account viscosity and surface tension and derived following expression:

$$R_b\ddot{R}_b + 3/2\dot{R}_b{}^2 = \frac{1}{\rho}\left(p_i - p_\infty - \frac{2\sigma}{R} - \frac{4\mu}{R}\dot{R}_b\right) \tag{11}$$

Where;

σ= Surface tension

μ= Dynamic viscosity of liquid

p_i=Pressure at the bubble wall

p_∞= Pressure in the liquid at infinity

Additionally, the heat difference plays important role in bubble parameter. When the heat difference is considered, Rayleigh-Plesset equation can be deduced as follow:

$$R_b'\ddot{R}_b' + 1{,}5\dot{R}_b'^2 = \varepsilon\left(\frac{R_{b0}'}{R_b'}\right)^{3\Upsilon} - 1 \tag{12}$$

Where;

R_b'=The dimensionless radius of bubble

R_{b0}'= The initial dimensionless radius of bubble

Υ= Special heat ratio

ε= Strength parameter

Influence of the bubbles are already studied in Ssu's work deeply, here, only main factors and phoneme mentioned briefly. In order to have detailed idea, the previous works should be checked. (Tsai, 2017)

2.4. Shock Factor

In order to quantify the shock severity, the following definitions must be considered. The shock factor value is described by (Reid, 1996). As in previous equations, the severity parameters are also based on explosive weight, stand-off distance from ship. If the measurement is performed to any part of the ship hull, it is called Hull Shock Factor (HSF) which presents the accessible energy from shock wave. It can be described as below:

$$HFS = \frac{W^n}{D}\left(\frac{1 + sin\theta}{2}\right) \tag{13}$$

On the other hand, as the angle value θ is large enough and close to 90°, it means the explosive is exactly under the center line of the ship. The Keel Shock Factor and Hull shock factor can be considered equal. The Keel Shock Factor can be written as follow:

$$KFS = \frac{W^n}{D} \tag{14}$$

Where;

W = Mass of the charge in TNT equivalence (kg)

D =The standoff distance from target (m)

n =The value varies slightly based on underwater experiment

θ =Shock wave angle is between vertical line to free surface and standoff distance line.

The maximum shock factor SF is described by taking n value as 1/2 as explained in (ISSC., 2006). Thus, the modified HFS and SF formulations can be shown below for maximum values.

$$FS = \frac{\sqrt{W}}{D} \tag{15}$$

$$HFS = \frac{\sqrt{W}}{D}\left(\frac{1 + sin\theta}{2}\right) \tag{16}$$

The standoff distance D and shock wave angle θ are illustrated in Figure 8 below.

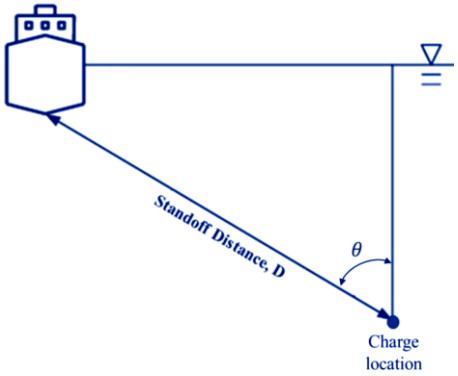

Figure 8 The sketch for the shock wave angle and standoff distance

The shock factor is one of the most important parameter to define the shock severity underwater explosion. As it is described previously with equations by (Reid, 1996), the different shock charges in different locations would give the same shock factor as an example, the big amount of explosive with high standoff distance would give same shock factor, which is obtained by small amount of explosive with short standoff distance. But the influence of two different explosions will be different. The large amount of explosive located far away from hull creates longer impulse time and bigger bubble which may cause whipping of the hull beam. On the other hand, small amount of explosive located near the hull will cause high bending moment blast damage. Therefore, the type and amount of the explosive as well as the standoff distance (distance from the charge to the hull) must be defined correctly to obtain realistic results.

3. SHIP DAMAGE DUE TO UNDERWATER EXPLOSION

The underwater explosion cause many effect on all over the vessel. As mentioned previously, the damage on a ship subjected to an underwater explosion generally depends on the amount and type of explosive, the location of the charge etc. The main consequences regarding the ship are explained briefly in following sections.

3.1. Blast Damage

The blast damage was studied by (Keil, 1961). These kinds of damages often occur when a high amount of explosive detonates at a short stand-off distance.

As mentioned in the shock factor section, the closer the explosive charge, the more damaged the ship especially. Also the more powerful explosive, the more influence on the ship.

A so-called blast damage generally occurs when the charge detonates near the ship and free surface. In case of contact explosion, the blast of the explosive is more effective than the shock wave generated by the explosion and traveling towards the ship hull. In this case, the blast causes large plastic deformations on the hull and even perforation as shown in Figure 9.

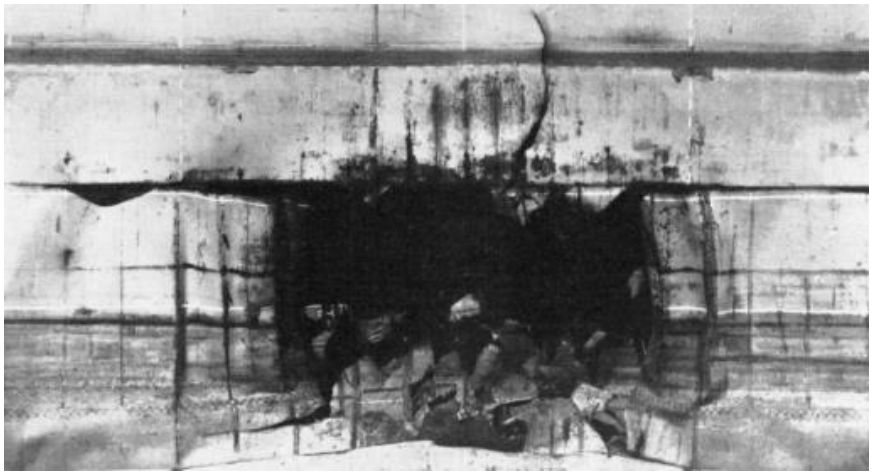

Figure 9 Blast damage on a side shell of a vessel (Keil, 1961)

The blast damage is the one of the more severe damage that may occur on the vessel. If the ship is exposed to short standoff distance and high powerful event, it would cause high plastic deformation and hole on the hull. This situation reduces the ultimate hull bending moment. On the other hand, the blast may decrease seriously the bulkheads or/and double hull water tightness and, in some cases, lead to the sinking of the ship.

3.2. Bubble Pulse Damage

After the shock wave loading on to the ship hull, the bubble pulse will also exert a pressure load on the ship hull. The bubble migrates upwards and downwards by changing the pressure inside it. When these oscillations occur near the ship, the hull and bubble will move together as illustrated in Figure 10.

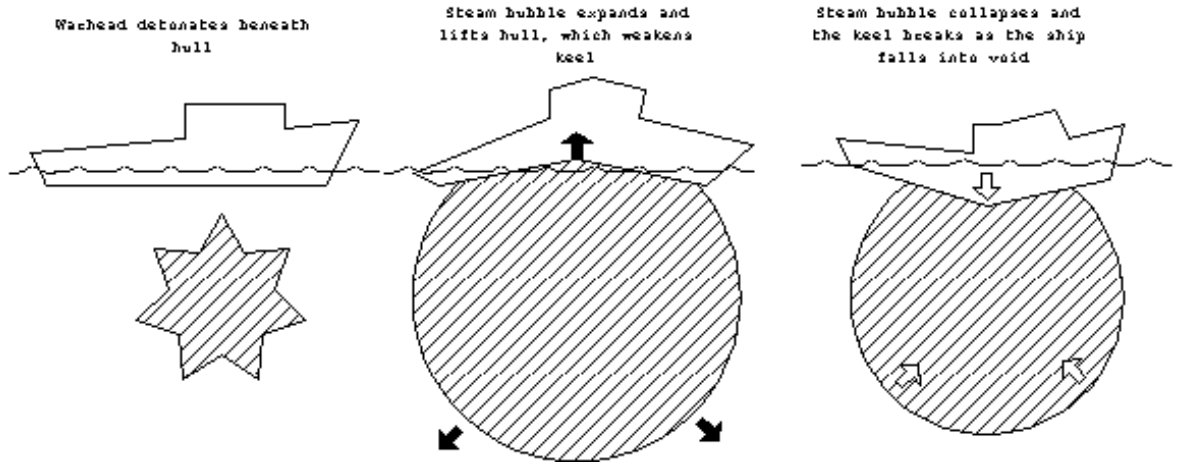

Figure 10 The ship behavior with bulb pulse – available from (https://www.reddit.com/r/gifs/comments/370frt/torpedo_ripping_ship_in_half/)

When the bubble oscillations match one of the bending natural frequencies of the ship hull-beam, resonance situation occurs and causes a harmonic high bending moment as well as high accelerations all along the hull girder. This phenomenon is called the whipping (Reid, 1996).

This whipping damage is more severe on the ship than on submarine since the submarine generally operates underwater and water damping helps to restrain the whipping effect. However, a surface ship is free to move easily upward without water damping effect.

3.3. Bubble Collapse Damage

The pressure difference leads to oscillating bubble collapse. According to (Costanzo, 2010), the explosive gas bubble may collapse on the free surface or on a solid body such as the hull of a surface ship or submarine. The oscillating bubble near the surface meets the pressure difference which causes to reduce the bubble volume and increase the pressure inside the bubble. In case of bubble collapse, the pressure change occurs suddenly, the bubble collapses on the hull and creates a high velocity water jet. This high velocity water jet (130-170 m/s range) is often able to perforate the vessel hull. (Reid, 1996)

3.4. Damages on Equipment and Machinery

The energy generated by UNDEX (shock wave and gas bubble pulsations) propagates from the water to the ship hull and is then transferred to webs, bulkheads, decks and super-structures.

It is worth noting that the elastic waves transmit very well with only small amount of reduction from ship bottom to top deck. The velocity varies around - +%20-30 range from bottom to top in the ship structure.

On the other hand, the acceleration levels inside the structures vary pretty largely through the bulkheads. Another case, the acceleration on the decks are less than the bulkheads on same deck level since shock load is transmitted vertically well. In order to understand this case easily, schematic variation of velocity and acceleration were illustrated in Figure 11. (Reid, 1996)

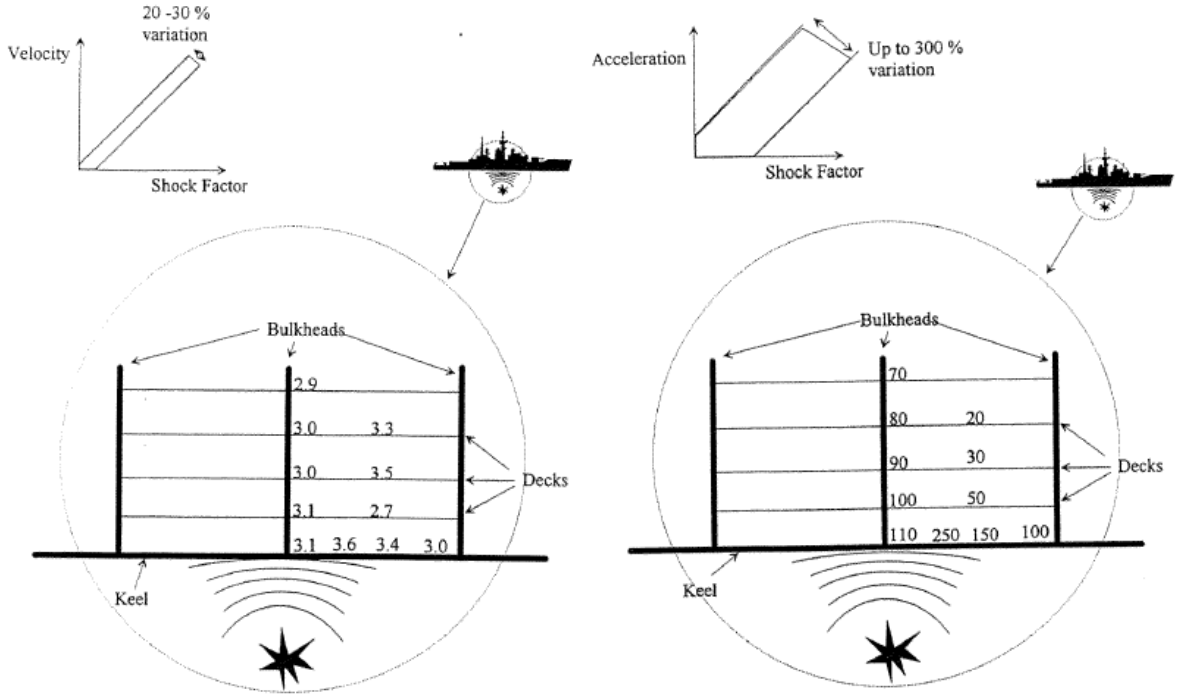

Figure 11 Schematic variation of velocity (left) and acceleration (right), when the ship submitted to UNDEX, (Reid, 1996)

Regarding the equipment installed on-board, damage may occur if their response in term of acceleration and displacement to a shock load is too high. Indeed, high accelerations and displacements may damage the vital equipment of the vessel switchboards, generator, radar, pumps and so on. Especially electronic equipment are very sensitive to shock waves due to high variation of electrostatic, magnetic electrostatic field, material dielectric strengths etc. In

Figure 12, on-board equipment damage is examined in three different perspectives on acceleration, velocity, displacement over time.

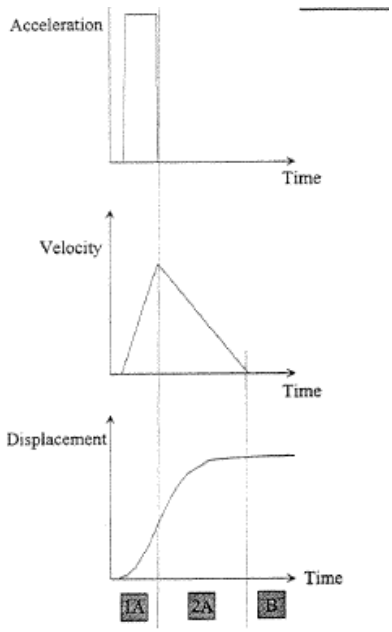

Figure 12 Time-history response for damage of equipment (Reid, 1996)

The general damages are seen in region 1A, where high accelerations occur while displacements remain comparatively low. The equipment or components may fail since they are made of brittle material and do not withstand the compression and buckling.

In region 2A, there isn't any more acceleration as the shock wave has vanished. Therefore, velocities are decreasing but displacements continue to increase. Possible failures that may occurred are tensile failures for instance inside welds.

There isn't any more acceleration and velocity in region B. But high displacements still exist in this region. The main failures come from bending and misalignment due to high displacement.

This study will be an important guide to consider the length of the transient shock analysis. As it is seen in Figure 12, the region B should be also considered to get the response of the displacement as well.

4. SHOCK RESPONSE SPECTRUM

4.1. Introduction

The shock response spectrum is one of the most important tools to represent simply the loading of a shock wave impulse. It is calculated by considering a transient shock input signal which is generally provided as a time evolution of displacement, velocity or acceleration.

In order to build shock response spectrum, a serie of SDOF linear oscillators (like a mass-spring system) with increasing natural frequencies are submitted to a given transient shock input as shown in Figure 13. The maximum responses (in term of displacement, velocity or acceleration) of these oscillators (which occur at their natural frequency) are then calculated and the combination of these maxima allows to build and plot the shock response spectrum (Alexander, 2009) such as the one presented in Figure 13. In other words, each of single degree of freedom system has its own particular response to a given impulse. The shock response spectrum is built by taking each peak of the displacement/velocity/acceleration response of the SDOF systems.

An example to shock response spectrum is presented respectively from left side to right side, from the lowest frequency to highest frequency (f1-f6) in Figure 13.

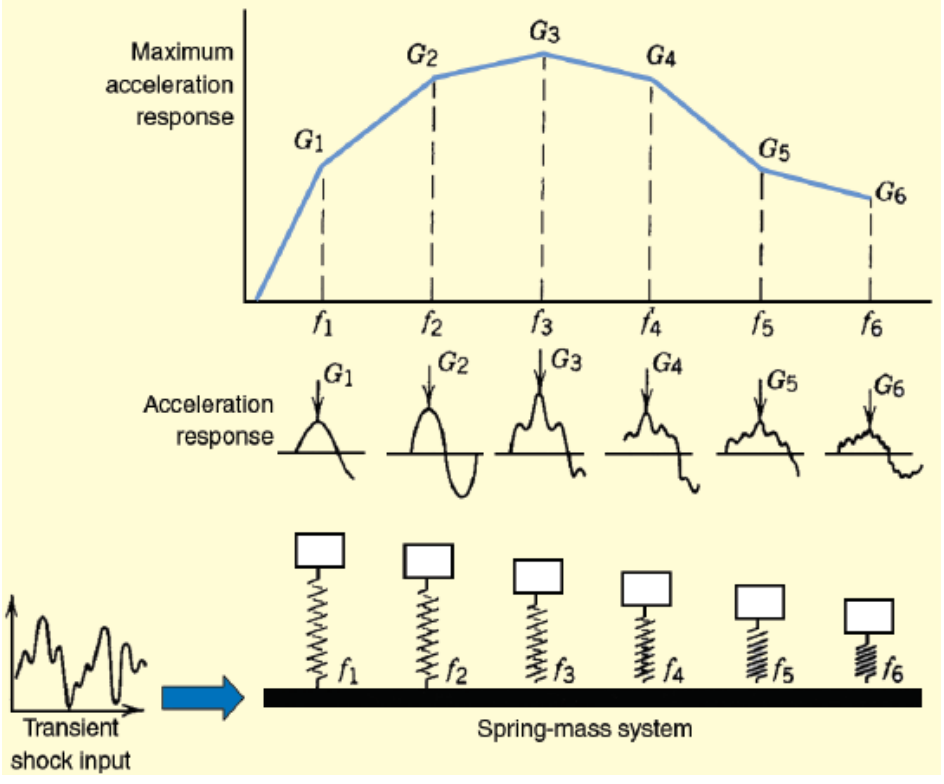

Figure 13 Building of a shock response spectrum, (Alexander, 2009)

It is worth noting that when building such SRS, the base of the structure is assumed to be stiff enough so that the motion of the oscillators do not influence the base of the structure.

4.2. Shock Response Spectrum Calculation

In previous section, the shock response spectrum has been briefly presented and it was demonstrated how the shock response spectrum can be obtained simply. In this section, the calculation process is detailed. In order to calculate SRS (Shock Response Spectrum), the mathematical model of single degree of freedoms (SDOFs) are used as described in part 4.2.1.

Even, it can thought how (SDOFs) presents the real equipment for SRS analysis. For this manner, it can be considered that every equipment and structures have particular natural frequencies at which the maximum response will occur. As one particular SDOF system has same natural frequency than the equipment, both systems will give same response for same effective weight and shock input. Of course, a sufficient number of SDOF oscillators shall be used to obtain fair enough precision when building the SRS.

Shock response spectrum theory is not only used for on-board equipment shock response analysis, it is also commonly used as a powerful tool for buildings seismic analysis, aircraft taking off, landing, pyrotechnic shock etc.

4.2.1. Single degree of freedom model

First, the equation of the motion is written to the single degree of freedom (SDOF) system which is illustrated in Figure 14. (Irvine, 2002)

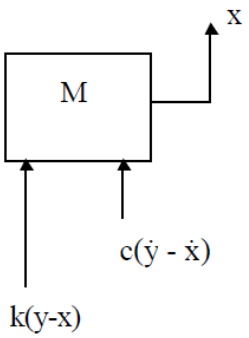

Figure 14 A single degree of freedom body (Irvine, 2002)

$$m\ddot{x} + c\dot{x} + kx = c\dot{y} + ky \tag{17}$$

Where, y is the displacement at the base plate, x is the displacement of the SDOF body, m is the mass, c is the damping parameter and k is the spring stiffness in (Eq. 17).

If the relative displacement between the base plate and the mass is written as $z = x - y$, the motion equation can be defined as below in (Eq. 18):

$$\mathrm{m}\ddot{\mathrm{z}} + \mathrm{c}\dot{z} + \mathrm{kz} = -\mathrm{m}\ddot{y} \tag{18}$$

Natural frequency ω_n, damping ratio ξ and amplification factor Q are defined as follows.

$$\omega_n = \sqrt{\frac{k}{m}} \tag{19}$$

$$\xi = \frac{1}{2Q} = \frac{c}{2\sqrt{km}} \tag{20}$$

$$Q = \frac{\sqrt{km}}{c} = \frac{1}{2\xi} \tag{21}$$

In order to write the equation in natural frequencies form, the following substitutions are used in final.

$$\omega_n{}^2 = \frac{k}{m} \tag{22}$$

$$2\xi\omega_n = \frac{c}{m} \tag{23}$$

Reporting such substitutions into (Eq. 18) $\mathrm{m}\ddot{\mathrm{z}} + \mathrm{c}\dot{z} + \mathrm{kz} = -\mathrm{m}\ddot{y}$ the equation of motion becomes:

$$\ddot{\mathrm{z}} + 2\xi\omega_n\dot{z} + \omega_n{}^2\mathrm{z} = -\ddot{y}(t) \tag{24}$$

Where $\ddot{y}(t)$ is an arbitrary function for the general case.

(Eq. 24) has not got a closed form solution. Thus, the solution of the problem must be carried out by a convolution integral approach. Then, the convolution integral is transformed to a series for the case that $\ddot{y}(t)$ is in digitized data form. (Demir, 2015).Afterwards, the series of digital data shall be converted to a digital recursive filtering relationship to speed up the calculation. The resulting definition for the absolute acceleration is given by the following expression:

$$\begin{aligned}\ddot{x}_i = {} & +2exp[-\xi\omega_n\Delta t]cos[\omega_d\Delta t]\ddot{x}_{i-1} - exp[-2\xi\omega_n\Delta t]\ddot{x}_{i-2} + 2\xi\omega_n\Delta t\ddot{y}_i \\ & + \omega_n\,\Delta t\,exp[-\xi\omega_n\Delta t]\left\{\left[\frac{\omega_n}{\omega_d}(1-2\xi^2)\right]sin[\omega_d\Delta t]\right. \\ & \left. - 2\xi cos[\omega_d\Delta t]\right\}\ddot{y}_{i-1}\end{aligned} \tag{25}$$

Where,

$$\omega_d = \omega_n\sqrt{1-\xi} \tag{26}$$

The equation above is used to obtain the shock response spectrum maximum values calculated for each SDOF's oscillators. Full derivation of the shock response spectrum calculation is detailed in Irvine's paper (Irvine, 2002).

The MATLAB® code which has been developed in the framework of this thesis is based on Irvine's work published by support of NASA (National Aeronautics and Space Administration).

4.2.2. Half sine (Input function)

A SRS generators may be validated by applying a known shock impulse. For this case, one of the most popular testing function is the half-sine acceleration time function which can be used to build the shock response spectrum. As an example, let us consider an half–sine function as input impulse, with an amplitude of 50 G and a duration of 11 ms. This signal is applied to 4 SDOF systems whose natural frequencies are respectively 30 Hz, 80 Hz, 140 Hz. The calculation uses an amplification factor Q=10 corresponding to a viscous damping ratio of 5%. Both half sine pulse and SDOF systems response are plotted in Figure 15. (Irvine, 2002)

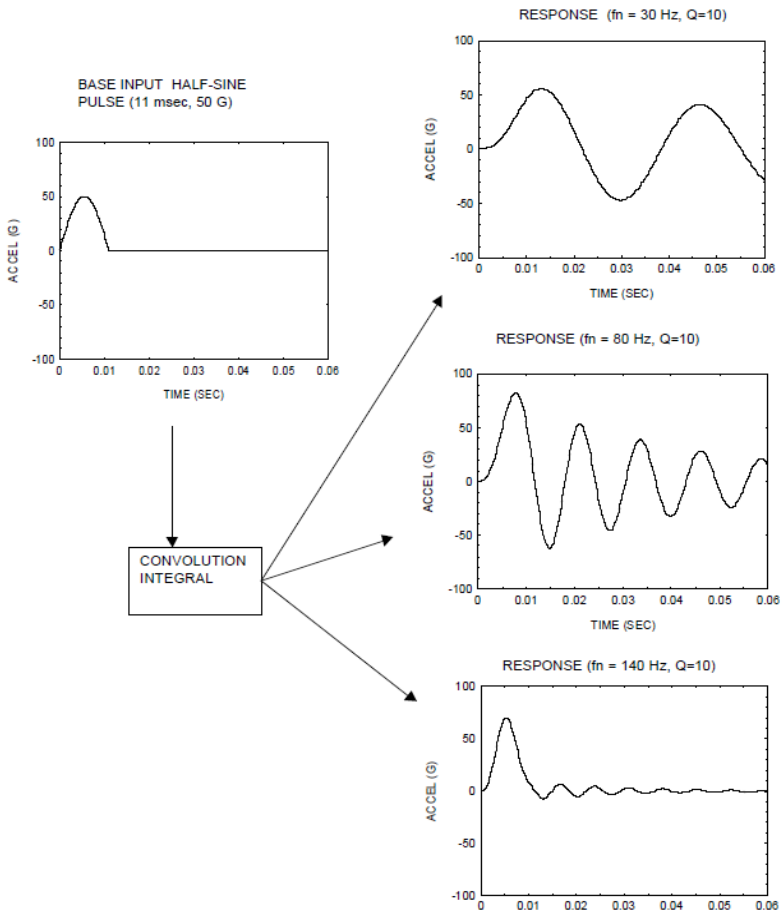

Figure 15 Half-sine input function and response of SDOF system- (Irvine, 2002)

In Figure 15, the time evolution of the shock responses can be seen schematically. Maximum peak levels are then identified for 30 Hz, 80 Hz, 140 Hz oscillators and used to build the shock response spectrum, as shown in Figure 16 where the maximum responses of all SDOF's oscillator's, whose natural frequencies vary from 5 to 1000 Hz, have been plotted. The resulting curve is the so-called SRS.

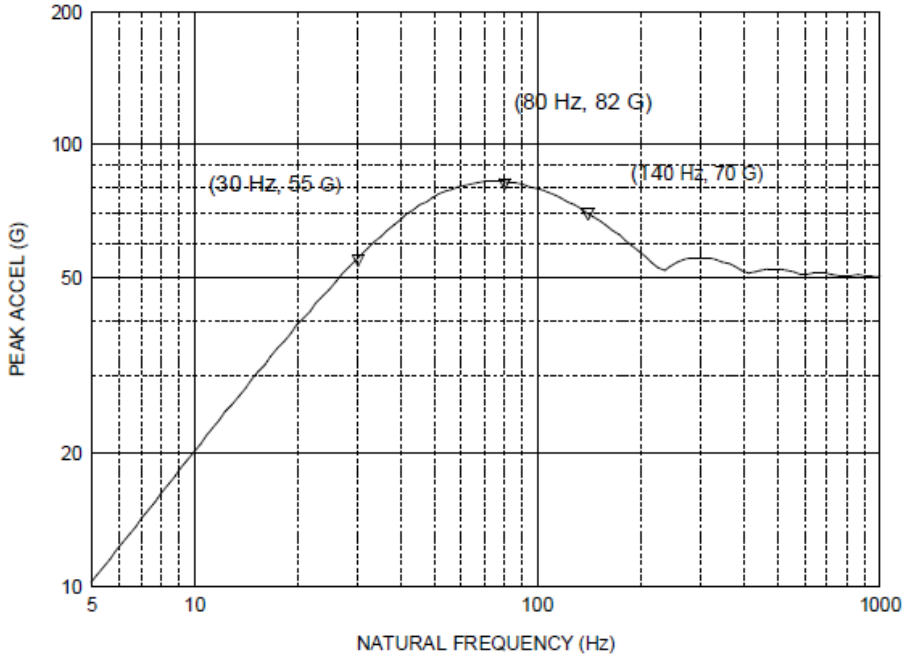

Figure 16 Shock response spectrum of half-sine impluse- (Irvine, 2002)

4.2.3. Shock response spectrum generators

Shock response spectrum calculation can be programmed by using different coding languages such as FORTRAN, MATLAB® and C/C++. In addition, ANSYS software provides a special command to generate SRS by use of acceleration or displacement time-history input.

In the framework of this master thesis, MATLAB® and ANSYS were used for SRS generation. Irvine, uses two different Kelly-Richman and Smallwood algorithms for SRS generation starting from acceleration time-history input. Smallwood approach is commonly used in the industry and taken as a reference for SRS generation (Irvine, 2012).Unfortunately, there is not any information about the algorithm used for SRS generation in ANSYS theoretical manual. Moreover, two different tools (ANSYS and MATLAB® codes) are compared each other using the same input signal.

4.2.4. Comparisons of SRS generator by input of half-sin impulse

The half-sin impulse was computed to verify the SRS generators, in the same time different approaches are studied for comparison in this part.

50G, 11 ms transient half-sinus acceleration, plotted in Figure 17, was used as input to generate the SRS and compare the different algorithms.

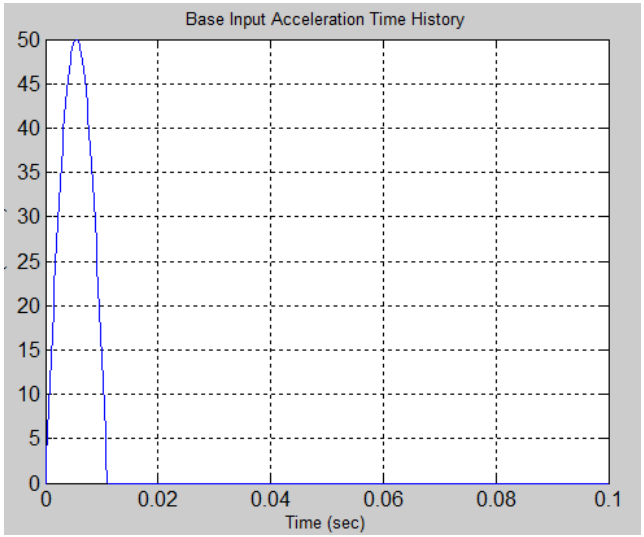

Figure 17 Half-sin base input, avaliable from www.noisestructure.com/products/SRS.php

Resulting three different SRS are compared in Figure 18. The first one is obtained by using the special ANSYS command, the second and third one are respectively calculated from Matlab programming of Smallwood and Kelly-Richman algorithms.

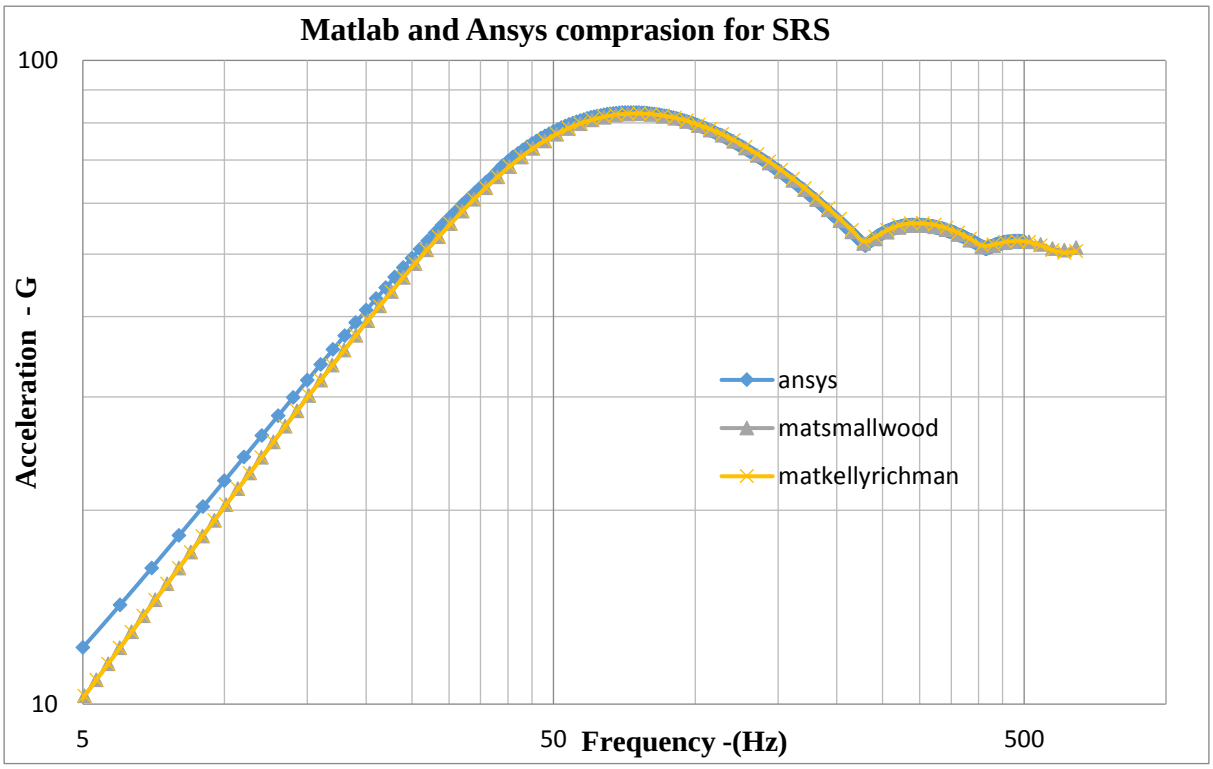

Figure 18 The SRS of the half-sin shock impulse with different tools

From Figure 18, it appears that the 3 derived SRS from 50G, 11 ms transient half-sin shock impulse are very similar to the one calculated by Irvine (see Figure 16), except the SRS obtained from ANSYS where the acceleration levels are slightly overestimated at low frequencies (5-40Hz).

4.2.5. SRS for Mid-point of the semi-cylinder structure

A semi-cylinder immersed structure is studied by Ssu-Chieh Tsai, 2017 as a previous work of this thesis. This simplified structure is created to study fluid-structure interaction with Lewis coefficient. As a sample input, the middle point (node 676) on the deck is considered for SRS generation. The simplified structure and the node 676 are illustrated in Figure 19.

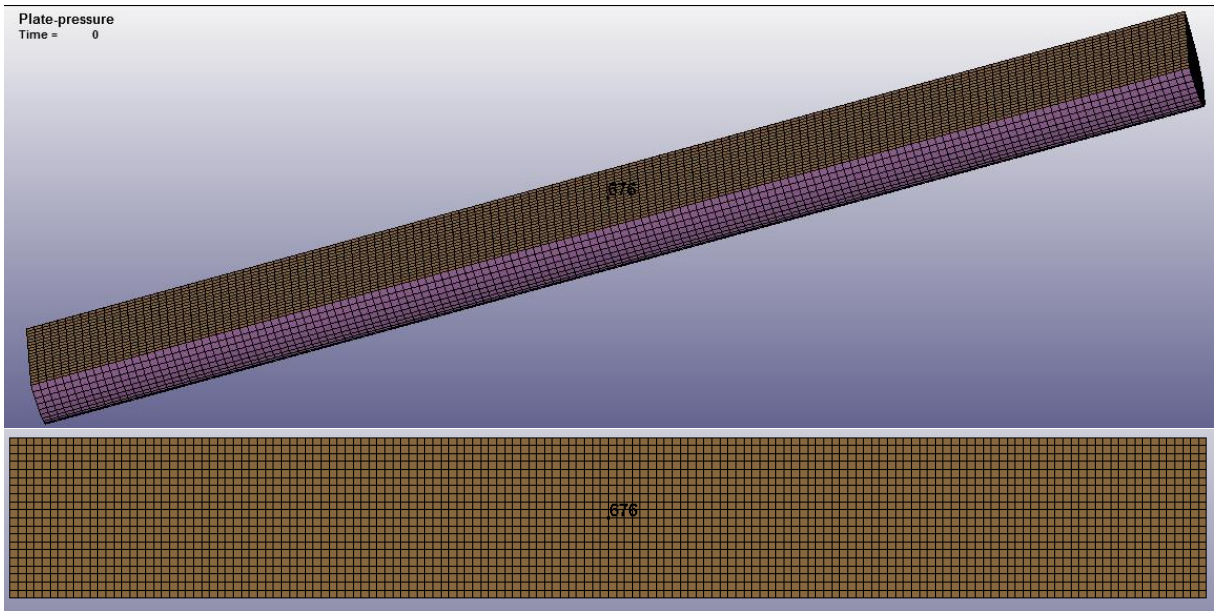

Figure 19 Simplified ship structure, (Tsai, 2017)

Displacement, velocity and acceleration time history data can be obtained on the dedicated point as a shock impulse for SRS generation. As previously mentioned, ANSYS can generate a SRS from a displacement time history. Therefore, three different SRS are plotted to examine and compare these two SRS generators. Two of these SRS are obtained from acceleration and displacement time history input in ANSYS, the other SRS is generated from acceleration time-history input in MATLAB. The results are presented in Figure 20.

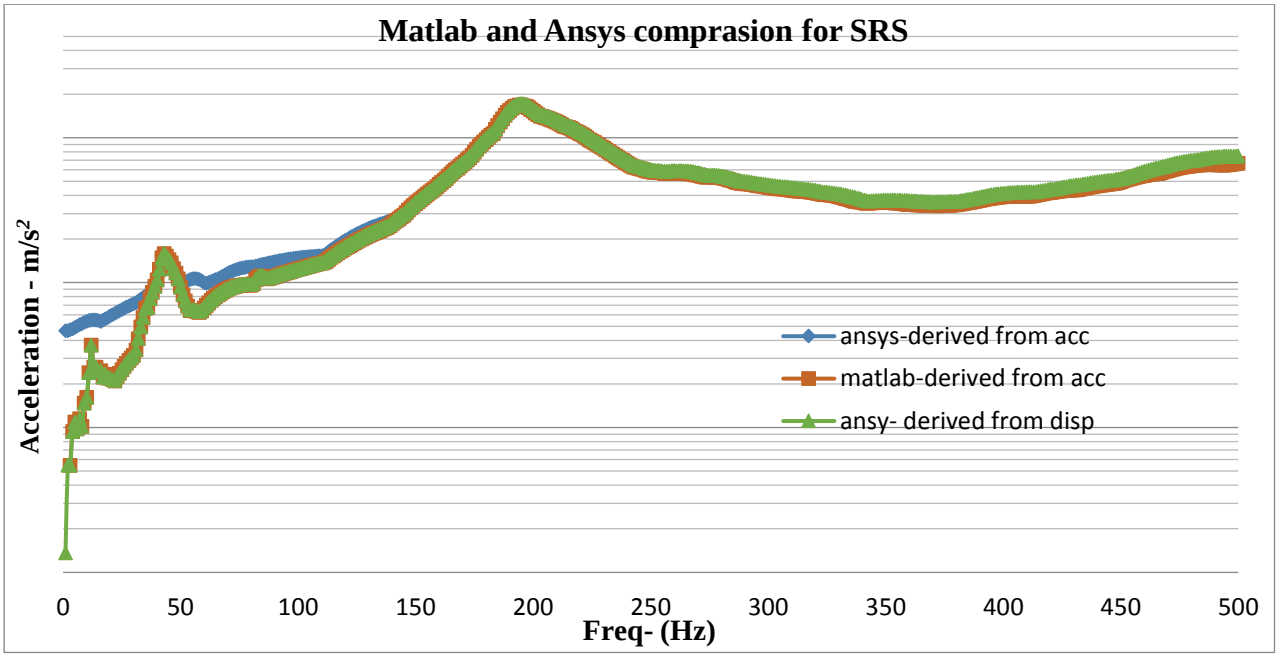

Figure 20 Comparison of SRS generators

It is noticeable that the SRS derived from acceleration-time history on MATLAB and SRS derived from displacement time-history on ANSYS are almost the same. Yet, the SRS derived from acceleration time-history in ANSYS gives unexpected results in low frequency range [0-45 Hz].

Thus, one can conclude that ANSYS command used with displacement time-history is applicable for SRS analysis. In other words, a SRS must be generated in ANSYS from a displacement time-history input. The same SRS can be generated by using MATLAB code developed in the framework of this thesis from an acceleration history-time input.

4.2.6. Shock response spectrum in Tri-axial Plots and Shock design spectrum

Tri-axial plots are is especially used in naval applications and allows to represent in a same graph a SRS in terms of displacement, velocity and acceleration. All three responses are plotted in logarithmic graph as shown in Figure 21. The relations between the main parameters (acceleration, velocity and displacement) related to frequency are given below (Eq. 27):

$$A = \omega V = \omega^2 X \tag{27}$$

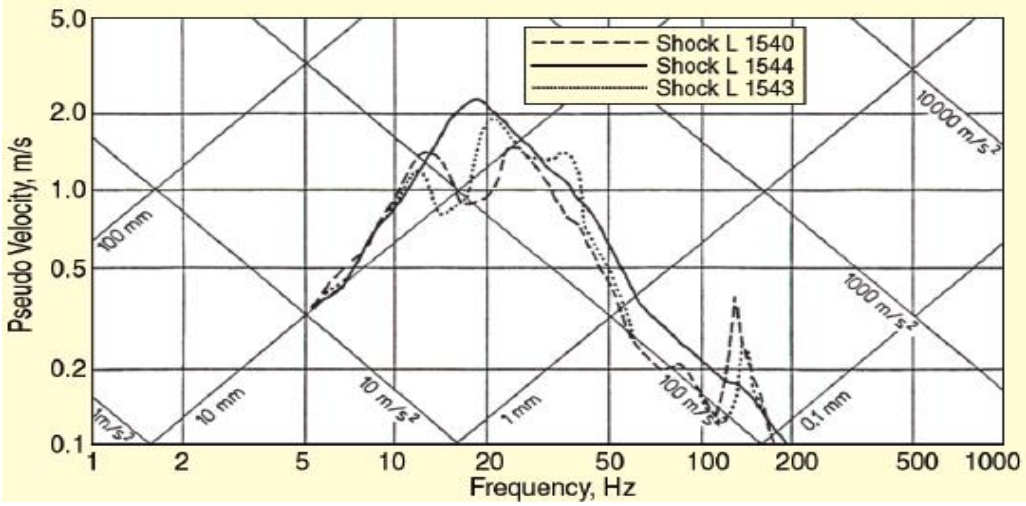

Figure 21 Response spectrum for given three different shock- (Alexander, 2009)

As it is seen in Figure 21, the vertical axis presents the pseudo velocity and horizontal axis presents the frequency. In addition, positive 45 degree grid lines present the displacement and negative 45 degree grid lines present the acceleration.

It is worth noting that design shock spectrum plot is generally issued to design safe on-board equipment. In order to obtain the shock design spectrum, the average of response spectrum in dedicated region is calculated by taken into account many number of response spectrums. In case of error and mistakes in the analysis, some statistical coefficients are added to smooth the average shock response spectrum plots. As an example, a design shock spectrum is illustrated in Figure 22.

4.2.7. Assessment Criteria from Shock Response Spectrum (BV043/85)

German federal armed forces published a building specification which contains the techniques to obtain shock response spectrum. BV043/85 presents the reference criteria for on-board equipment subjected to shock load and it is commonly taken as a reference in navy industry.

Generally, the shock load of equipment is specified by customer in the form of a shock design spectrum curve as shown in Figure 22. Thus, shipyards require reliable equipment for the obtained shock spectrums. (YAO Xiong-liang, 2008)

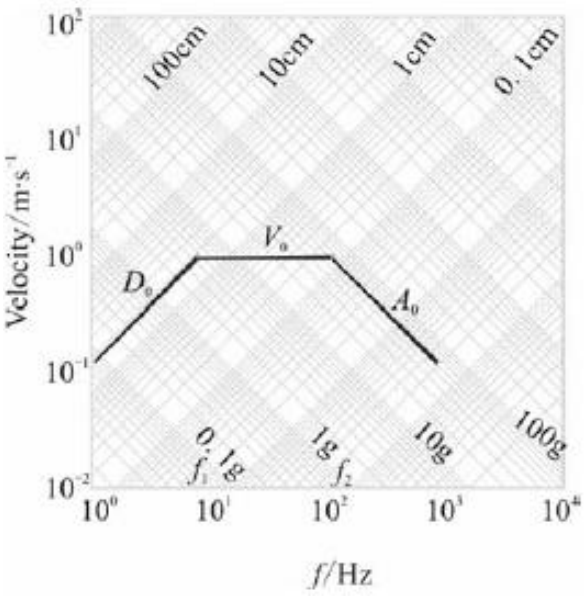

Figure 22 Shock design response spectrum, (YAO Xiong-liang, 2008)

In the figure, the constant displacement D_0, velocity V_0 and acceleration A_0 are defined. Also, the frequency range of constant velocity can be obtained as follows.

$$f_1 = V_0/2\pi D_0 \tag{28}$$

$$f_2 = A_0/2\pi D_0 \tag{29}$$

5. DYNAMIC DESIGN ANALYSIS METHOD (DDAM)

DDAM is a modal method which is used to qualify the supporting structure and equipment strength in an underwater explosion case. As a different from direct shock analysis method, this method is used SRS (Shock Response Spectrum) theory and structure of equipment itself. Thus, the structural information is used in modal analysis which gives most participating modes, natural frequencies, and other modal properties for DDAM analysis. In final stage, response of the structure can be obtained applying modal summation method. (Remmers, O'Hara, & Cunniff, 1996)

The dynamic design analysis method (DDAM) is commonly used in naval industry for many years. In early 50's, it was used to evaluate the shock response of embarked equipment by American and British NAVY's. Nowadays DDAM is used and taken as a reference in all over the world because of its rapidity and efficiency for shock design of the equipment. (McCarthy, 1995) NAVSEA

In DDAM, on-board equipment or structures are discretized in equivalent mass – spring systems (finite element meshes) subjected to a shock response spectrum, the objective being to calculate the response of the equipment/structure in term of displacements, velocity, and acceleration but also to determine the stress state inside the structures. DDAM method has been implemented in several finite element software such as NASTRAN, ANSYS, etc.

As input, acceleration shock response spectrum may is usually obtained from on-board experimental tests and/or operational data records performed at different locations of a pattern vessel.

When the shock design spectrum is achieved, DDAM can be processed through five different phases. (Navarro, 2015)

- Problem definition
- Mathematical modelling
- Motion& Dynamic computation
- Evaluation
- Limitations of DDAM- NRL coefficients

5.1. Problem Definition

The design of the structure which is going to be studied is characterized by the shock grade, the location of the mounted structure/equipment and the shock design value.

5.1.1. Shock grade

The items on the naval structure are characterised in two different shock grade, Grade A and Grade B. Grade A means that the system, equipment or structure is important to ensure the ship safety and/or to keep its mission. Grade B items are not necessary for safety or mission of the ship but these items can be dangerous for the grade A items or crew members. Following items can be considered as Grade A (essential-mission): ship control and command, propulsion, navigation and communications, countermeasures, fire control, etc.

5.1.2. Mounting location

The response of an equipment/system depends on mounting location since the shock wave travels all along the ship, decreasing progressively as it is explained in part 3.4. The equipment/system is generally classified as hull mounted, deck mounted or shell mounted. (Navarro, 2015)

- Hull mounted

This means that the equipment is mounted on the main hull frame system like main transversal frames, inner bottom, shell plating above waterline and structural bulkhead which present a bulkhead between the inner bottom and the main deck.

- Deck mounted

The equipment is mounted on decks platforms, non-structural bulkheads, platforms, structural bulkheads above the main deck.

- Shell mounted

The equipment is located on shell plating below the waterline.

Figure 23 presents the different mounting locations to be considered for shock design values definition during the problem definition phase.

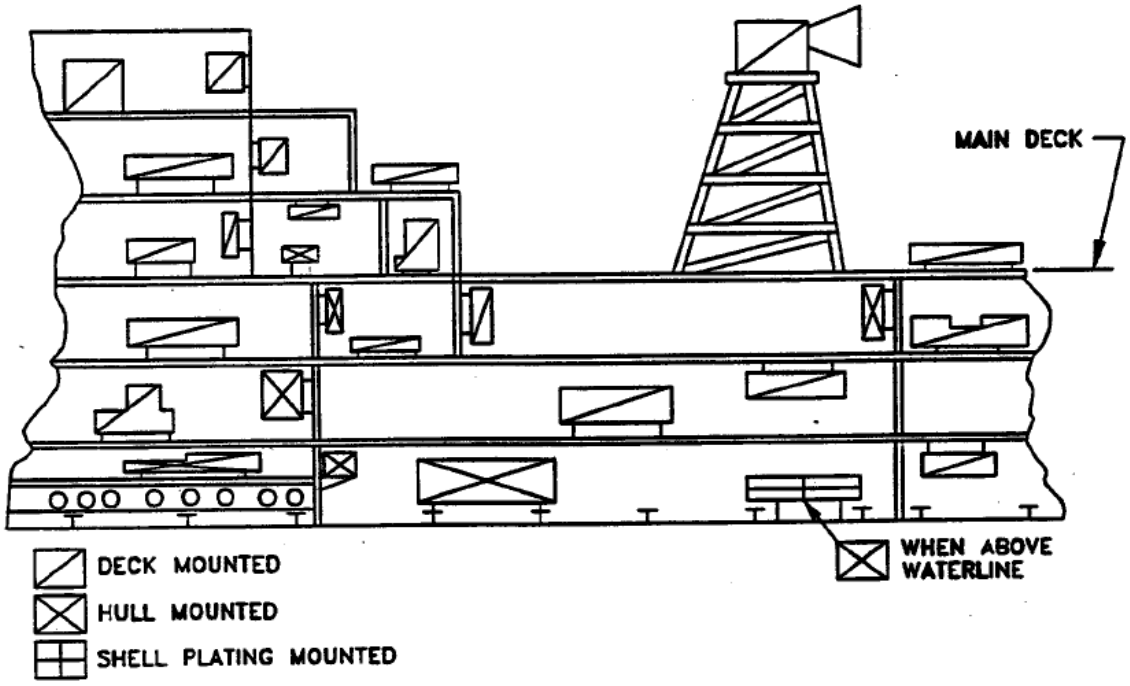

Figure 23 Mounting system of items (McCarthy, 1995)

In the case of an equipment which is mounted on to two or more different mounting locations, the higher specified shock design value should be considered for the shock analysis of the equipment.

When this figure is examined carefully, it can be seen the transmission of the shock load along the ship structure. For example, an equipment mounted on the main structural bulkheads and another one located in the stiffeners have same shock design value. Basically, the decreasing shock design values are related to Shell plating, Hull and Deck.

5.1.3. Shock design values

The shock design values are important to implement DDAM according to the case of study. The sufficient and proper design values must be used by the designer to respect the owner requirements. The different design values are explained as follows:

o Elastic shock design values

These values should be used when it is necessary to preserve the original physical dimensions after exposure of the shock, especially where high precision clearances are needed such as propeller shafting. Foundations for rotating auxiliary equipment should be designed, elastically; proving that plastic deformation or tilting of the mounting surface will not occur, or will not impaired the ship performance. Proper selection of shock design values should be considered by the designer and the contractor. (Navarro, 2015)

- Elastic-Plastic shock design values

When some plastification of the equipment/system is admitted, dynamic design analysis is anyway required.

- Special criteria for displacement

This design value is used where deflections are more critical than stresses for critical items. In this case, this is the displacement limit which is considered for the analysis. Calculated from elastic shock design values, this displacement should not exceed a required critical limit

- Special criteria for Hold-Down/locating devices

In cases where foundations are designed to suit elastic-plastic, velocity limited shock design values should be developed by the use of the elastic shock values, e.g. for the analysis of bolting dowels, and similar hold down locating devices. This analysis should be performed to devices attached to the shipboard foundation. Hold-Down locating devices which are not at the foundation of the equipment shall follow the design criteria that apply to other structural elements of the equipment.

5.1.4. Critical areas

Critical areas are defined as the areas where some equipment tends to exceed the failure criterion in shock loading. These critical areas would cause functional corruption of the system. Therefore, the designer should redevelop the model with necessary information such as stress, deflection in these areas. The specified critical systems are referred as the rudder, main propulsion excluding propeller, masts, main reduction gear. (Navarro, 2015)

5.2. Mathematical Modelling

This part presents the mathematical model of the system in dynamic analysis point of view such as considering mass and structural element. (Navarro, 2015)

As a shock load is not unidirectional, the study should be carried out separately for each three principal direction (athwart ship, vertical, fore and aft) and shock strength of the equipment to each direction should be evaluated individually. For a Multi Directional Response (MDR), a single mathematical model may be enough for the three directions of input. The mathematical modelling phase passes through the following steps:

- Basic model
- Frequency estimations
- Mass lumping

- Mass locations
- Definition of structural model
- Special modelling criteria

5.2.1. Basic model

One of the fundamental assumptions necessary for the application of DDAM is the selection of a fixed base. A fixed base acts as rigid stationary boundary in the direction of the shock, transmitting the shock motion to the mounted equipment or structure. The fixed base is assumed to be the interface between the system foundation and the ship structure. Proper selection of the fixed base, whether it is hull or deck mounted, will also define the proper selection of the shock design values. It is necessary for the model to reflect the flexibilities of the interface which can affect the system response. (Navarro, 2015)

5.2.2. Frequency calculation

Fixed base natural frequency calculations are used to determine the components which are critical. These components may require a separate mass or masses to properly model them. The cut-off frequency is defined as the highest mode of vibration to be considered by the conditions specified. In other words, the components of the model which are below the cut-off frequency shall be modelled.

5.2.3. Mass lumping

Once the critical areas are identified, the modelling of the problem should be done taking into consideration the following points:

a) Model simplicity: The model should be as simple as possible, without omitting important information.

b) High frequency components should be lumped together: high frequency components with adjacent frequencies will need to be merged together.

c) Low frequency elements should be modelled as separated masses.

d) Shock test items shall not be included in the model. The rules focus on the analysis only on representative systems.

5.2.4. Mass locations

The masses of the representative equipment should be in relation with a fixed origin. A proper system of coordinates should be used, in relation to the fixed frame of reference.

5.2.5. Definition of structural model

The structural model which is linear, elastic, having a mathematical description, can also be represented by a finite element model. The structural model, describes the item in terms of physical characteristics, which when combined with concentrated masses will produce a dynamic characteristics representative of the equipment, or system.

5.2.6. Detailed modelling criteria

During the coefficient computation phase and dynamic computation phase, all the resilient mounting characteristics shall be taken into consideration for the mathematical modelling. For equipment that has piping connections, which is not separated from the model, the analyst shall include the weight, up to five feet (1.52 m) of piping, including its content as mass when modelling the equipment.

At the locations, where foundations are grounded on deep frames, such inner bottom structure, built-in tanks, or similar structure above, this structural flexibility should be taken into account. The incorporation, of this flexibility may lead to a reduced shock response calculation.

5.3. Motion & Dynamic Computation

The equation which governs the motion of a discretized structure/system subjected to a shock load may be written as:

$$[M]\ddot{X} + [C]\dot{X} + [K]X = Fe \qquad (30)$$

Where $\ddot{X}$ is acceleration vector, $\dot{X}$ is velocity vector, X is displacement vector, $[M]$ is mass matrix, $[K]$ is stiffness matrix, Fe is external force and $[C]$ is damping matrix which, as it be seen latter, is not taken into account in DDAM calculations. (McCarthy, 1995)

During the internship and master thesis, DDAM analyses were carried out using both NASTRAN and ANSYS finite element solvers. The modal matrix equation for multi degrees of freedom system may be written as:

$$-\omega^2[M]\{\Phi\} + [K]\{\Phi\} = 0 \qquad (31)$$

By solving this equation, the natural frequencies and corresponding mode shapes of the structure/system can be obtained.

Motion equations and dynamic computation parts are explained with more details in DDAM derivation and equations part with formulation and coefficients for DDAM.

5.4. Evaluation

Evaluation part is an essential part to determine the level of influence in the deflection and stress levels in the equipment and foundation with specific criteria and rules. In order to evaluate the DDAM analysis properly, the explanations are followed. (McCarthy, 1995)

5.4.1. Modal analysis

Modal analysis must be carried out to get the natural frequencies and mode shapes of the system. When a situation with closely spaced mode occurs (several natural frequencies are in a range defined by ±10% of the mean value), a reduction process should be applied for the modal summation (see part 5.4.4).

The number of modes to be consider in DDAM analysis must be chosen such as the modal effective mass equals or exceeds 80% of the total mass of the system. On the other hand, according to DDAM requirements, the modal truncation frequency might be taken equal to 250Hz as an upper level. This is due to the fact that, by experience, typical on-board equipment are less influenced by high frequency excitations. Moreover, during an underwater explosion, the high frequencies shock waves are generally absorbed by the ship structures or their environment.

Afterwards, for each considered mode, the response of the structure submitted to the shock response spectrum is evaluated in term of displacements, velocities, accelerations or stress levels.

These modal responses are finally combined as presented in part 5.4.3 to calculate the maximum shock response of the overall system/structure.

5.4.2. Stress calculation

In order to obtain the modal stresses, the Von-Mises stress theory is used in a structure which is submitted to normal stress and shear stress. The formulation can be seen below for unidirectional stress.

$$\sigma_a = \sqrt{\sigma_n^2 + 3\tau_s^2} \tag{32}$$

In the formula, σ_a is the modal equivalent stress related to the dedicated mode number a, σ_n is the normal stress and τ_s the shear stress.

If the stress is not only one direction, the equivalent modal stress can be calculated by following formulations below.

$$\sigma_a = \sqrt{\sigma_x^2 + \sigma_y^2 - \sigma_x\sigma_y + 3\tau_{xy}^2} \text{ for stresses on x and y direction} \quad (33)$$

$$\sigma_a = \sqrt{\sigma_x^2 + \sigma_y^2 + \sigma_z^2 - \sigma_x\sigma_y - \sigma_y\sigma_z - \sigma_x\sigma_z + 3(\tau_{xy}^2 + \tau_{xz}^2 + \tau_{yz}^2)} \quad (34)$$

for stresses on x, y and z direction.

Where;

σ_a= Equivalent modal stress related to the dedicated mode number *a*,

$\sigma_{x,}\sigma_{y,}\sigma_z$= Normal stresses respectively along x, y, z axis

$\tau_{xy}, \tau_{xz}, \tau_{yz}$= Shear stresses respectively in xy, xz, yz plans.

5.4.3. Summation methods

Many different summation methods exist to calculate the maximum response of the structure by summing the most participating modes. In naval industry, NRLSUM is commonly used for DDAM analysis. The other summation methods are Square Root of Sum of Squares (SRSS), Complete Quadratic Combination (CQC), Double Sum (DSUM), etc.

Naval Research Laboratories (NRL) presents a summation procedure which allows to calculate the total shock response (stress, deflection, etc.) by combining the responses of the modes. The following formulation is used to obtain total shock response.

$$R_i = |R_{ia}| + \sqrt{\left(\sum_{b=1}^{N} R_{ib}^2\right) - R_{ia}^2} \quad (35)$$

Where;

R_{ia}= The largest modal stress or deflection among the selected modes at ith point.

R_{ib}= Contribution of each member of stress or deflection at ith point.

Only comparing the shock load stress with failure criteria would not be enough to decide if failure occurs or not. Therefore, the operating stress must be added to obtain the total stress which will be compared with the failure criteria.

$$\sigma_{total} = |\sigma_{shock}| + |\sigma_{oprt}| \quad (36)$$

5.4.4. Evaluation of the response

This part is dedicated to evaluate the response of the equipment whereas NRL summations method gives greater results than allowable limits. The following reduction process should be considered. (McCarthy, 1995)

In a case, a closely spaced mode would cause the high response, so closely spaced mode must be checked for reduction in modal summation phase. If closely spaced mode doesn't cause high response, the model should be redesigned again to reach permissible limit.

The closely spaced modes method (CSM) combines the closely spaced modes into one particular mode which presents the both following modes. Closely spaced mode can be applied in modal summation phase of DDAM and Spectrum analysis in ANSYS.

The algebraic summation method (ASM) is an alternative method for combination of modal responses. This method sums modal responses which conserve the phase relationship between the modes. The same set of modes for NRL summation shall be implemented for this method.

5.5. Limitations of DDAM-NRL coefficients

The coefficients in Dynamic Design Analysis Method are obtained from the experimental results and then, is implemented to analytical formulation. Beside it is very fast and applicable in most of the cases, it has some drawbacks and limitations. Therefore, these limitations must be concerned clearly by the designer.

Firstly, the method assumes that the equipment is considered linear elastic in the analysis. Plastification is not considered. Furthermore, the SRS analysis is not very efficient in low frequency range therefore, the DDAM analysis is not recommended for low frequency response analyses (< 5 Hz). Finally, as explained previously, the occurrence of closely spaced modes requires to use special appropriate approaches.

The specified coefficients given by NRL for building shock design spectrum are derived from real scale model experiences by recording the data during the experiments. The lack of this coefficients is that there is not any distinction between different types (and sizes) of the ships (frigate, patrol vessel etc.). On the other hand, these coefficients presume that the shock input value is same at any location based on shock design spectrum for given model. For instance, deck mounted equipment has same shock design spectrum whatever is the level of the deck. (McCarthy, 1995)

6. DERIVATION OF DDAM EQUATIONS

The concept of the DDAM theory was explained in part 5, now the derivation of the equations will carry out in this part. This section takes reference from NEi Nastran Dynamic Design Analysis Method (DDAM) Handbook. (Nastran, 2009)

6.1. Structure Dynamics

The basic dynamic equation can be written in matrix form without damping for free vibration as shown below. Damping factor does not need to be considered for modal analysis. In DDAM analysis, the damping is already included in shock design spectrum so it is not considered for the dynamic response calculation.

$$[M]\ddot{X} + [K]X = 0 \tag{37}$$

In order to solve the problem:

$$X = \sin(\omega t) \tag{38}$$

Then, it is applied to original equation,

$$-\omega^2[M]\bar{X}\ \sin(\omega t) + [K]\bar{X}\ \ \sin(\omega t) = 0 \tag{39}$$

This equation refers to an eigenvalue problem, there is one solution when X =0, but there would be many number of solution when the derivative of $([K] - \omega^2[M])\bar{X}$ term is zero. Thus, every each solution generates a particular ω eigenvalue and corresponding eigenvector which is presented as ϕ symbol. This obtained eigenvalue refers to natural frequency of the system also, this eigenvalue is available for each degree of freedom in M (mass) and K (stiffness) matrices. In order to examine the equation easily, the X vector is normalized as 1. Then, the Generalised Mass matrix (diagonal) is defined as follows:

$$\{M_a\} = \phi^T[M]\phi \tag{40}$$

And corresponding generalised stiffness matrix (diagonal):

$$\{K_a\} = \phi^T[K]\phi \tag{41}$$

Both matrices components are related to the eigenvalues (natural circular frequencies):

$$\omega_i = \sqrt{\frac{K_i}{M_i}} \tag{42}$$

Note that the eigenvectors are orthogonal, $\{x_i\}\{x_j\} = 1\ and\ \{x_i\}\{x_j\} = 0$. This mathematical property will be used later on.

6.2. Modal Effective Mass

The normal modal analysis plays an important role on DDAM analysis. Further, modal effective mass should be known what important modes are to use in the spectrum analysis.

Arbitrary shapes can be obtained by linear combination of scaled eigenvectors. Therefore, a rigid body vector will be generated at the interest of the response direction. The rigid body vector is presumed as linear summation of the elastic modes of structure multiplies scale factors of the structure. This summation is the result of displacement unit at all nodes in structural model.

So the rigid body vector D_r can be defined as follow:

$$D_r = \sum \phi\varepsilon \tag{43}$$

In (Eq. 43), ε is a scaling factor vector on the eigenvectorϕ.

The Participation Factor is a definition of what portion of each mode participates to the rigid body vector. It can be presented by (Eq. 44):

$$P_a = \frac{\phi_a^T[M]\{D_r\}}{\phi_a^T[M]\phi} \tag{44}$$

$[M]$ is the mass matrix of the system and $\{D_r\}$ is rigid body vector. If the participation factor equation is implemented with mass normalised eigenvector, the Participation Factor term becomes as shown below:

$$P_a = \frac{\phi_a^T[M]\{D_r\}}{1} \tag{45}$$

The rigid body vector $\{D_r\}$ is simplified as a vector of 1s for a practical point. Then, the summation of participation factor for a mode can be written as following (Eq. 46):

$$P_a = \sum_{i=1}^{N} \phi_{ia} M_i \tag{46}$$

In (Eq. 46), i presents the degree of freedom, a is mode number of the component and N number of degrees freedom.

Total mass of the system can be obtained by sum of square of participation factors as shown (Eq. 47):

$$M_{total} = \sum_{a=1}^{N} P_a^2 \tag{47}$$

Modal effective mass is the portion of total mass of the system which is obtained for each mode. Modal effective mass is achieved by sum of the square of the participation factor on each degree of freedoms.

$$M_{eff\ a} = \sum_{i=1}^{N} (\phi_{ia} M_i)^2 \, , lb \ or \ kg \tag{48}$$

The modal effective mass is multiplied by g gravity in order to have proper units in shock response calculation. The modal effective weight can be seen by following (Eq. 49):

$$W_a = \frac{M_{eff\ a} * G}{1000} \ kips \quad or \quad W_a = M_{eff\ a} * G \ lbs \tag{49}$$

In SI unit system, the modal effective mass is considered instead of modal effective weight and it is used kg unit for DDAM analysis.

Implementation of DDAM requires that the modal effective weight must satisfy, in each direction, at least 80% of the weight of the system. Thus, the most effective modes shapes and frequencies are achieved in the modal analysis for DDAM.

6.3. Response Spectrum Analysis using NRL Coefficients

The concept of the shock response spectrum was explained in part 4. In this part, how to generate shock response spectrum and shock design values by coefficients will be carried out for the whole DDAM analysis. In the DDAM analysis, specified coefficients from NRL-1396 report can be used as an input for the shock response spectrum analysis.

6.3.1. Coefficients

The significant coefficients are obtained from the shock design spectrums which have been built from underwater explosion experiments in real scale patterns. In this process, the data are collected considering mounting locations for two main types of vessel, surface ship and submarine as shown in Table 2. (O'Hara B. a., 1963)

Table 2 DDAM coefficients for acceleration and velocity shock value- NRL-1396

Input Acceleration Shock Value Cofficeints		A	B	C	D	E	F
Submarine	Hull mounted system	10.4	0	1	480	20	1
	Deck mounted system	5.2	0	1	480	20	1
	Shell mounted system	5.2	0	1	480	20	1
Surface Ship	Hull mounted system	20	1	49.5	450	6	2
	Deck mounted system	10	1	49.5	450	6	2
	Shell mounted system	10	1	49.5	450	6	2
Input Velocity Shock Value Coefficients		A	B	C			
Submarine	Hull mounted system	20	480	20			
	Deck mounted system	10	480	20			
	Shell mounted system	100	480	20			
Surface Ship	Hull mounted system	60	12	6			
	Deck mounted system	30	12	6			
	Shell mounted system	120	12	6			

Additionally, Figure 24 illustrates to indicate the specified mounting location for given coefficients.

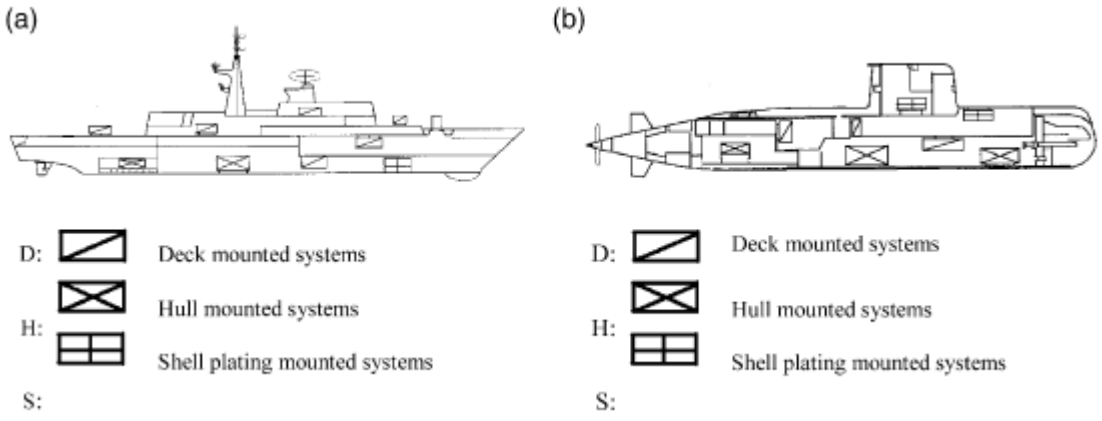

Figure 24 Indication of mounting locations, (Cho-Chung-Liang&Min-Fang-Yang&Yuh-Shiou-Tai, 2001)

Furthermore, the input shock design values in shock response spectrum can be obtained by using modal effective weight and coefficients. The input acceleration and the velocity at certain mode can be calculated by following formulas respectively:

$$A_0 = A\left[\frac{BW_n^2 + CW_n + D}{(E + W_n)^F}\right] \tag{50}$$

$$V_0 = A\left[\frac{B + W_n}{(C + W_n)}\right] \tag{51}$$

W_n=Modal effective weight at certain mode shape

The coefficients can also be presented in another form (Eq. 52&53). Actually, this format is generally used for DDAM applications in Nastran and in ANSYS finite element software.

$$A_0 = AF_i \frac{AA(AB+M)}{(AC+M)} \quad V_0 = VF_i \frac{VA(VB+M)}{(VC+M)} \tag{52}$$

For Surface ship with Hull or Shell monted

$$A_0 = AF_i \frac{AA(AB+M)(AC+M)}{(AD+M)^2} \quad V_0 = VF_i \frac{VA(VB+M)}{(VC+M)} \tag{53}$$

For all other ship types and mounting locations

M=Modal effective weight at certain mode shape, kips unit in BIN system and kg in SI unıt system.

O'Hara and Belsheim's coefficients give exactly the same shock design spectrum as the coefficients in Table 3. The only difference is the way of demonstration. In order to apply NRL coefficients in finite element solver such as ANYS and NASTRAN, Table 3 will be more applicable.

Table 3 DDAM coefficients for finite element solvers (SIEMENS, 2004)

Shock criteria	VA	VB	VC	AA	AB	AC	AD
SURF/DECK/ELASTIC	30	12	6	10	37.5	12	6
SURF/HULL/ELASTIC	60	12	6	20	37.5	12	6
SURF/SHELL/ELASTIC	120	12	6	40	37.5	12	6
SURF/DECK/ELPL	30	12	6	10	37.5	12	6
SURF/HULL/ELPL	60	12	6	20	37.5	12	6
SUB/DECK/ELASTIC	10	480	100	5.2	480	20	20
SUB/HULL/ELASTIC	20	480	100	10.4	480	20	20
SUB/SHELL/ELASTIC	100	480	100	52	480	20	20
SUB/DECK/ELPL	10	480	100	5.2	480	20	20
SUB/HULL/ELPL	20	480	100	10.4	480	20	20

In Table 3, the abbreviations refer respectively: SURF= Surface ship, SUB=Submarine, DECK= Deck mounted, HULL= Hull mounted, SHELL=Shell mounted, ELASTIC= Elastic deformation criteria, ELPL= Plastic deformation criteria.

On the other hand, the direction of the shock is as important as the location of the equipment. According to experimental results, the level of the shock varies depending on the direction. Thus, the directional weighting coefficients are composed as illustrated in Table 4.

Table 4 Directional coefficients for DDAM analysis with coefficients (SIEMENS, 2004)

nsurf/nstruc/nplast	VF(1)	VF(2)	VF(3)	AF(1)	AF(2)	AF(3)
SURF/DECK/ELASTIC	0.4	0.4	1	0.4	0.4	1
SURF/HULL/ELASTIC	0.2	0.4	1	0.2	0.4	1
SURF/SHELL/ELASTIC	0.1	0.2	1	0.1	0.2	1
SURF/DECK/ELPL	0.2	0.2	0.5	0.4	0.4	1
SURF/HULL/ELPL	0.1	0.2	0.5	0.2	0.4	1
SUB/DECK/ELASTIC	0.8	2	1	0.8	2	1
SUB/HULL/ELASTIC	0.4	1	1	0.4	1	1
SUB/SHELL/ELASTIC	0.08	0.2	1	0.08	0.2	1
SUB/DECK/ELPL	0.4	1	0.5	0.8	2	1
SUB/HULL/ELPL	0.2	0.5	0.5	0.4	1	1

In Table 4 above, VF and AF refer to directions identified by (1), (2), and (3), respectively

- (1) = Fore/aft, x-direction
- (2) = Athwart-ship, y-direction
- (3) = Vertical, z-direction

NRL Coefficient - DDAM analysis is mainly adapted to BIN (British unit) system since it is commonly used in US and the British navies. In order to apply these coefficients to SI unit system properly, Table 5 was considered in conversion phase.

Table 5 Conversion of DDAM coefficients to SI unit system- (Schaller, 2008)

AF	Direction coefficent same=1
AA	Multiply by (9810/386)=25.4145
AB	Multiply by (386*0.453437/1000)=0.175027
AC	Multiply by (386*0.453437/1000)=0.175027
AD	Multiply by (386*0.453437/1000)=0.175027
VF	Direction coefficent is same=1
VA	Multiply by (386*0.453437/1000)=0.175027
VB	Multiply by (386*0.453437/1000)=0.175027
VC	Multiply by (386*0.453437/1000)=0.175027
Amin	Minimum input acceleration 6 G=58860 mm/s^2

When DDAM coefficients are used in SI unit system (mm, T, s, N, MPa), they should follow this conversion step in Table 5. (Schaller, 2008)

According to NAVSHOCK requirements, the minimum shock input acceleration is defined as 6 G (gravity). Therefore, the minimum shock acceleration must be 2316 in/sec^2 or 58860

mm/s^2 equal to 6 G (gravity) as it is shown in a sample of shock design spectrum presented in Figure 25.

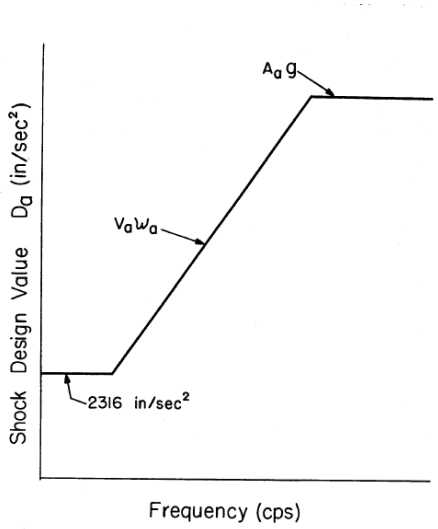

Figure 25 A design shock spectrum - (Belsheim&O'Hara, 1963)

Figure 25 presents that the velocity sourced acceleration shock design value is seen in the slope of the graph, also, acceleration sourced shock design value is seen horizontally in the graph. Hence, it can be interpreted that the velocity sourced shock value can be considered as more important at low frequencies. Nevertheless, acceleration sourced shock value is more significant in the high-frequency range.

6.4. Assessment of DDAM Responses

The acceleration shock input value at each natural frequency can be obtained by the SRS shock response spectrum (sourced by NRL coefficients or transient analysis). After that, the acceleration response at ath mode and ith node can be assessed by (Eq 54).

$$a_{ia} = P_{ia}\phi_{ia}A_0 \tag{54}$$

Where,

a_{ia}=Response acceleration of the equipment at at ith node an ath mode

P_{ia}=Participation factor at at ith node an ath mode

ϕ_{ia}=Eigen vector at at ith node an ath mode

A_0=Acceleration shock input value from SRS or NRL coefficients

Then, velocity at that mode can be calculated from the acceleration divided by the natural frequency.

$$v_{ia} = \frac{a_{ia}}{\omega} = \frac{P_{ia}\phi_{ia}A_0}{\omega} \tag{55}$$

Also, displacement can be calculated from the acceleration divided by the square of the natural frequency.

$$u_{ia} = \frac{a_{ia}}{\omega^2} = \frac{P_{ia}\phi_{ia}A_0}{\omega^2} \tag{56}$$

In order to obtain force, displacement can be used at each mode shape. The displacement between two nodes and stiffness of the spring can be used to obtain the force, for instance, in a spring-mass system.

$$F_{na} = K_n(u_{ia} - u_{ja}) \tag{57}$$

Where,

F_{na}= Force at ath mode

K_n= Stiffness of the spring

u_{ia}=Displacement at ith node

u_{ja}= Displacement at jth node

Whereas the response is obtained for each mode, a summation procedure can applied to combine responses of the structure at each mode. Many different summation methods exist such as the root mean square method, the NRC grouping method, the double sum method and the complete quadratic combination.

Generally, the root mean square method is appropriate to find the peak response from the combination each i modes as shown in (Eq. 58)

$$\Gamma_{RMS} = \sqrt{\sum(\Gamma_i)^2} \tag{58}$$

However, DDAM uses another summation method which is applicable and generally used for naval applications, the so-called NRL (Naval Research Lab) sum. It fundamentally takes the absolute of the maximum response and then, sums the root mean square of the rest of the responses as shown in (Eq.59)

$$\Gamma_{NRL} = |\Gamma_{MAX}| + \sqrt{\sum(\Gamma_i)^2 - (\Gamma_{MAX})^2} \tag{59}$$

Where,

Γ_i= Responses (displacement or stress) at each of i modes.

Γ_{MAX}= Maximum response among all modes.

NRL sum is considered for all DDAM calculations in this thesis.

7. DDAM ANALYSIS OF A CANTILEVER BEAM

In this part, a DDAM analysis is carried out for a simple cantilever beam in MSC Nastran and ANSYS finite element solvers with different mesh sizes. Obtained numerical results are then compared with analytical results referenced by (Cho-Chung-Liang&Min-Fang-Yang&Yuh-Shiou-Tai, 2001).

This analysis is carried out in MSC Nastran with BIN unit system, and in ANSYS with SI unit system. Since the reference results are presented in British Unit system, the analysis is performed in British Unit system (BIN) as well. Whereas the analysis is performed in BIN unit system, the results are converted to SI unit system. Finally, the results are presented in both unit systems and the discrepancy between numerical and analytical results is discussed.

Note that only transverse directed shock is applied to the cantilever beam. Because of this, the modal analysis and spectrum analysis are only performed along x-transverse direction.

7.1. Model Description

The cantilever beam is considered as shell mounting system and clamped at the edge of the beam. The main dimensions and material properties of the cantilever beam are given in Table 6. Also, the schematic illustration can be seen in Figure 26.

Table 6 Main properties of the cantilever beam

Main Properties of a Cantilever Beam		
L	72 (in)	1.8288 (m)
h	4.64 (in)	0.117856 (m)
b	1 (in)	0.0254 (m)
E	2,9e7 (psi)	2e11 (N/m^2)
ρ	0.00073 ($lbf{\cdot}s2/in^4$)	7803.7 (kg/m^3)

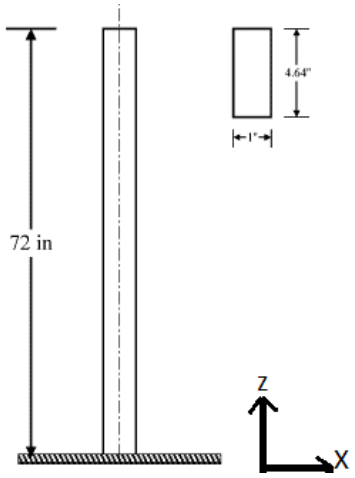

Figure 26 Main dimensions of cantilever beam

The modelling of the cantilever beam is performed using MSC Patran with three different mesh sizes, which are respectively a 3D solid element model with grid element size 0.5 inch (12.7 mm), a beam element model with element size 8 inch (0.2 m) and a beam element model with element size 1 inch (25.4 mm). Moreover, the same geometry is modelled in ANSYS as beam structure with element size 25.4 m, which is equivalent to one of MSC. Patran model.

The boundary conditions of the cantilever beam are shown below.

$$u(0) = u'(0) = 0, \tag{60}$$

$$u''(L) = u'''(L) = 0$$

The expression means that one extremity of this beam $(z = 0)$ is clamped and the other extremity $(z = L)$ is free to move in all directions.

7.2. Natural Frequencies and Mode Shapes

In order to analyse this beam shock response using DDAM method, firstly the modal analysis should be performed properly since the DDAM analysis is based on modal combination. The comparison of resulting circular frequencies for the cantilever beam with reference file is shown in Table 7. It is worth noting that the relative error is calculated according to reference results.

Table 7 Modal analysis of the cantilever beam

Mode No	Reference	Nastran - Element size - (0.2 m)		Nastran - Element size - (25.4 mm)		Nastran – SOLID-Element size - (12.7 mm)		ANSYS, SI unit, Element size- (25.4 mm)	
	Radians (rad/sec)	Radians (rad/sec)	Discr.	Radians (rad/sec)	Discr.	Radians (rad/sec)	Discr.	Radians (rad/sec)	Discr.
1	181.7	179.6	1.2%	180.6	0.6%	181.9	-0.1%	180.5	0.7%
2	1134.0	1094.3	3.5%	1115.1	1.7%	1118.9	1.3%	1109.6	2.2%
3	3176.1	2957.5	6.9%	3051.0	3.9%	3045.3	4.1%	3018.4	5.0%
4	6223.4	5528.8	11.2%	5791.3	6.9%	5745.3	7.7%	5689.4	8.6%

During the analysis, it was noted that increasing the number of finite elements allows to increase the number of calculated mode shapes as well. Also, it would be noticed in Table 7 that when the number of modes increases, the error between analytical and numerical solutions increases too. Because discrepancy between theoretical and numerical results are increasing while the number of modes increases.

Furthermore, the beam element model with 25.4 mm element size gives more precise results as compared with solid element one because the reference results are theoretically based on a beam theory. The solution in a beam element model with element size (25.4 mm) gives more accurate results among all results. That's why the same analysis in ANSYS is carried out for comparison.

Finally, the first four bending mode shapes of the cantilever beam can be seen respectively from left side to right side for a solid model in Figure 27.

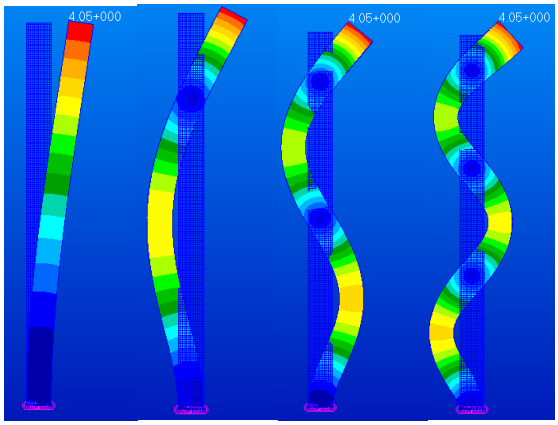

Figure 27 Main mode shapes (bending) of the cantilever beam

Once modal analysis has been performed, shock analysis is processed and presented in following part.

7.3. Shock Analysis of the Cantilever Beam

The shock analysis is performed by considering specific shock spectrum coefficients since the reference calculations take into account George J. O'Hara and Robert O. Belsheim`s coefficients which have been listed in section 6.3.1. As it is mentioned, the coefficients are based on shock design criteria such as location, type of vessel, etc. Thus, this study is performed for surface ship, shell mounted and elastic deformation region according to the reference file. The coefficients which are taken into account are listed in Table 8.

Table 8 Coefficients for Surface ship, Shell mounted and Elastic deformation

Shock criteria	VA	VB	VC	AA	AB	AC	AD
SURF/SHELL/ELASTIC (BIN)	120	12	6	40	37.5	12	6
SURF/SHELL/ELASTIC (SI unit: kg,m,Pa,s)	3.0496	2100.3	1050.1	1.0165	6563.5	2100.3	1050.1
Directional coefficient	Only x-transverse shock VF1=AF1=0.1						

Those coefficients are used to generate the shock response spectrum for DDAM analysis. In DDAM analysis, cut-off percentage of total effective mass is normally required as at least 80%, here, it is considered as 100% to obtain all mode shapes in the analysis and compare them with the reference results. Another requirement in DDAM analysis is the minimum acceleration shock input value which is required as 6 G in NRL report. These requirements are applied for DDAM analysis.

In order to compare numerical results with the reference ones, some conversions are done to have equivalent units in all cases.

In DDAM analysis, one of the most important parameters is the effective mass, which basically relies on a participation factor as explained before. The effective mass is used to define shock input values (if SRS is derived from coefficients). Also, it defines the contribution of each mode for the final response of the structure. In other words, the mode with the highest modal effective mass dominates the rest of the modes in the structural response. The effective mass is given for each mode in Table 9.

Table 9 Modal effective mass for the cantilever beam

Mode No	Reference		Nastran - Element size - (0.2 m)			Nastran - Element size - (25.4 mm)			Nastran – SOLID-Element size – (12.7 mm)			ANSYS, SI unit, Element size-(25.4 mm)	
	Effective mass (lbm-kg)		Effective mass (lbm-kg)		Discr.	Effective mass (lbm-kg)		Discr	Effective mass (lbm-kg)		Discr.	Effective mass (kg)	Discr.
1	0.15	26.3	0.15	26.1	0.7%	0.15	26.3	0.2%	0.15	26.1	0.7%	26.2	0.4%
2	0.05	8.4	0.05	8.2	2.8%	0.05	8.2	2.8%	0.05	8.1	3.7%	8.1	3.4%
3	0.02	2.8	0.02	2.8	-0.8%	0.02	2.8	-0.8%	0.02	2.8	0.8%	2.8	-0.7%
4	0.01	1.4	0.01	1.4	-2.6%	0.01	1.5	-5.8%	0.01	1.5	-3.3%	1.5	-4.6%

The highest modal effective mass is seen corresponds to the first bending mode. Afterwards, the modal effective mass is decreasing respectively in following modes. In next steps, the participation of modal effective mass to the whole system can be observed in Table 13.

In all cases, the results are obtained with less than 5 % relative error which is acceptable for this kind of analysis. Here, also, the best results are obtained with the beam element model solution based on 25.4 mm element size.

As a next step, the shock input acceleration values Ai*g and Vi*ω are presented respectively. These values are obtained by computation of specified NRL coefficients. In the same time, they will define shock response spectrum for DDAM analysis. Firstly, acceleration derived shock values are tabled in Table 10.

Table 10 Acceleration derived shock input values

Mode No	Reference		Nastran - Element size - (0.2 m)			Nastran - Element size - (25.4 mm)			Nastran – SOLID-Element size – (12.7 mm)			ANSYS, SI unit, Element size-(25.4 mm)	
	Ai*g (in/s^2 -m/s^2)		Ai*g (in/s^2 -m/s^2)		Discr.	Ai*g (in/s^2 -m/s^2)		Discr.	Ai*g (in/s^2 -m/s^2)		Discr.	Ai*g (m/s^2)	Discr.
1	1.9E+04	483.7	1.9E+04	484.3	-0.1%	1.9E+04	484.2	-0.1%	1.9E+04	484.3	-0.1%	475.1	1.8%
2	1.9E+04	489	1.9E+04	488.5	-0.1%	1.9E+04	488.5	-0.1%	1.9E+04	488.6	-0.1%	486	0.4%
3	1.9E+04	489.3	1.9E+04	489.8	-0.1%	1.9E+04	489.8	-0.1%	1.9E+04	489.8	-0.1%	489.2	0.0%
4	1.9E+04	489.6	1.9E+04	490.2	-0.1%	1.9E+04	490.1	-0.1%	1.9E+04	490.2	-0.1%	490.1	-0.1%

The input acceleration shock value is based on modal effective weight and coefficients. Although there is small discrepancy in modal effective mass calculation, the discrepancy in

input acceleration shock value is near zero as shown in table above. The reason is that the coefficients have a bigger influence than the modal effective weight in the calculation of the acceleration shock input values.

Another method to calculate the acceleration shock value is to derive from input shock velocity. This type of acceleration is also called *equivalent* input acceleration. As for acceleration shock input value, the input velocity is also calculated using coefficients listed in section 6.3. In order to obtain the equivalent acceleration shock value, input shock velocity is multiplied by natural circular frequency value of each mode ($Vi*\omega$) as shown in Table 11.

Table 11 Velocity derived shock values

Mode No	**Reference**		**Nastran - Element size - (0.2 m)**			**Nastran - Element size - (25.4 mm)**			**Nastran – SOLID- Element size - (12.7 mm)**			**ANSYS, SI unit, Element size- (25.4 mm)**	
	Vi*ω (in/s^2 -m/s^2)		**Vi*ω (in/s^2 -m/s^2)**		**Discr.**	**Vi*ω (in/s^2 -m/s^2)**		**Discr.**	**Vi*ω (in/s^2 -m/s^2)**		**Discr.**	**Vi*ω (m/s^2)**	**Discr.**
1	4.3E+03	109.8	4.3E+03	108.9	0.8%	4.3E+03	109.5	0.3%	4.3E+03	110.3	-0.5%	108.77	0.9%
2	2.7E+04	690.4	2.6E+04	665.8	3.6%	2.7E+04	678.4	1.7%	2.7E+04	680.7	1.4%	674.21	2.4%
3	7.6E+04	1936	7.1E+04	1801	7.0%	7.3E+04	1858	4.0%	7.3E+04	1855	4.2%	1838.6	5.0%
4	1.5E+05	3798	1.3E+05	3368	11.3%	1.4E+05	3528	7.1%	1.4E+05	3500	7.9%	3467.8	8.7%

Normally, the discrepancy in V_i input velocity is less than 1%, but the relatively high discrepancy observed in modal analysis influences the discrepancy in equivalent acceleration results proportionally in Table 11.

In generating shock response spectrum by coefficients, both input acceleration and equivalent acceleration shock values are compared for each mode. Then, the lower one of these two shock values is taken into account for the final input acceleration shock value. The final input acceleration values are seen in Table 12.

Table 12 Final input acceleration shock value

Mode No	Reference		Nastran - Element size - (0.2 m)			Nastran - Element size - (25.4 mm)			Nastran – SOLID- Element size – (12.7 mm)			ANSYS, SI unit, Element size- (25.4 mm)	
	Shock design value An (in/s^2 -m/s^2)		Shock design value An (in/s^2 -m/s^2)		Discr.	Shock design value An (in/s^2 -m/s^2)		Discr.	Shock design value An (in/s^2 -m/s^2)		Discr.	Shock design value An (m/s^2)	Discr.
1	4.3E+03	110	4.3E+03	109	0.8%	4.3E+03	109.5	0.3%	4.3E+03	110	-0.4%	110	0.2%
2	1.9E+04	488	1.9E+04	489	-0.1%	1.9E+04	488.5	-0.1%	1.9E+04	489	-0.1%	490	-0.1%
3	1.9E+04	489	1.9E+04	490	-0.1%	1.9E+04	489.8	-0.1%	1.9E+04	490	-0.1%	490	-0.1%
4	1.9E+04	490	1.9E+04	490	-0.1%	1.9E+04	490.1	-0.1%	1.9E+04	490	-0.1%	490	-0.1%

As explained above, the final input acceleration table is a combination of both input acceleration (Ai*g) and equivalent acceleration values (Vi*ω). Thus, acceleration input derived from velocity is only used for the 1st mode, the other final input accelerations are taken from acceleration derived shock input values. As another way of describing the final shock input values, the shock value at the 1st mode is velocity sourced and the others are acceleration sourced. In the end, the final acceleration values have a small discrepancy with reference result, less than 1 % for all cases.

Based on the final acceleration shock values, the shock response spectrum can be plotted as shown in Figure 28.

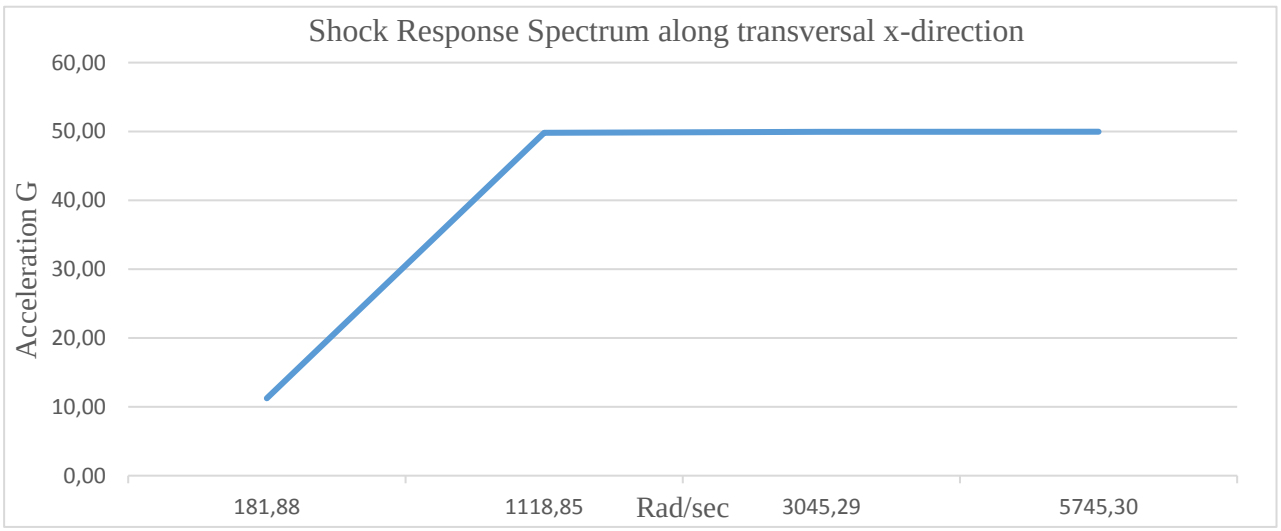

Figure 28 Shock response spectrum for this study

In next table, the percentage of the modal effective mass of the system is shown for each mode. NRL specification requires considering the participation of at least 80% of the modal

weight of the system for DDAM analysis. Whereas 80% of total modal weight is considered, only the first two or three modes are taken into account for modal summation in this analysis as shown in Table 13.

Table 13 Modal weight percentage at each mode

Mode No	Reference	Nastran - Element size - (0.2 m)		Nastran - Element size - (25.4 mm)		Nastran – SOLID- Element size - (12.7 mm)		ANSYS, SI unit, Element size- (25.4 mm)	
	Modal weight %	Modal weight %	Discr.	Modal weight %	Discr.	Modal weight %	Discr.	Modal weight %	Discr.
1	61.5%	61.1%	0.7%	61.4%	0.2%	61.1%	0.7%	61.3%	0.3%
2	19.7%	19.1%	2.8%	19.1%	2.8%	19.0%	3.7%	19.0%	3.4%
3	6.6%	6.6%	-0.8%	6.6%	-0.8%	6.5%	0.8%	6.6%	-0.1%
4	3.3%	3.4%	-2.6%	3.5%	-5.8%	3.4%	-3.3%	3.4%	-4.0%

As it is noticeable in Table 13 above, the first two modes dominate the other modes. Especially the participation of the 3rd and 4th modes are respectively around 6% and 3%, they are very low compared with the first two modes. In this analysis, the response of the cantilever beam will be influenced mostly by the first mode.

In the final response of the DDAM analysis, displacement values are compared with reference results. The displacement results calculated from NRL summation can be seen in Table 14.

Table 14 Displacement response of the cantilever beam

Reference		Nastran - Element size - (0.2 m)			Nastran - Element size - (25.4 mm)			Nastran – SOLID- Element size – (12.7 mm)			ANSYS, SI unit, Element size- (25.4 mm)	
Total displacement (in- m)		Total displacement (in- m)		Discr.	Total displacement (in- m)		Discr.	Total displacement (in- m)		Discr.	Total displacement (in/ m)	Discr.
0.22	0.0056	0.22	0.0056	-0.2%	0.22	0.0056	-0.3%	0.22	0.0055	0.6%	0.0056	-0.3%

As a final response, the results are obtained with less than 1% discrepancy for all cases. Moreover, the post process of displacement of the solid model cantilever beam is illustrated in Figure 29 to have an idea of how deflection would occur in this shock analysis.

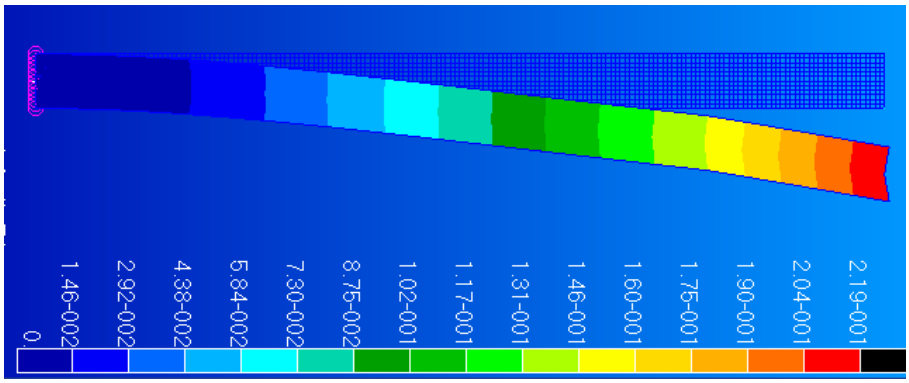

Figure 29 Final deflection of the solid model cantilever beam

As a conclusion, the analysis process of the shock spectrum and DDAM analysis are studied for a simple cantilever beam. At each time step, numerical results obtained are compared to a reference solution showing small discrepancy. It appears that using a fine meshed beam model allows to obtain for the cantilever beam almost the same results than the reference. Moreover, this analysis will be a guide for next DDAM analysis.

8. CASE STUDY: SHOCK ANALYSIS OF AN ANTENNA STRUCTURE

In this part, the shock analysis of an antenna structure is carried out by applying a different way of shock analysis methods. The geometry of the antenna structure is given by STX France, the antenna is located on the deck of the ship and fixed on the location where it is assembled.

The antenna is necessary and crucial for safety and operation of the ship. Thus, it is considered as Grade A items as explained in part 5.1.1. For this reason, the antenna structure is expected to remain in elastic deformation during the shock load.

Three main analysis methods may be listed as follows:

- NRL Coefficient DDAM analysis: Once, DDAM analysis procedure is applied to the antenna structure by using coefficients from NRL 1396 report according to the location of the equipment, grade of the equipment etc. This analysis is performed using ANSYS software.

- Transient analysis: a direct integration method was applied to a simplified ship structure, which has semi-cylinder model below the waterline. In this analysis, the antenna is attached on the deck of the ship and the response of the antenna is obtained using LS-DYNA explicit solver, dependent on the time in an underwater explosion case. The reason for using LS-DYNA explicit transient solver, the structural response of whole elements is analysed for each time step. Besides that, it takes much time due to the direct integration.

Moreover, explicit direct integration solver is very convenient for fluid-structure interaction, large or small displacement as well as the large velocity of particles. Furthermore, it is capable to solve non-linear loadings and structure behaviours. Therefore, it is applicable for underwater explosion analysis

- DDAM analysis from time history input: this DDAM analysis is performed with a different shock response spectrum, which is obtained from time-history input data obtained from a transient LS-DYNA analysis, instead of coefficients. In the analysis, the shock response spectrums are generated considering the time-history responses at the location of the equipment. Afterwards, the generated SRS is used for DDAM analysis.

Regarding non-disclosure agreement with STX France, the detailed geometries in the thesis are not shared. Also, the maximum stresses and displacements are not indicated as numerical value. They are indicated considering a particular reference value in the tables. Moreover, pressure, stress, acceleration levels on the graphs are not demonstrated numerically as well. This procedure is followed in next sections.

8.1. NRL Coefficient DDAM Analysis of the Antenna Structure

NRL Coefficient DDAM analysis is performed for the antenna structure to estimate the responses in case of UNDEX. The antenna structure is considered as a Grade A item and it is supposed to remain in elastic deformation domain.

As a sample equipment of a frigate, the geometry of the antenna is given by STX France. In structural point of view, the antenna is made of square beam steel structure and it is fixed on the deck. The geometry of the antenna can be seen in Figure 30.

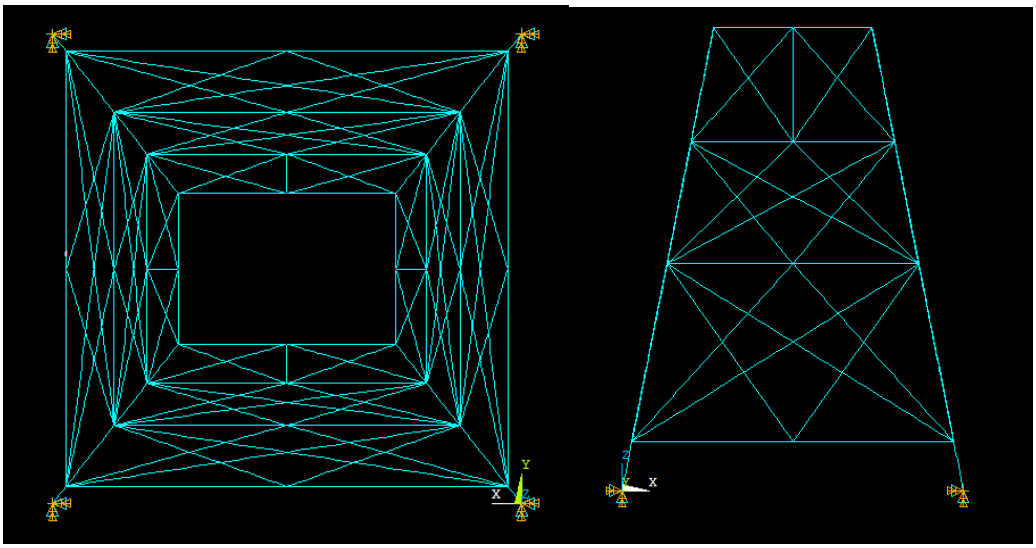

Figure 30 Geometry of the antenna

Table 15 Characteristics of high tensile steel used for the antenna

High tensile steel	Properties
E (MPa)	210000
ρ (kg/m^3)	7810
ν	0.3
σ_y (MPa)	800

Table 15 lists the mechanical characteristics of the high tensile steel (35NCD16) considered for the antenna.

Afterwards, meshing process is operated on the structure. The mesh size is important to catch the most participating mode shapes correctly. Furthermore, having quite fine mesh is also essential to obtain the stress and displacement results properly. Thus, the equipment has been meshed using 65mm element size.

Since the DDAM analysis is based on mode shapes participation, a modal analysis is first performed and then the modes are expanded regarding the direction of each shock load. The modal characteristics can be seen in Table 16.

Table 16 Modal analysis of the antenna structure

MODE No	ANSYS	NASTRAN	X direction	Y direction	Z direction
	Frequency (Hz)	Frequency (Hz)	Percentage of the modal effective mass		
1	110.98	110.99	95.4	0	0
2	115	115.01	0	94.69	0
3	170.18	170.18	0	0	0
4	175.49	175.50	0	0	0.36
5	180.45	180.45	0	1.49	0
6	189.36	189.36	1.42	0	0
7	197.75	197.76	0	0	0
8	226.2	226.20	0	0	89.94
	Total percentage of modal effective mass		96.82	96.18	90.3

In the modal analysis, the cut-off frequency is considered as upper level 250 Hz. This is due to the fact that, by experience, typical on-board equipment is less influenced by high frequency excitations as explained in part 5.4.1.

As it is seen in Table 16, the total percentage of the modal effective mass passes the significant limitation of 80% for DDAM analysis at each shock direction. It means that the analysis can be performed confidently for this study.

The DDAM coefficients from NRL report are used to analyze the response of the equipment according to shock criteria of the antenna. Since the antenna is located in the deck of the surface ship and it is expected to remain in elastic deformation region, the coefficients in Table 17 are applied to generate shock response spectrum for this analysis.

Table 17 Shock design coefficients for the antenna structure-Deck mounting system

Shock criteria	VA	VB	VC	AA	AB	AC	AD	
SURFACE SHIP/DECK MOUNTED /ELASTIC DEFORMATION	Velocity shock design coefficients			Acceleration shock design coefficients				
	30	12	6	10	37.5	12	6	BIN Unit system
	0.7624	2100.324	1050.16	0.254145	6563.513	2100.324	1050.16	SI unit system
	Directional Coefficients							
	VF(1), x directed shock	VF(2), y directed shock	VF(3), z directed shock	AF(1), x directed shock	AF(2), y directed shock	AF(3), z directed shock		
	0.4	0.4	1	0.4	0.4	1		

In the application of DDAM method, the shock analysis is also performed for the antenna. The main parameters of DDAM are presented such as the most participating modes, modal effective mass, input acceleration value etc. The shock analysis is shown in Table 18 for each shock direction.

Table 18 Shock analysis summary for the antenna structure- Deck mounting system

Shock design analysis at X directed shock						
MODE No	Frequency (Hz)	Participation factor	Modal effective mass (kg)	Input acceleration shock value (m/s^2)	Input acceleration shock value G	Percentage of modal effective mass%
1	110.98	41.51	1723.18	266.61	27.17	95.4
6	189.36	-5.038	25.377	484.44	49.38	1.42
Shock design analysis at Y directed shock						
MODE No	Frequency (Hz)	Participation factor	Modal effective mass (kg)	Input acceleration shock value (m/s^2)	Input acceleration shock value G	Percentage of modal effective mass%
2	115	-41.35	1710.05	267.51	27.26	94.69
5	180.45	5.16	26.6223	484.15	49.35	1.49
Shock design analysis at Z directed shock						
MODE No	Frequency (Hz)	Participation factor	Modal effective mass (kg)	Input acceleration shock value (m/s^2)	Input acceleration shock value G	Percentage of modal effective mass%
4	175.5	2.487	6.18548	1222.5	124.6	0.36
8	226.2	-40.28	1622.1	684.34	69.69	89.94

In another case, the antenna structure is considered as hull mounting equipment to compare the results with transient and DDAM analysis from time history input. The reason is that the base of the antenna structure is mainly located (three legs of the fixed base) above bulkheads.

Whereas the equipment is hull mounting system, the shock design values will be higher than a case of the deck mounting system. Also, both cases will be in elastic deformation criteria since the antenna is Grade A item. The following coefficients in Table 19 are considered for DDAM analysis.

Table 19 Shock design coefficients for the antenna structure-Hull mounting

Shock criteria	VA	VB	VC	AA	AB	AC	AD	
SURFACE SHIP/HULL MOUNTED /ELASTIC DEFORMATION	Velocity shock design coefficients			Acceleration shock design coefficients				
	60	12	6	20	37.5	12	6	BIN Unit system
	1.5248	2100.32	1050.16	0.50829	6563.513	2100.324	1050.2	SI unit system
	Directional Coefficients							
	VF(1), x directed shock	VF(2), y directed shock	VF(3), z directed shock	AF(1), x directed shock	AF(2), y directed shock	AF(3), z directed shock		
	0.2	0.4	1	0.2	0.4	1		

The acceleration and velocity coefficients are different from the deck mounting ones. Besides that, the directional coefficients are different as well. Thus, the new SRS will vary according to the new coefficients. After the implementation of NRL coefficients, the shock analysis values and parameters of DDAM analysis are obtained and listed in Table 20.

Table 20 Shock analysis summary for the antenna structure- Hull mounting

Shock design analysis at X directed shock						
MODE No	Frequency (Hz)	Participation factor	Modal effective mass (kg)	Input acceleration shock value (m/s^2)	Input acceleration shock value G	Percentage of modal effective mass%
1	110.98	41.51	1723.18	266.61	27.17	95.4
6	189.36	-5.038	25.377	484.44	49.38	1.42
Shock design analysis at Y directed shock						
MODE No	Frequency (Hz)	Participation factor	Modal effective mass (kg)	Input acceleration shock value (m/s^2)	Input acceleration shock value G	Percentage of modal effective mass%
2	115	-41.35	1710.05	535.02	54.54	94.69
5	180.45	5.16	26.6223	968.3	98.71	1.49
Shock design analysis at Z directed shock						
MODE No	Frequency (Hz)	Participation factor	Modal effective mass (kg)	Input acceleration shock value (m/s^2)	Input acceleration shock value G	Percentage of modal effective mass%
4	175.5	2.487	6.18548	2445	249.24	0.36
8	226.2	-40.28	1622.1	1368.7	139.52	89.94

The input acceleration shock values in hull mounting system are obtained differently when using NRL coefficients. Especially, the acceleration shock input value is increased twice at y and z directed shock in hull mounting condition. The rest of the properties are obtained in the same way since they are based on the modal analysis of the antenna.

Finally, the response of the antenna can be obtained applying the modal summation method for each direction. The convenient summation NRLSUM method is considered for this study. Moreover, the operational load should be also considered in the evaluation of DDAM, it is considered as 0 since this structure does not have any significant operational loads. In the end, the displacement and stress results obtained for two different cases are presented in Table 21.

Table 21 Response of the antenna structure by NRL summation

Shock response at	X directed shock-Deck mounted	X directed shock-Hull mounted	Y directed shock-Deck mounted	Y directed shock-Hull mounted	Z directed shock-Deck mounted	Z directed shock-Hull mounted
Total Displacement (mm)	0.5 $Disp_{DDAM\text{-}NRL\text{-}y\text{-}HULL}$	0.5 $Disp_{DDAM\text{-}NRL\text{-}y\text{-}HULL}$	0.5$Disp_{DDAM\text{-}NRL\text{-}y\text{-}HULL}$	$Disp_{DDAM\text{-}NRL\text{-}y\text{-}HULL}$	0.42 $Disp_{DDAM\text{-}NRL\text{-}y\text{-}HULL}$	0.83 $Disp_{DDAM\text{-}NRL\text{-}y\text{-}HULL}$
Maximum von-Mises Stress (MPa)	0.54 $\sigma_{DDAM\text{-}NRL\text{-}y\text{-}HULL}$	0.54 $\sigma_{DDAM\text{-}NRL\text{-}y\text{-}HULL}$	0.5 $\sigma_{DDAM\text{-}NRL\text{-}y\text{-}HULL}$	$\sigma_{DDAM\text{-}NRL\text{-}y\text{-}HULL}$	0.32 $\sigma_{DDAM\text{-}NRL\text{-}y\text{-}HULL}$	0.63 $\sigma_{DDAM\text{-}NRL\text{-}y\text{-}HULL}$

In Table 21, each value is presented taking reference of the maximum response of the antenna at Y-directed shock-Hull mounted as highlighted in the table.

In such type of structure, instead of displacement values, the maximum stress values are much more important for the evaluation of response results. Besides, the location of the maximum stress helps to detect the most critical spots in the structure. Figure 31 & 32 present the locations of the maximum stress respectively at x, y, and z directed shock from left to right.

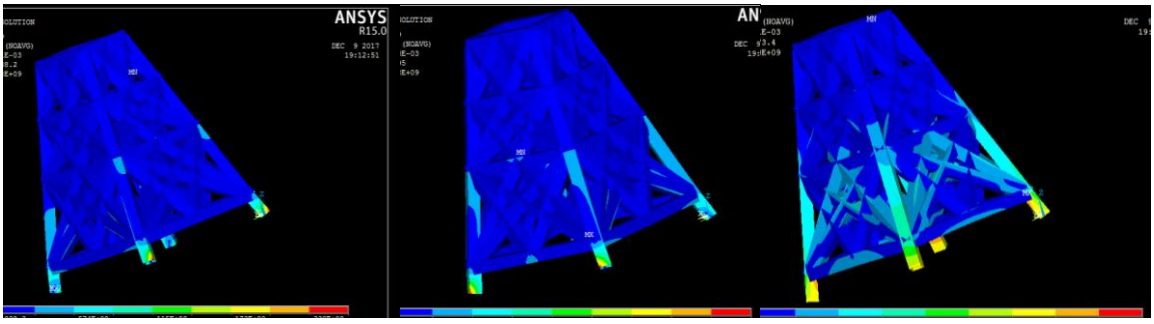

Figure 31 Post-processing of NRL Coefficient DDAM analysis of the antenna - Deck mounted

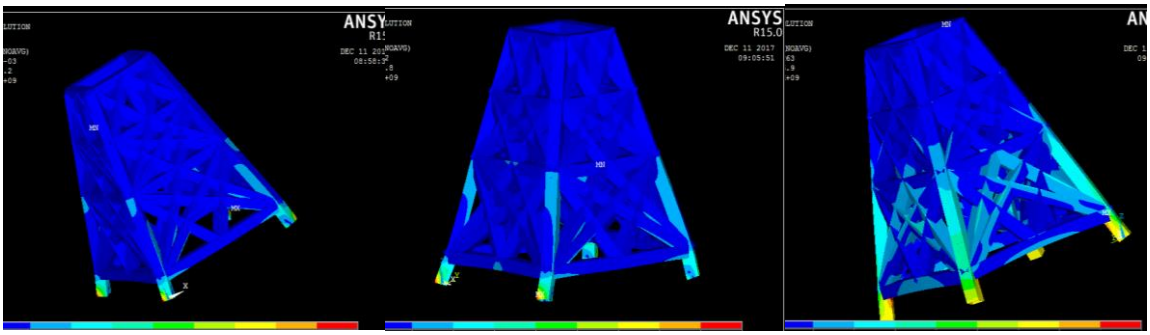

Figure 32 Post-processing of NRL Coefficient DDAM analysis of the antenna - Hull mounted

In both cases, it appears that the most critical parts are detected in same locations since DDAM analysis is based on modal analysis. In the analysis, the only differences occur on the acceleration shock input value, which influences the response of the antenna.

The maximum von-Mises stress appears at the legs of the antenna at three different direction of the shock. Especially at x and y directed shocks, the maximum stress is obtained at the root of the structure, where it is fixed to the deck. Yet, the maximum stress at z directed shock can

be seen at the junction points between legs and the rest of the antenna structure. This is due to the fact that, stress and displacement responses are calculated based on summation of the most participating modes in DDAM analysis.

Thus, these parts of the structure would be critical in case of an underwater explosion. It also appears that the highest levels of stress are observed when the antenna, mounted on the hull, receives a shock acting along y-direction. In this case, the structure should be reinforced or designed to better withstand such loading.

8.2. Transient Analysis of the Antenna

Here, the process of the transient analysis will be explained starting from modelling to post-process phase. Three different transient analyses are performed in this part.

8.2.1. Modelling of simplified ship

Transient analysis is applied to a simplified ship model, which is similar regarding its properties to a frigate. Most of the characteristics of the frigate are considered such as the location of the decks, the shell thickness, the bulkheads, the girders and the mass of the frigate as well. For simplification, the hull of the ship is modeled as a semi-cylinder (elliptical) and Lewis coefficients (Kim&Koo, 2015) are considered to estimate the water added mass coming from the interaction between the ship hull and the surrounding water.

The modeling process is performed in ANSYS Workbench and then the model is exported as LS DYNA input file. The main dimensions of the simplified ship are shown in Table 22.

Table 22 Main dimension of the simplified ship

Part	Dimension (m)
Length overall	Around 100
Breath	Around 12

Only the main structural components such as transversal bulkheads, frames, girders and different deck have been modeled as shown in Figure 33. Pillars have also been modeled at each section in starboard and port side.

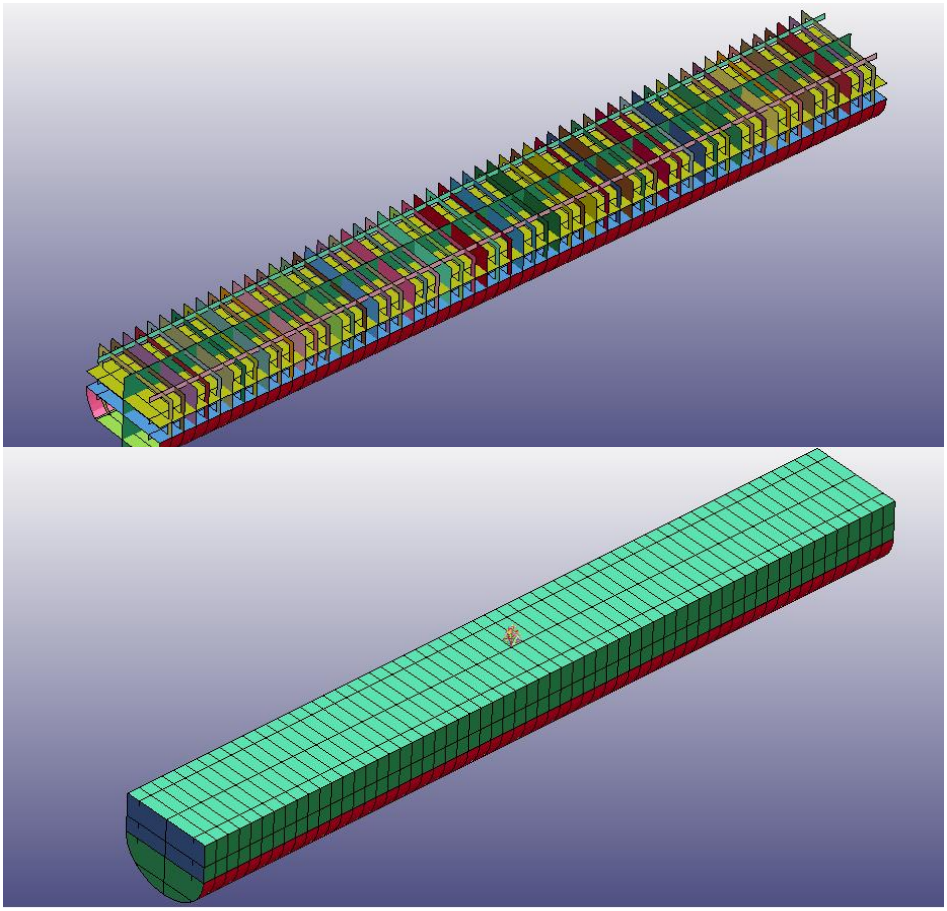

Figure 33 Model of simplified ship

The structural dimensions of the model and the principal weights are not presented in the thesis because of non-discloser agreement between the author and STX France. Nevertheless, **Erreur ! Source du renvoi introuvable.** gives a clear idea about the structure.

After the modeling of the ship, the meshing process is also carried out in ANSYS workbench. The mesh size plays an important role in both duration and quality of the analysis. Since the structure is very big, a coarse mesh is applied globally with 0.8 m element size. First, a *global model* approach is considered for the transient analysis.

8.2.2. Global model, finer mesh around equipment

First of all, the antenna structure is studied with the global model using a coarse mesh all over the simplified ship structure and a finer mesh in the neighboring of the equipment.

To study the influence of the mesh size on the shock response of the equipment, two different mesh sizes (50mm and 200mm) are considered around the antenna, as shown in Figure 34.

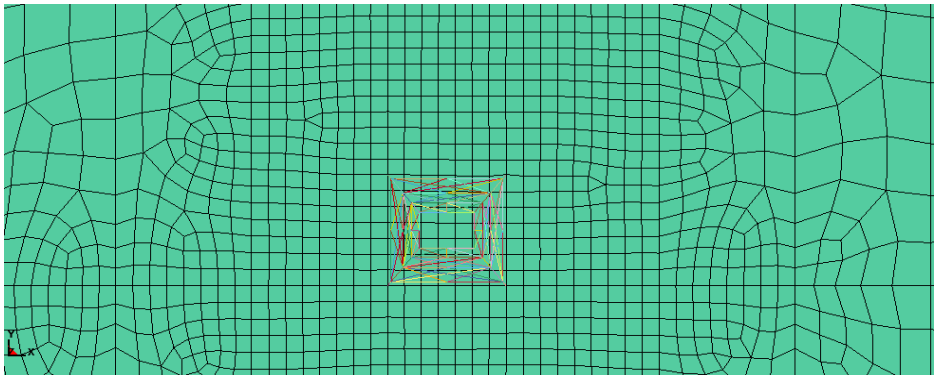

a . 200mm element size mesh

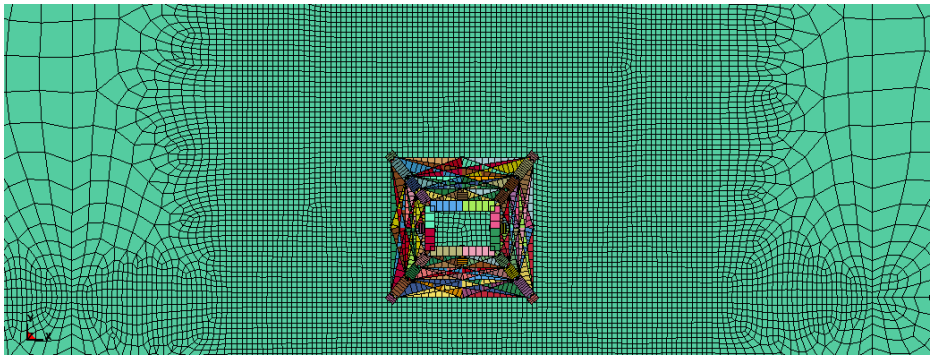

b . 50mm element size mesh

Figure 34 Element size around equipment respectively coarse to fine in global models

In order to obtain correct results in SRS and transient analyses, the mesh size must be fine enough to present the mode shapes at the particular natural frequency. As an example in this study, the SRS is supposed to be well presented between 100 to 240 Hz according to the modal analysis of the antenna, so that the mesh size of the simplified ship must be fine enough to catch the corresponding mode shapes until around 240 Hz. That's why modal analysis is performed locally to examine the mode shapes on the simplified ship structure. **Erreur ! Source du renvoi introuvable.** presents a mode shape at 38.3 Hz post-processed on a ship section coarsely meshed (left) and a mode shape at 248 Hz post-processed near the antenna where the mesh has been refined (right)

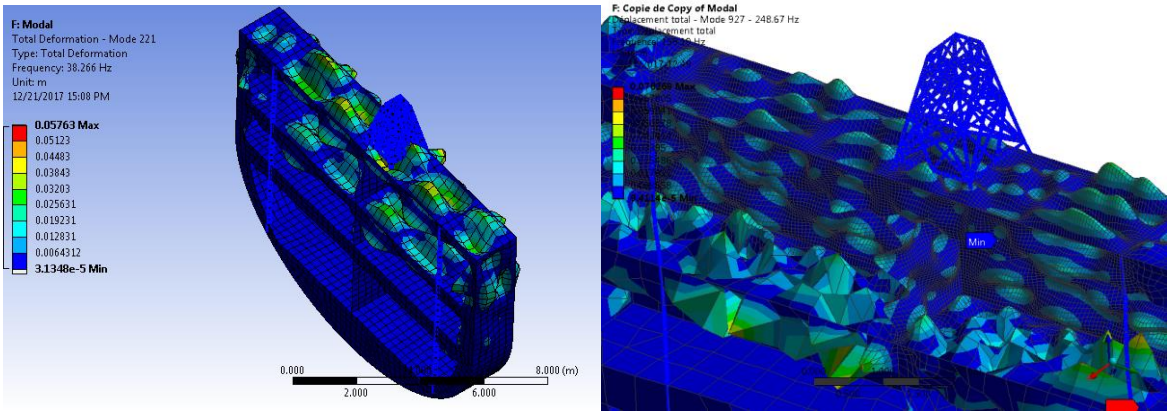

Figure 35 Modal analyses left=global coarse mesh(element size=0.8m), right=fine mesh around equipment(elemetsize=0.05m)

In Figure 35, it can be noticed that the shape of the modes are correctly represented in the neighboring of the antenna until 248 Hz with the fine mesh (50mm element size) model. However, considering a coarse mesh (0.8 m element size), mode shapes are badly represented after 25 Hz. As an example, the left part of **Erreur ! Source du renvoi introuvable.** shows that the mode shape at 38 Hz is not correctly represented.

8.2.3. Section model- Fine mesh

Transient analyses were performed and, as it will be shown in the next sections, unrealistic results were obtained with both global models. It was concluded that meshing the structure only locally is not convenient for the SRS determination and for transient analysis. Because the shock wave propagates all over the structure from ship bottom to weather deck. Whereas the mesh is coarse in bottom structure and fine only in the deck, unrealistic shockwave will propagate from the bottom to the deck. Thus, the response of the structure will not be correct neither in the antenna's deck and nor in the rest of the structure.

In order to overcome this problem, one section of the ship bounded by two bulkheads is only studied. In this study, a 50mm mesh size is considered which allows to obtain well fit modes shapes until 248 Hz. The model of this structure can be seen with the antenna structure in Figure 36.

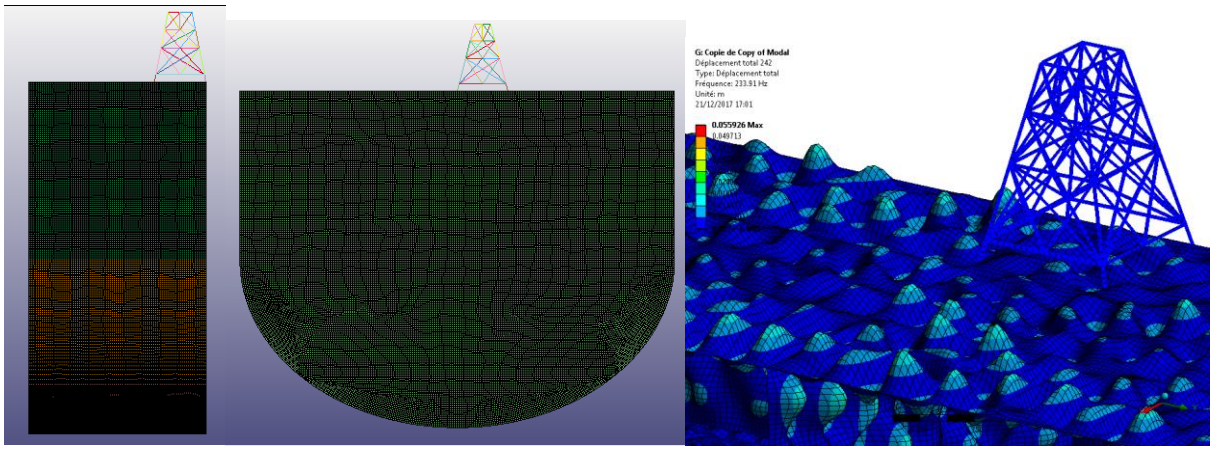

Figure 36 Section model fine mesh

In addition, some boundary conditions are applied to the extremity of the transverse bulkhead of the section model, it is supposed to have zero displacement at transitional x direction and rotational y direction (Ux=0, Ry=0).

8.2.4. Boundary conditions and loads

This model solely considers the steel ship without any deadweight and outfitting. Therefore, the weight of deadweight and outfitting must be included to have the same weight than the corresponding frigate. This additional weight is distributed using lumped masses along the decks except the top deck. Similarly, the water added mass calculated using Lewis coefficients is distributed on the wetted surface of the hull. Lewis coefficients used for the water added mass estimation can be seen for a cylinder in Table 23.

Table 23 Lewis coefficients for cylindrical geometry (Kim&Koo, 2015)

L/2r	α
1.2	0.62
2.5	0.78
5	0.9
9	0.95
∞	1

$$Madd = \alpha * \rho * \left(\frac{(\pi * r^2) * L}{2}\right) \quad (61)$$

In (Eq. 61),

$Madd$ = Added mass in kg,

α= Coefficient for added mass

ρ = Density of the fluid in kg/m^3

L = Length of the ship in m

r = Radius of the geometry, draught is considered in m

The other case is that gravity is not applied to the model since the hydrostatic pressure is not considered in the calculation, because the influence of hydrostatic pressure is very low compared to pressure field due to the underwater explosion. Whereas both hydrostatic pressure and gravity are not considered in the simulation, the model will be in a stable situation. Even if the gravity load is not considered, the inertia of the added mass and weight of the ship will be taken into account in the calculations.

In this transient analysis, the pressure field was considered from explosion including fist shock wave and the first two bubble pulses. Pressure loads from the explosive charge are applied to the entire hull of the structure elements below the waterline.

The macro files to generate pressure file already exist in STX sources, thanks to Mauricio and Ssu's works. It was ready to apply to a new simplified ship's hull. Only the properties of the explosive are modified such the shock factor, the amount of explosive etc. The explosive initial conditions used for the simulation are listed below in Table 24.

Table 24 Initial conditions in Barras' study- (Barras, 2012)

	Properties
mc	TNT charge mass, mc=500 kg
di	Distance from explosive to free surface, di=50+draught
r	Distance from explosive to standoff point, r=50m
ρc	Density of the explosive, ρc= 1600 kg/m^3
SF	Shock factor= 0.447

Also, the location of the charge is an important parameter to define shock factor. In this study, the location of the explosive charge and a ship in section view are shown in Figure 37.

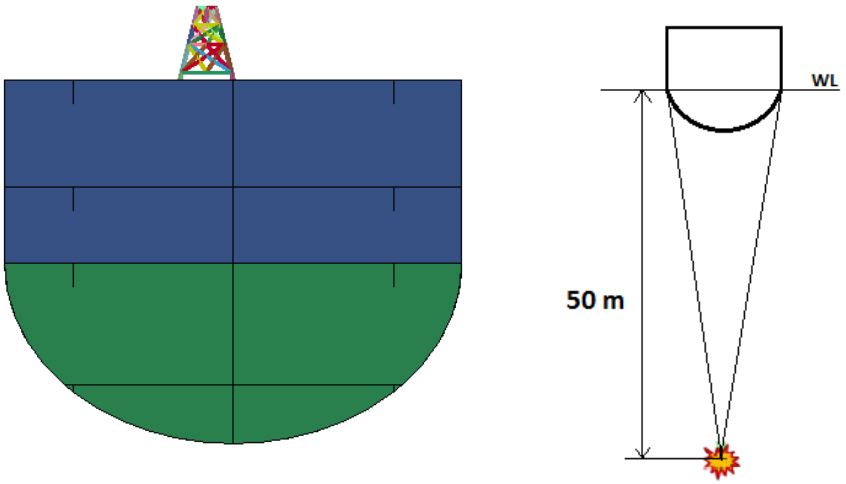

Figure 37 Location of the charge and ship

As explained, a pressure time evolution is considered for the transient analysis. The maximum pressure levels are applied to the element located at the junction point of ship bottom and the middle of the ship hull. The time evolution of the maximum pressure load seen by structure is illustrated in Figure 38.

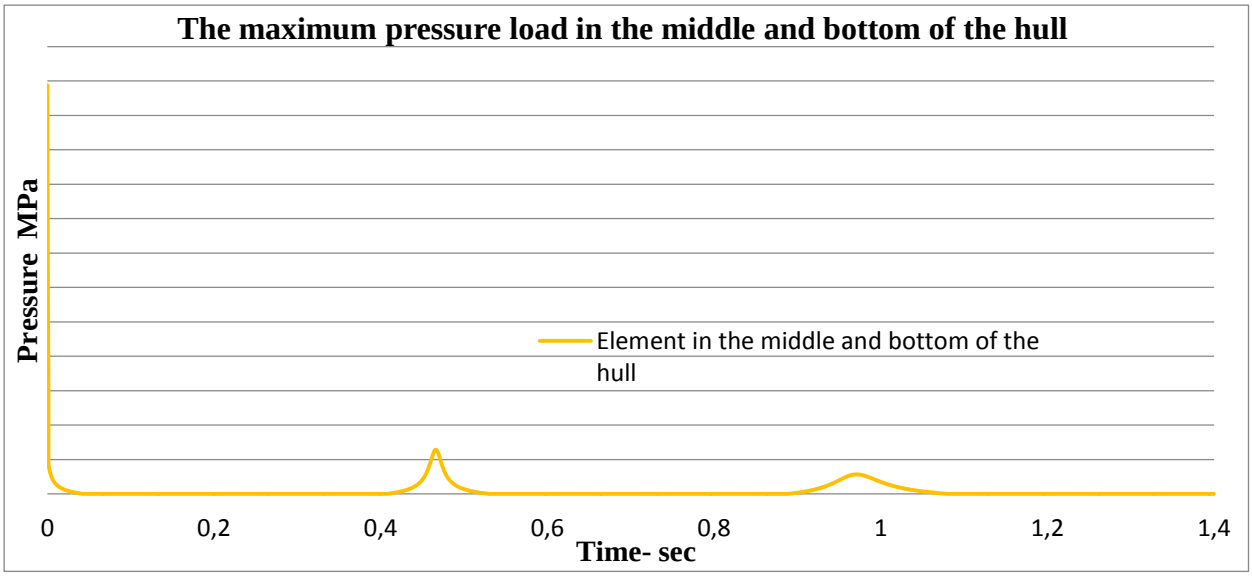

Figure 38 Maximum pressure loads in the bottom of the hull

In Figure 38, it is noticeable that the first shock wave is very sudden and has very high-pressure load in short time duration. Then, the pressure peaks observed at 0.45 and 0.9s are due to the two first pulsations of the explosive gas bubble.

8.2.5. Results of the finite element transient analysis

From the transient analysis, time evolutions of Von-Mises stresses may be post-processed. Three simulations are run for around 2.2 seconds. The stress state in the antenna is post-processed to assess its survivability regarding military shock loading. Generally,

displacements are rather post-processed for resilient mounted equipment which may have extremely large movements when subjected to an underwater explosion. Von-Mises stresses time histories post-processed for the three different studies are compared in Figure 39.

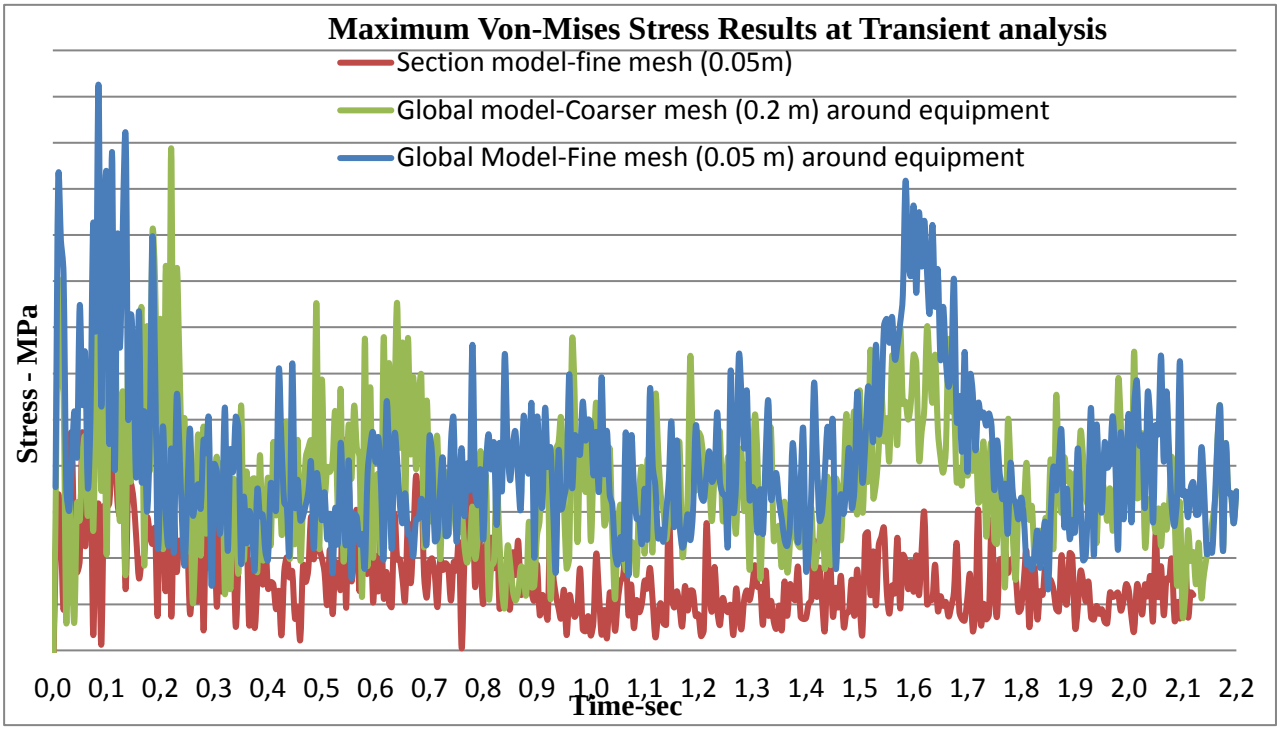

Figure 39 Stress results in the transient analysis

In Figure 39, the stress values obtained in global models are completely unrealistic. On the other hand, the section model with fine mesh has the lower stress value compared with global models, and the stress levels in section with fine mesh are closer to reality. Even if the results are not realistic in global models, the following explanations can be extracted regarding Figure 39.

In three cases, the maximum stress can be seen after the first shock wave as expected because the first shock wave is very sudden with high pressure and energy in a very short time period. Therefore, it influences the antenna structure which is a high-frequency range equipment.

The influence of the shock wave and bubble pulsations are observed in the antenna with some delay. Even the first shock wave acts between 0 – 0.043 s, the influence of it can be seen between 0.05 -0.15. Also, the effect of bubble pulsations is observed with some delay in the global model analyses, as it is seen in 1.6-1.7s. The reason is that the propagation of the shock wave all over the structure, takes time to reach the base of the antenna.

On the other hand, the influence of bubble pulses are not observed in section model with fine mesh since bubble pulsations influence only ship hull beams (global model).

The maximum Von-mises stress values in transient analysis can be seen in Table 25 .

Table 25 Maximum Von-Mises stress values obtained from the transient analysis

Transient Analysis	Global model, coarse mesh (0.2m) around equipment	Global model, finer mesh (0.05m) around equipment	Section model fine mesh (0.05 m)
Total response of the equipment (Max-Von-Misses stress) in MPa	**1.95 $\sigma_{max\text{-}trans\text{-}section\ model}$**	**2.17 $\sigma_{max\text{-}trans\text{-}section\ model}$**	$\sigma_{max\text{-}trans\text{-}section\ model}$

In Table 25, the maximum stress values in transient analysis are indicated proportional to the maximum stress in section model with fine mesh as highlighted in the table.

The yield stress of the antenna material is 800 MPa. Therefore, the antenna structure should have plastified in global models. However, all simulations are carried out using elastic behavior law, which does not account for plastification. That's why it can be said that such stress levels are unrealistic high and badly calculated. This is due to fact that, the flexibility of structure is not modeled correctly in high-frequency.

However, the maximum stress in section model is still in elastic behavior law in contrary with global models.

8.3. DDAM Analysis from Time History Input

In this part, a DDAM analysis is carried out for the same antenna structure by using a specific SRS, which is derived by the transient analysis, instead of using particular DDAM coefficients.

For this study, the SRS should be obtained at the location, where the antenna is mounted. Therefore, the shock response spectrums are calculated respectively at the base point of the antenna structure as shown in Figure 40.

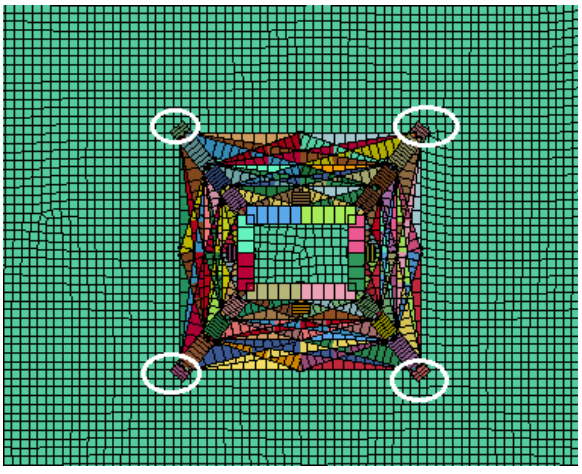

Figure 40 Locations, where time-history data considered

The Shock response spectrums are obtained considering the displacement time-history data post-processed along each direction (x, y and z) from the transient analysis. A representative shock response spectrum of the antenna is obtained for each direction (x, y and z).

In order to compare three different transient analyses, the maximum SRS values are plotted in a single figure. The comparison of shock response spectrums along each direction can be seen in Figure 41.

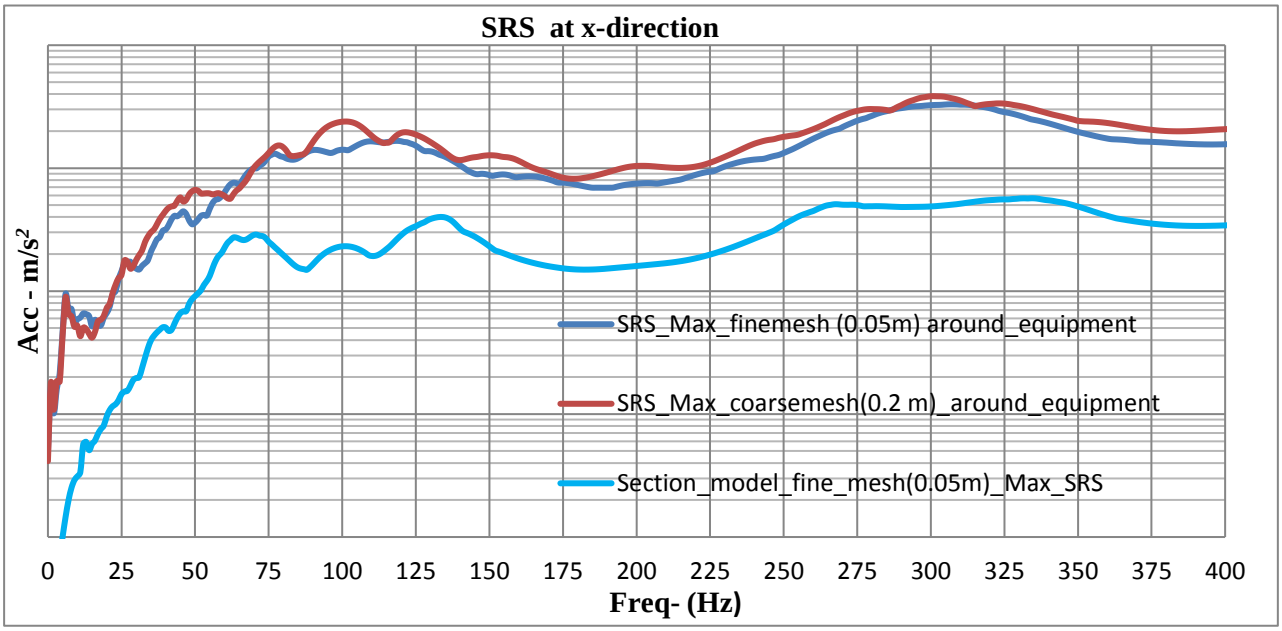

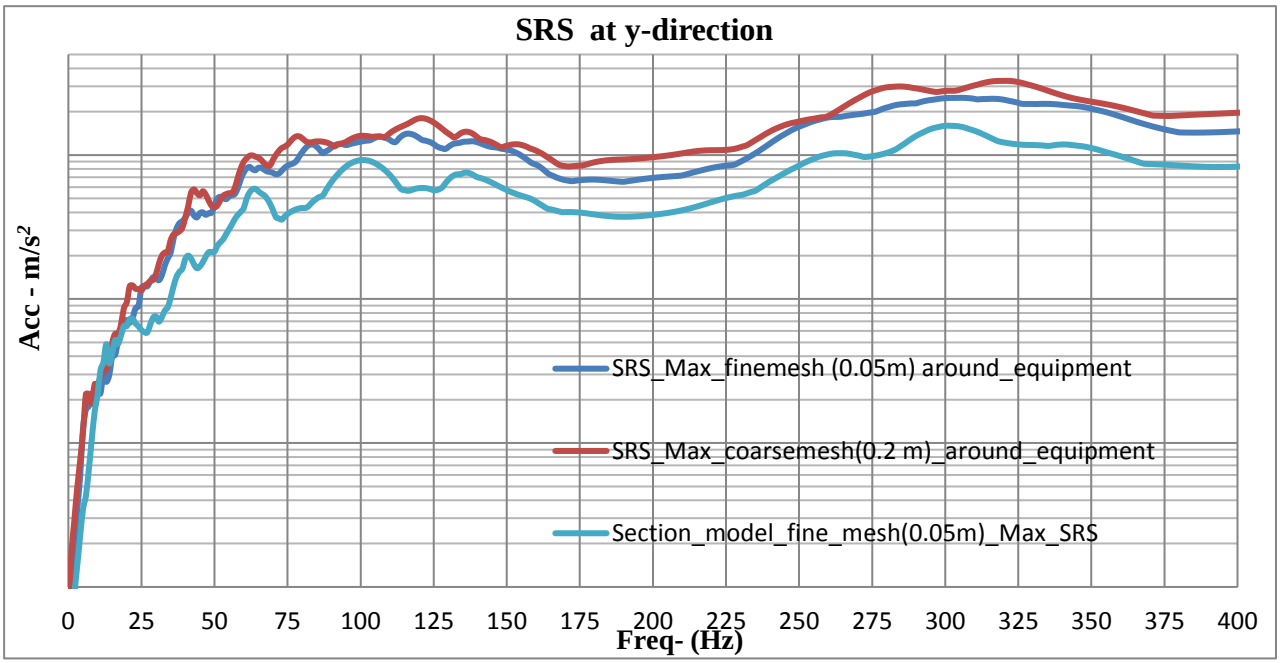

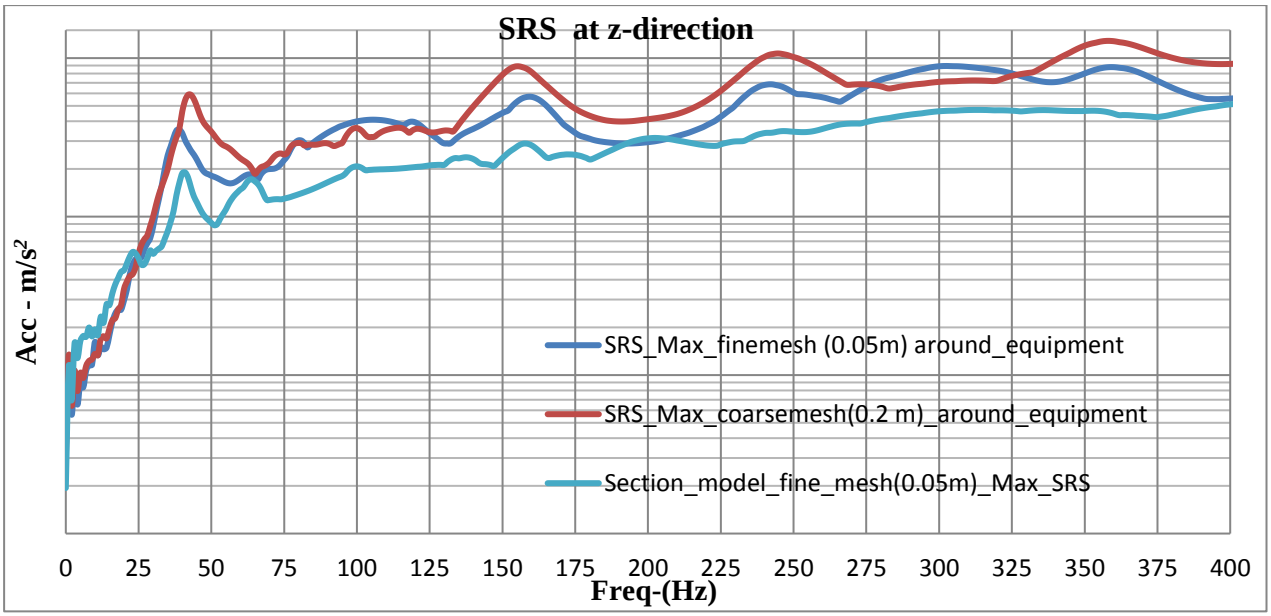

Figure 41 Shock response spectrum values at each directed shock from three different transient analyses

In the graphs above, it can be noticed that using a finer mesh for modelling both the ship section and the deck supporting, the antenna leads to a significant decrease of antenna feet accelerations, around 80% along x-direction and 50% along y- and z- directions.

Then, the SRSs obtained are used to calculate the mode participation factor and the input acceleration for the modes considered in DDAM analysis, as shown in Table 26.

Table 26 Summary of DDAM Analysis from Time History Input

SET	Freq (Hz)	Effective mass kg	Participation factor	Input acceleration shock value m/s^2 (Global model coarser mesh around equipment)	Input acceleration shock value m/s^2 (Global model finer mesh around equipment)	Input acceleration shock value m/s^2 (Section model fine mesh)	% Modal effective mass for DDAM analysis
X directed shock							
1	110.99	1723.18	41.51	2073.6	1561.6	199.53	95.4
6	189.36	25.377	-5.038	961.76	793.5	176.88	1.42
Total response of the equipment (Max-Displacement) in mm				2.17 Disp-DDAM-section model	1.71 Disp-DDAM-section model	0.21 Disp-DDAM-section model	
Total response of the equipment (Max- Von-Mises stress) in MPa				**3.05 $\sigma_{max\text{-}DDAM\text{-}section\ model}$**	**2.3 $\sigma_{max\text{-}DDAM\text{-}section\ model}$**	0.3 $\sigma_{max\text{-}DDAM\text{-}section\ model}$	
Y directed shock							
2	115.01	1710.05	-41.35	1669.6	1393.2	678.83	94.69
5	180.45	26.6223	5.16	1087.8	714.05	446.18	1.49
Total response of the equipment (Max-Displacement) in mm				1.73 Disp-DDAM-section model	1.5 Disp-DDAM-section model	0.7 Disp-DDAM-section model	
Total response of the equipment (Max- Von-Mises stress) in MPa				**2.25 $\sigma_{max\text{-}DDAM\text{-}section\ model}$**	**1.86 $\sigma_{max\text{-}DDAM\text{-}section\ model}$**	0.91 $\sigma_{max\text{-}DDAM\text{-}section\ model}$	
Z directed shock							
4	175.50	6.18548	2.487	5512.3	3701.5	2447.9	0.36
8	226.20	1622.1	-40.28	7788.7	5121.2	2938.2	89.94
Total response of the equipment (Max-Displacement) in mm				2.7 Disp-DDAM-section model	1.75 Disp-DDAM-section model	Disp-DDAM-section model	
Total response of the equipment (Max- Von-Mises stress) in MPa				**2.7 $\sigma_{max\text{-}DDAM\text{-}section\ model}$**	**1.78 $\sigma_{max\text{-}DDAM\text{-}section\ model}$**	$\sigma_{max\text{-}DDAM\text{-}section\ model}$	

In Table 26, the maximum stress and displacement values in DDAM analysis from time-history input are indicated proportional to the maximum ones in section model with fine mesh (z-directed shock) as highlighted in the table.

This table shows that the maximum stress levels obtained from both global models are unrealistically high, whatever is the fineness of the deck mesh near the antenna. In the same conditions, the use of NRL coefficients to build the SRS and run a DDAM analysis leads to stress levels which are around 4 times less than the ones obtained here.

When the ship structures (hull, bulkheads and decks) are models using a coarse mesh, their flexibility in high frequency range is not correctly modelled. In other words, these structures

are too rigid. As a consequence, almost the entire shock wave is transmitted from the ship bottom to the antenna feet, without being filtered by the hull/bulkheads/deck deformation. Resulting accelerations post-processed at the base of the antenna are then unrealistically too high. For this reason, global models will not be considered anymore in the following sections.

8.4. Comparison between the Transient Analysis and DDAM Analysis from Time History Input

The DDAM Analysis from time history input can be used as an alternative method of the transient analysis. It is a method based on the SRS (shock response spectrum) theory. In industry, this method is user-friendly, easy to apply and much faster (around 40 times) than a transient analysis.

According to studies by (Ding, 2011) and (Morgan, 2015), the DDAM Analysis from Time History Input gives generally 10-15 % more conservative results than the transient analysis. Thus, both analyses are expected to have similar results.

As shown in previous section, the results seem reliable and realistic using the section model fine mesh.

However, the transient analysis gives the results dependent on time, the maximum and most critical cases are obtained by the DDAM analysis since the shock response spectrum theory stands on the maximum response of the single degree freedom system. Therefore, the stress response of the antenna for three different models is compared in a single graph as shown in Figure 42.

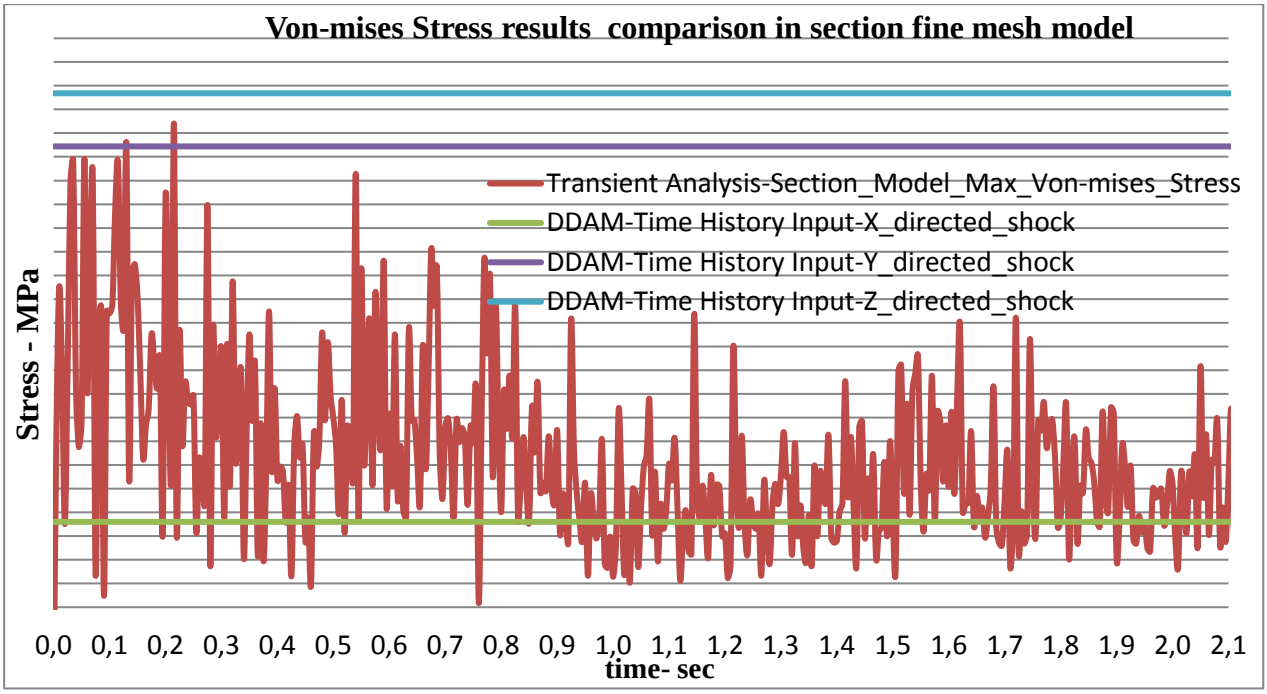

Figure 42 Stress result comparisons in section fine mesh model

Here, obtained Von-Misses stress levels are compared for both analyses. The DDAM analysis gives the most critical cases for each shock direction. On the other hand, a time evolution of Von-Mises stress levels is post-processed from transient analysis. Therefore, the maximum Von-Mises stress results are shown proportional to the maximum stress in the transient analysis in Table 27.

Table 27 Maximum Von-mises stress results for section fine mesh model

Section Model with fine mesh	DDAM Analysis from Time History Input-x directed shock	DDAM Analysis from Time History Input-y directed shock	DDAM Analysis from Time History Input-z directed shock	Transient analysis
Total response of the equipment (Max Von-mises stress) in MPa	0.31 $\sigma_{max\text{-}trans\text{-}section\ model}$	0.96 $\sigma_{max\text{-}trans\text{-}section\ model}$	1.05 $\sigma_{max\text{-}trans\text{-}section\ model}$	$\sigma_{max\text{-}trans\text{-}section\ model}$

The maximum stress in DDAM is obtained as 5% higher than the maximum stress in transient analysis when the structure is submitted to z-direction SRS, corresponding to the highest shock response spectrum level. In the transient analysis, there are many stress values varies depending on time. In order to have an equivalent comparison, the maximum one will be considered since DDAM is used for absolute maximum response of the equipment.

When the maximum stress values are compared, it can be noticed that the DDAM analysis seems to be 5% more conservative than transient analysis.

In addition, the locations of the maximum stress values are examined. In both cases, the maximum stress occurs at the junction element of the base of the structure. This can be seen more precisely in Figure 43.

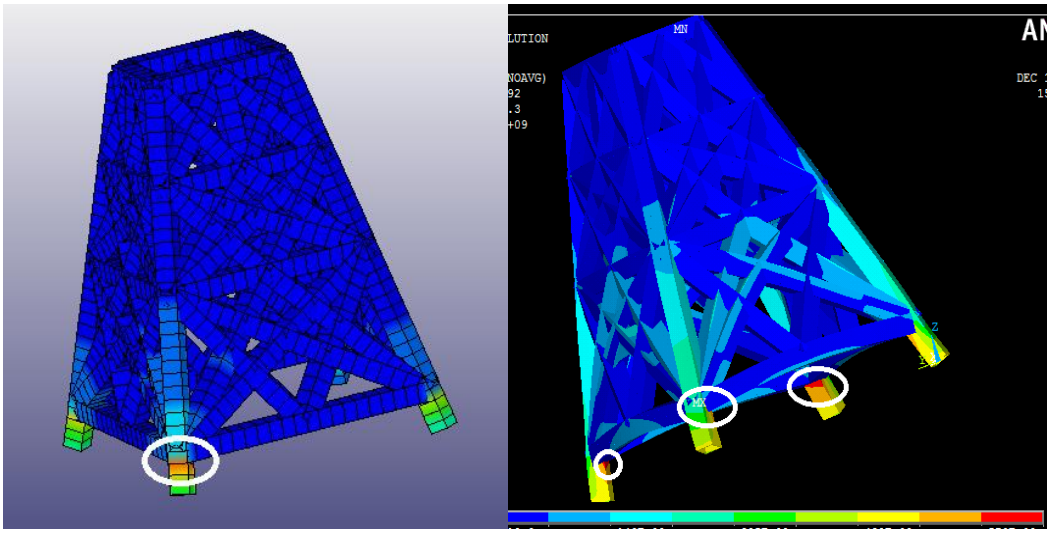

Figure 43 The location of the maximum stresses (Left=transient, right=DDAM)

In the DDAM analysis, the absolute maximum stress is at the junction elements. This is occurred by modal combination method since DDAM considers the most participating mode shapes at z-direction for this case. Then, it combines the responses in these modes to find a final absolute response. Therefore, the location of the maximum stress in the DDAM exactly depends on most participating mode shapes along that direction.

In the transient analysis, the maximum stress value is also observed at the junction element of the base of the structure as shown in the left figure. But the maximum stress values are always changing depending on time. If the transient analysis is post-processed for the full duration of the analysis, it can be seen that the maximum stress values are always seen at the base of the structure in the bottom where it is assembled or in the junction element between base of structure and rest.

Moreover, the DDAM analysis gives the same tendency as the absolute maximum stress values for x and y directed shocks can be seen in Figure 44.

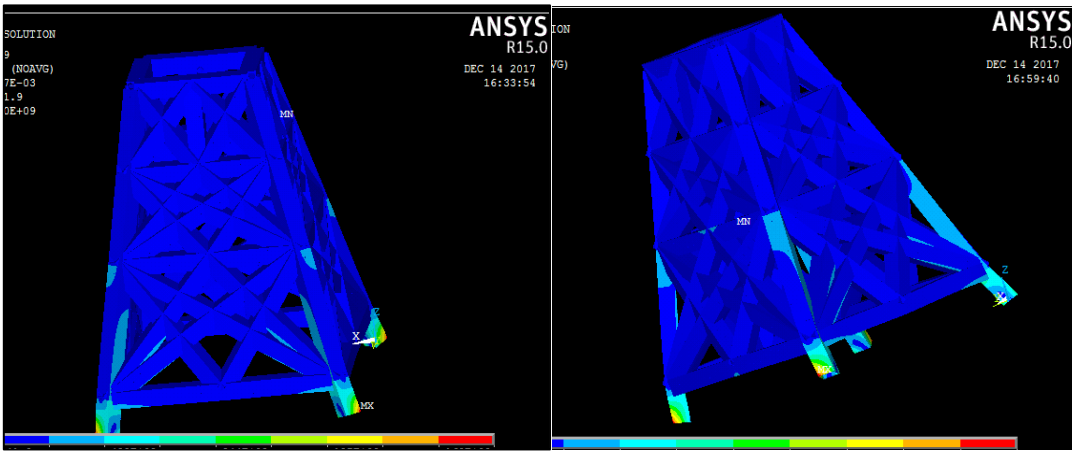

Figure 44 The location of maximum stress values respectively at x and y directed in DDAM analysis

Additionally, some of maximum stress values and their locations in the transient analysis are demonstrated for two different time steps in Figure 45.

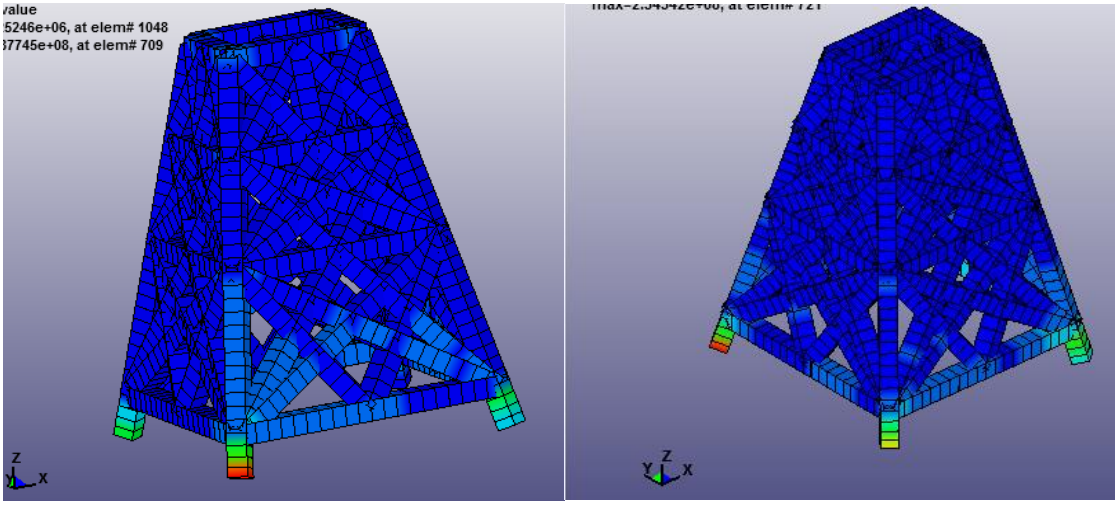

Figure 45 Some samples of maximum stress values in the transient analysis

It can be noticed that DDAM analysis is very powerful to define the location of the maximum stresses. As shown in Figure 45, the maximum stress can also be observed in the base of the antenna structure like in DDAM analysis when the shock is applied along x or y directions.

Finally, the following conclusions can be extracted regarding the two different methods.

- DDAM gives between 5 - 10 % more conservative stress results compare to transient analysis.
- DDAM is a very powerful approach to define the most critical area as of the structure.
- Shock response spectrum is a very powerful tool and easy to implement for shock analysis.
- DDAM is faster than transient analysis.

8.5. Conclusions for the Antenna Structure

Here, the final comparison is carried out by considering the most critical results from the three different main shock analysis methods. The most critical cases are compared in Table 28.

Table 28 Final maximum stress values in three different shock analysis methods

	NRL Coefficient DDAM-Y directed shock Hull mounted	(Section model fine mesh) DDAM Analysis from Time History Input-Z directed shock	(Section model fine mesh) Transient analysis
Total response of the equipment (Max-Von-mises stress) in MPa	0.77 $\sigma_{\text{max-trans-section model}}$	1.05 $\sigma_{\text{max-trans-section model}}$	$\sigma_{\text{max-trans-section model}}$

In fact, there are two different main results, the first one is obtained by DDAM analysis using coefficients of NRL report 1396 and the other one is obtained from section fine mesh model of the simplified ship model by applying pressure field.

DDAM from time history input and transient analyses lead to very close results.

As explained, NRL coefficients are obtained from particular acceleration shock spectrum which is obtained from experimental tests and operational data records. They are related to some pattern vessels and depend on the location of the equipment subjected to underwater explosion. In addition, they include some safety factor. Therefore, the results related to NRL coefficient DDAM analysis are expected to have more conservative than the results obtained from the section model fine mesh.

Yet, in the antenna study, the results based on NRL coefficient DDAM analysis are not conservative. This can be justified by the limitations of NRL coefficients and the way of performing the transient analysis.

On one hand, the main limitations of DDAM-NRL coefficients can be seen below;

- DDAM-NRL coefficients are obtained from formulations which are based on experimental results.
- The specified shock design spectrum is derived from real scale model experiences by recording the data during the experiments. The lack of NRL coefficients is that there isn't any distinction between the type and size of ships such as frigate, patrol vessel etc.

- DDAM-NRL presumes that the shock input value is same at any mounting system. For instance, a deck mounting system has same shock design spectrum whatever is the location of considered deck.
- As these distinctions are very critical for the analysis, the alternative methods would be applied to proper results (such as a transient analysis).

On the second hand, the way of performing the transient analysis and DDAM analysis from time history input are listed below;

- In the analysis of the antenna, the shock input signal (acceleration at the base of the antenna) is assessed from a simplified ship structure model (ship's hull is modeled as a half-cylinder)
- The signal is obtained from a "dry" model, where water inertia effects are modelled by using lumped masses determined from Lewis coefficients. This leads to very conservative results as the fluid structure interaction should also include radiating damping and cavitation effects, which tend to restrain the acceleration of the hull structure.
- The analysis is applied only on a local section model. Therefore, the propagation of the shock wave would not be same as in the global model of the ship.
- No damping is considered when performing the transient analysis. In reality, some energy is dissipated by damping during the propagation of the shock wave between the ship bottom and the deck supporting the antenna.

9. SHOCK LEVELS IN DIFFERENT MOUNTING LOCATIONS

In order to get the severe level of the locations in the simplified ship structure, shock response spectrums are studied in different locations to obtain the influence of the different deck levels and main mounting systems such as shell mounting, hull mounting, and deck mounting systems. The section fine mesh model was taken into account for this study.

In reality, the equipment is assembled on the structural support elements such as longitudinal stiffeners, girders, etc. in a ship. As explained before, the structure of the ship is simplified. That's why there are not any longitudinal stiffeners and other supports. Therefore, the deck mounting system is considered on the girders instead on the stiffeners, moreover, the hull mounting system is taken into consideration on junction point between a bulkhead and a girder and junction point between a girder and a pillar. On the other hand, the shell plating system is considered exactly on the shell plate below the waterline. Fifteen different points are considered for this study as shown in Figure 46.

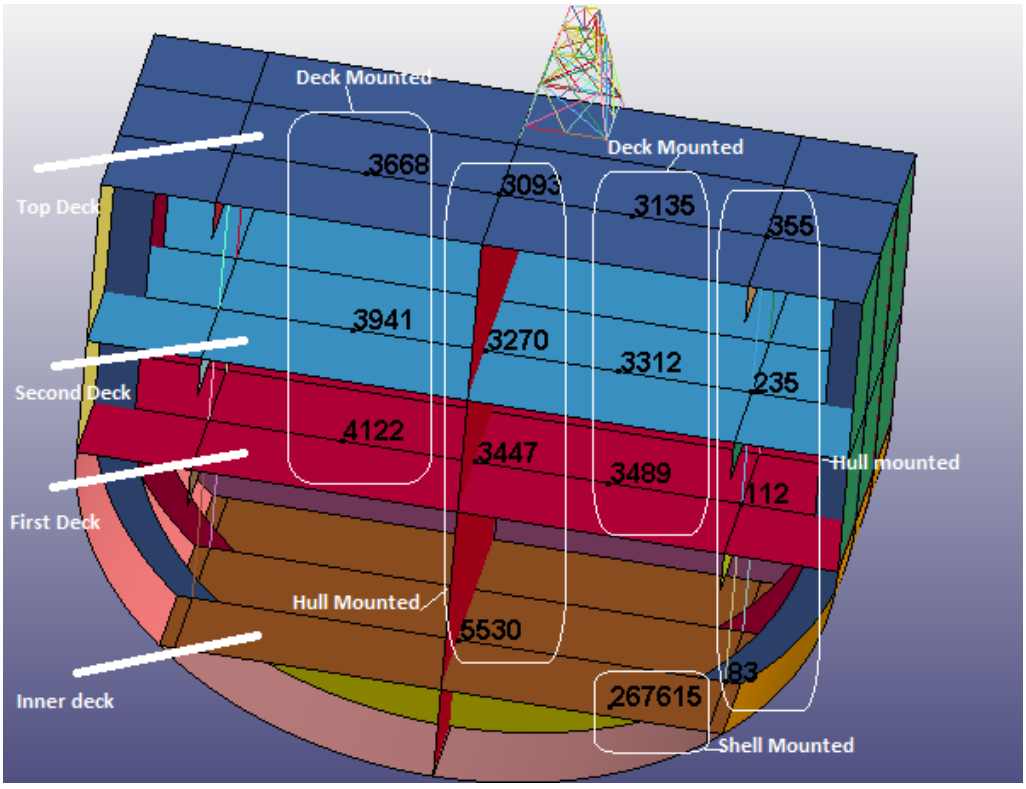

Figure 46 Consideration of the mounting location

Moreover, NRL coefficients also give the relation between shock load, mounting system, and the direction of the shock. As the ship is modelled as a simplified structure, the mounting systems in the simplified ship model do not match with the ones in NRL specifications.

Therefore, NRL-DDAM coefficients will not be comparable in this case. The main purpose of this study is to give an idea about shock severity in different locations and directions.

First of all, the shock response spectrums are plotted at each directed shock for each mounting system and level of deck. The shock response spectrums can be seen respectively at x, y, and z directed shock in Figure 47.

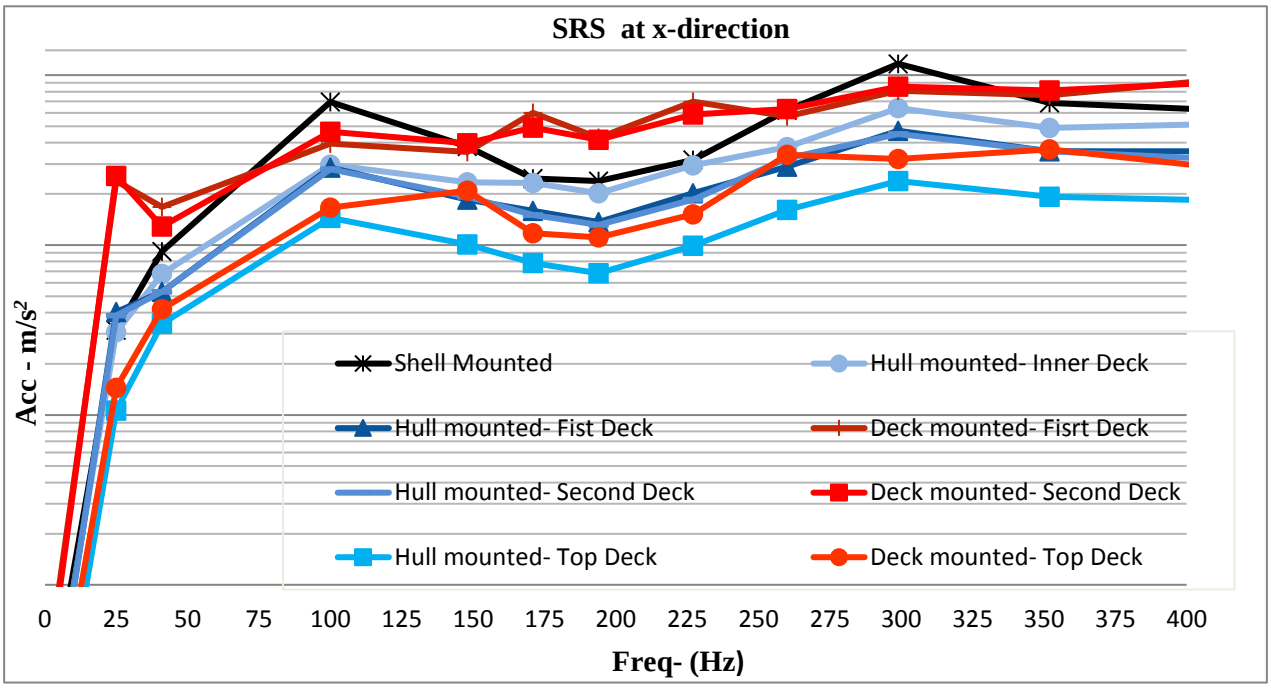

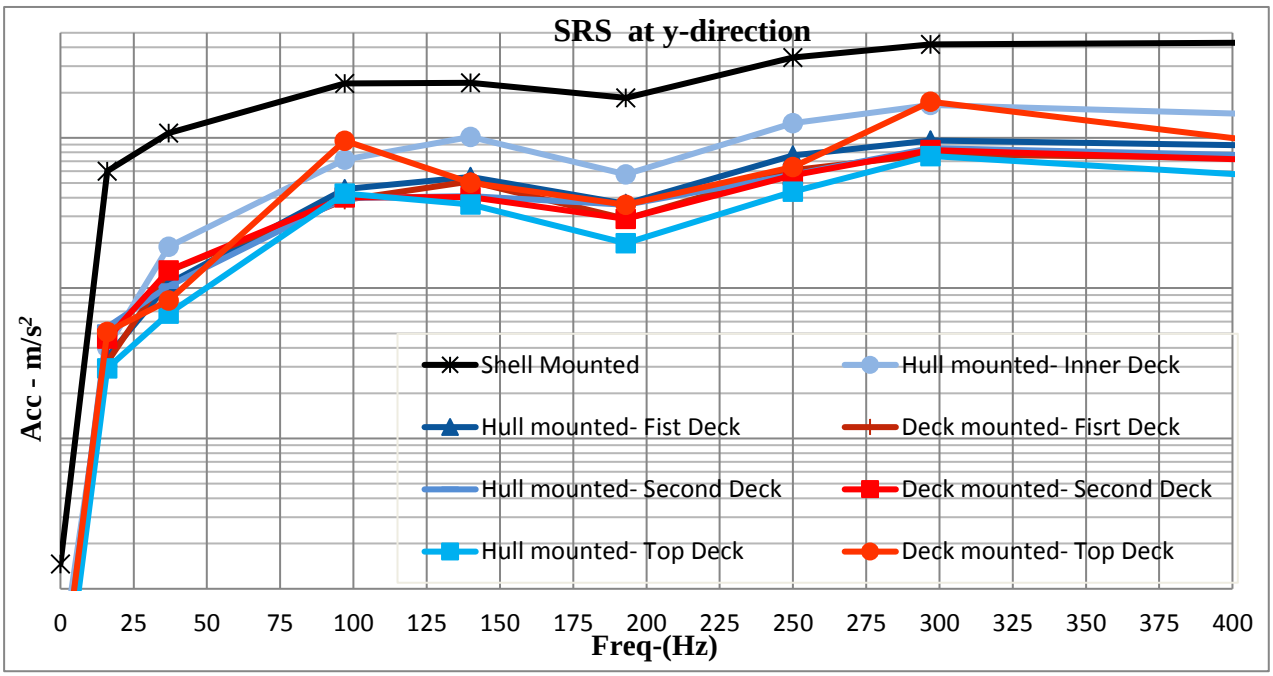

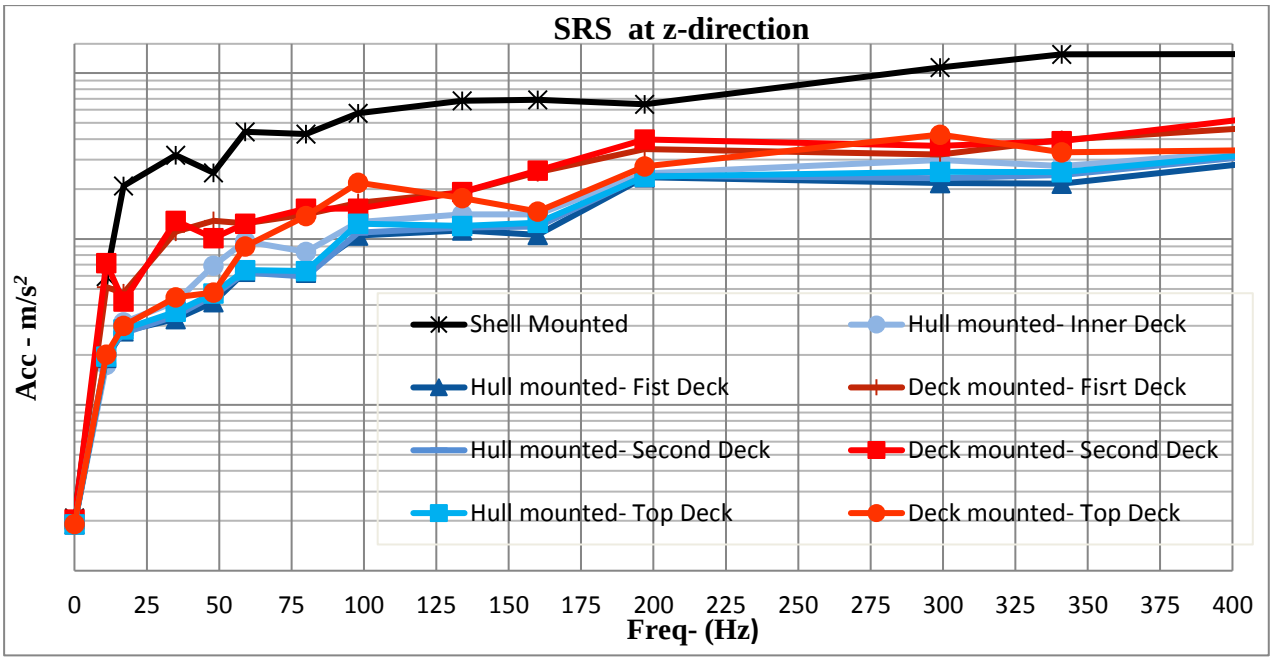

Figure 47 Shock response spectrums at each mounting locations on different deck levels

Here, it can be noticed that the shell mounting system has the highest response particularly at y and z directed shock load. Only at x directed shock response, the shell mounting system does not have the highest response at all frequencies.

Generally, the deck mounting system has higher response as compared to the hull mounting system. This is due to the fact that, the hull mounting is located in more stiff structures and the deck mounting system is located above the main frames, which are less stiff structures.

The other case is that the response level of the mounting locations varies with the level of the deck. At x and y directed shock, the level of the shock severity is generally decreasing from inner deck to top deck as shown in the graphs. As z directed shock is considered, it can be seen that the deck mounting system has a higher response than the hull mounting system.

Secondly, the average shock responses of the mounting systems are studied to compare the shock levels. This case is dedicated to define shock levels in the mounting systems, not the level of the deck. The average shock response spectrums at x directed shock are plotted as shown in Figure 48.

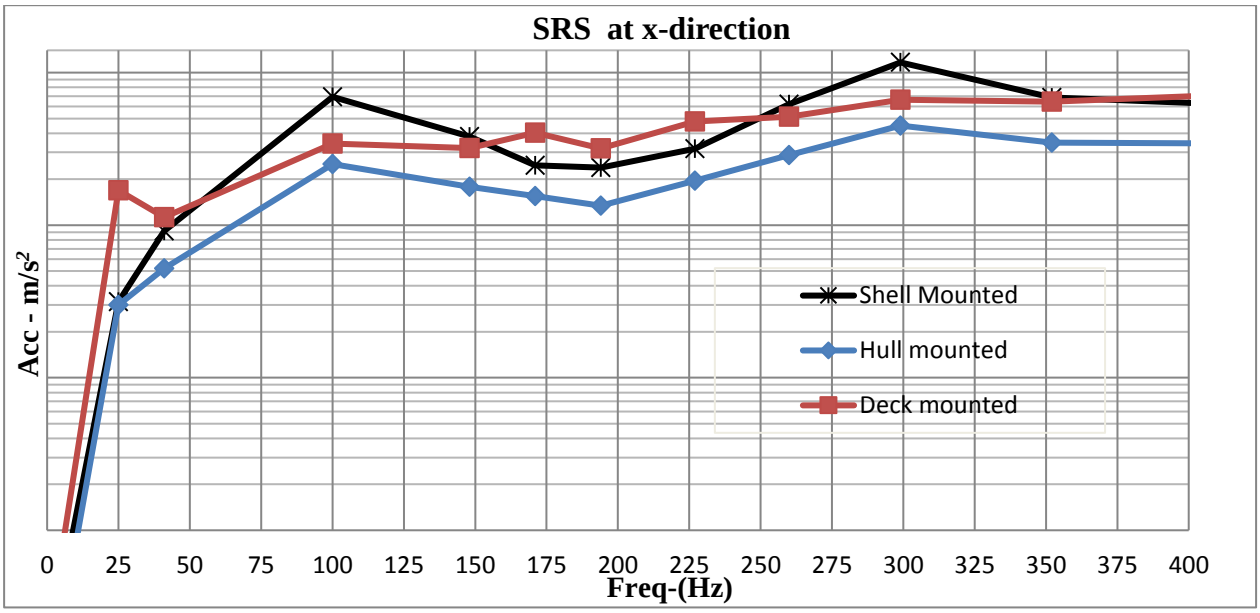

Figure 48 Shock response spectrums at each mounting locations at x directed shock

In figure 48, the hull mounting system has less response as compared to the deck mounting system at all frequency range. However, the shell mounting system doesn't give the highest response at all frequencies. The highest response in hull mounting system can be seen between 50 - 150 Hz and 250 - 350 Hz at x directed shock. Also, the shell mounting system gives two times more response in comparison with the hull mounting system in the graph.

Moreover, the average shock response spectrums at y directed shock are plotted as shown in Figure 49.

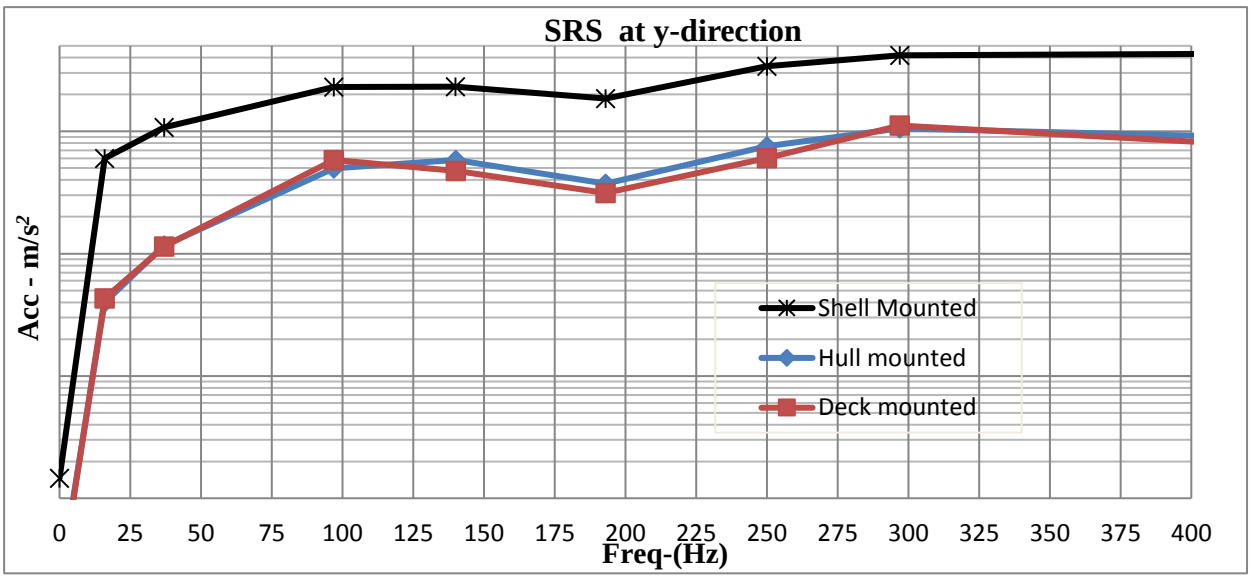

Figure 49 Shock response spectrum at each mounting locations at y directed shock

The interesting point is that the hull and the deck mounting systems have an almost same response at y directed shock load because the stiffness of the points is almost same in the hull and the deck mounting systems at y-direction.

Moreover, the highest response is seen in the shell mounting system. Also, the response in the shell mounting system is about five times higher than the hull and the deck mounting systems at y-directed shock.

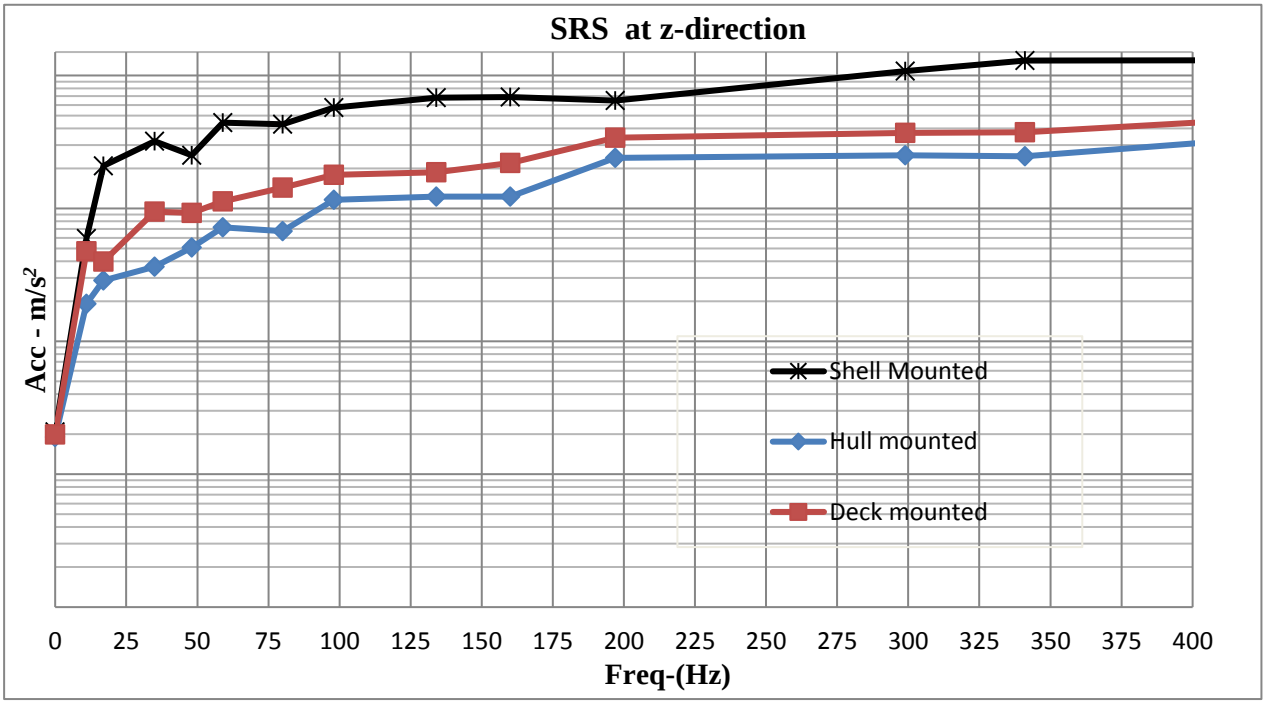

Figure 50 Shock response spectrums at each mounting locations at z directed shock

Figure 50 presents the average shock response spectrums at z directed shock for three different mounting systems. The severity level of the shock can be seen respectively in shell, deck and hull mounting systems. The shell mounting system gives 3.5 times higher response than the deck mounting system. Also, the deck mounting system gives 1.5 times higher response than the hull mounting system.

Apart from x-directed shock, the shell mounting system has the highest response with a huge difference at y and z directed shock.

In third part, the directional comparison is carried out. Thus, the shock response spectrums at each direction are compared in a single mounting system. The directional response is compared for the shell mounting system in Figure 51.

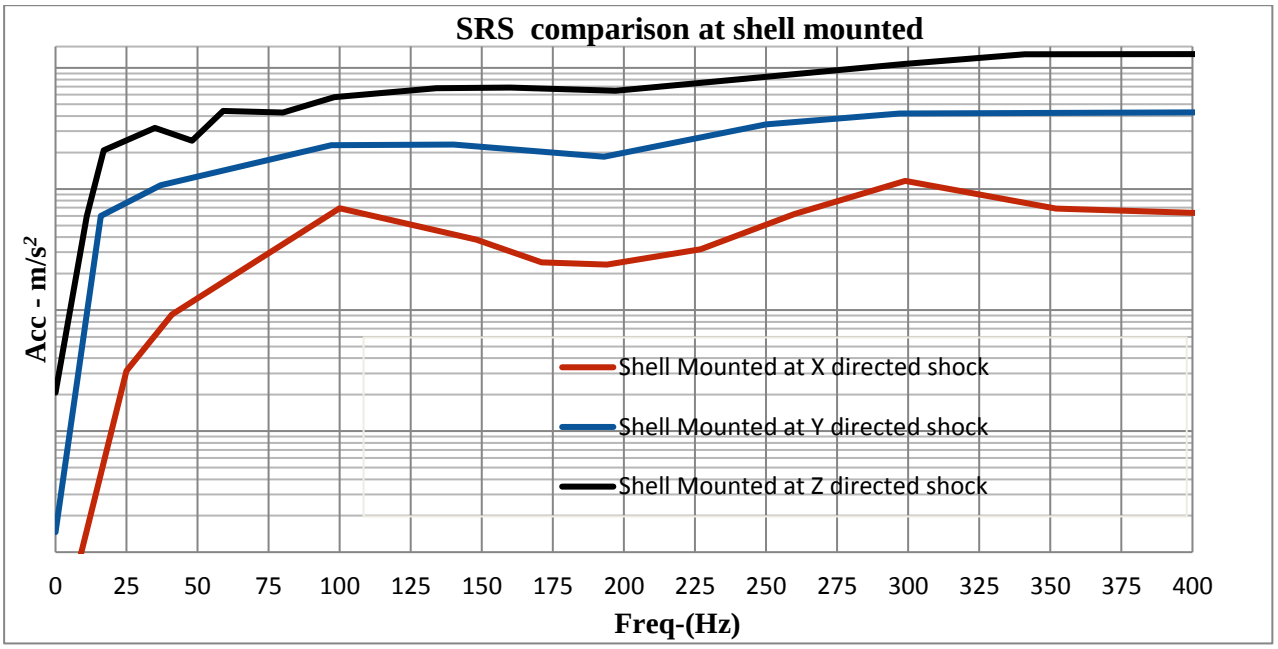

Figure 51 Directional shock response spectrums at shell mounting system

The highest response is obtained at z directed shock as expected. Also, the shock response is decreasing respectively from z directed shock to x directed shock. Approximately, z directed shock is 2.5 times higher than y directed shock. Also, y directed shock is 6 times higher than x directed shock.

The directional response spectrums are shown for the hull mounting system in Figure 52.

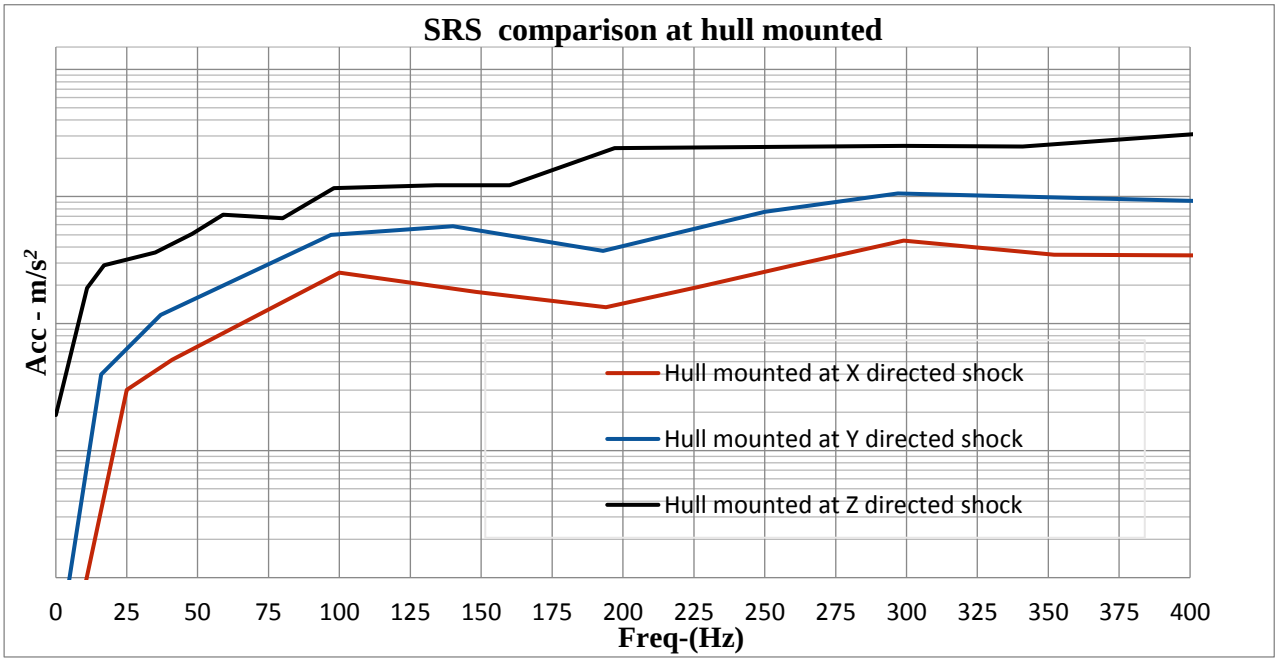

Figure 52 Directional shock response spectrums at hull mounting system

The directional shock ratio at the hull mounting system is similar to shell mounting system. However, the spectrum value at the shell mounting system is around 2.5 times higher than

hull mounting system. Here, the maximum response is also at z directed shock. Furthermore, the relation between directions in the hull mounting system is that z directed shock is 2.5 times higher than y directed shock and y directed shock is 5.5 times higher than x directed shock.

As another case, the directional response spectrums in the deck mounting system are demonstrated in Figure 53.

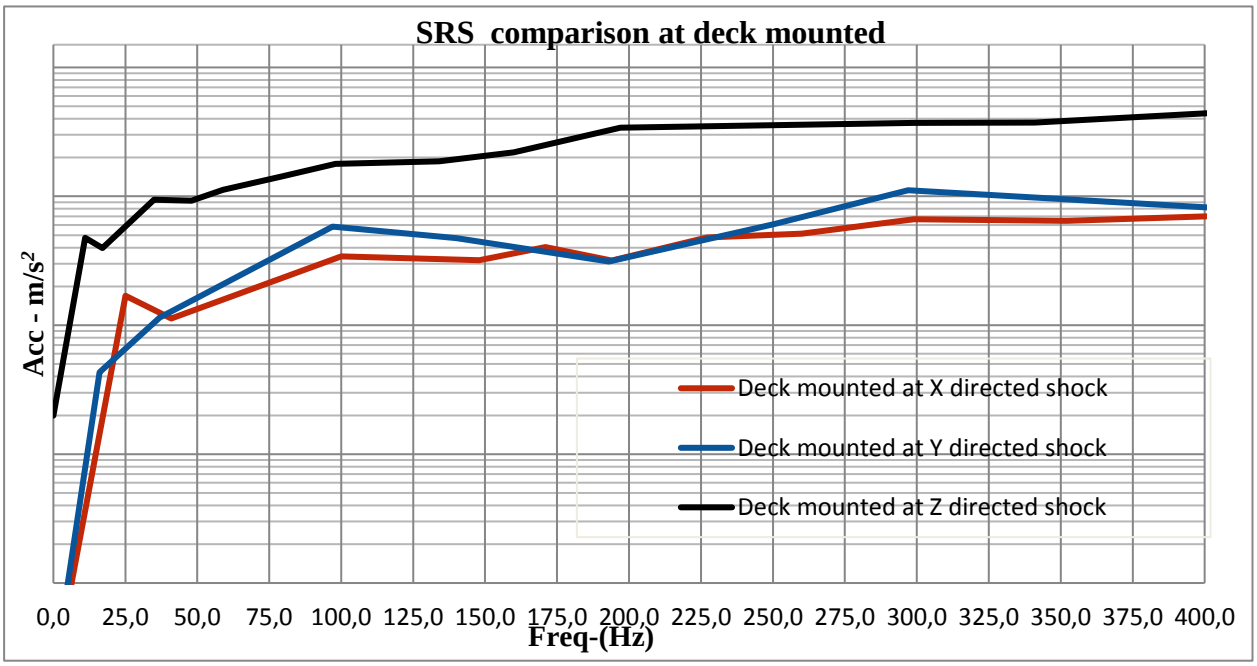

Figure 53 Directional shock response spectrums at deck mounting system

Apart from the hull and the shell mounting systems, the directional shock response spectrums behave differently at the deck mounting system since the response spectrums are almost similar at x and y directed shocks in the deck mounting system. Again, z directed shock load has the highest response and it gives almost 6 times higher responses compare to x and y directed shock loads.

As a conclusion in this study, these two parameters (the level of the deck and mounting system) are very important to define the level of the shock, for instance, the shock severity is decreasing from the bottom to the top of the ship structure. Despite the fact that, DDAM coefficients give only single shock response spectrums for each direction and the mounting location.

Furthermore, the structure of the ship is important for shock response spectrums. As obtained in the results, the stiffness of the structure influences the response of the structure. The high response occurs in less stiff structures in the same deck level.

10. CONCLUSION

After analysing the main methods for estimating the response of the equipment, DDAM analysis from time history input has been found as most convenient and fastest method. Although the transient analysis is very reliable, it takes too much computational time. Therefore, DDAM analysis from time history input can applied for equipment analysis since it is very fast and gives convenient results as well. In case of detail analysis or DDAM cannot handle with a problem, applying a transient analysis would be necessary for some analysis.

This thesis can be concluded as follows.

- The available DDAM-NRL coefficients are achieved by experimental tests in 1963. They are very old and it is not very convenient for new type of the ships.
- The transient analysis should be applied to fine enough meshed model, which is able to catch correctly the modal behavior of the equipment.
- DDAM analysis would be applied for any kind of equipment and any location by using the shock response spectrum which are be calculated from time-history data post-processed from transient analysis.
- For the antenna studied in this thesis, DDAM analysis from time history input and the transient analysis lead to roughly similar results.
- DDAM analysis can be used as an alternative solution of a transient analysis.
- In the last part, the different shock spectrums are studied and comparisons of shock severities are demonstrated.

This thesis is only dedicated in the antenna structure and the beam structure, however, the same methods can be applied any type of equipment on any part of the ship.

11. ACKNOWLEDGEMENT

Firstly, I would like to express my sincere gratitude to all the people who contributed for the development of this thesis, notably to my supervisor Prof. Hervé Le Sourne, who followed my duties with patient and attention during the 3th semester of EMSHIP program in ICAM. Also, his supports helped me a lot for writing of this thesis and researches.

In addition, I would like to express my thanks to the department of Acoustic and Vibration in STX France, where I had a chance to perform my internship, especially to Engineer Mr. Simon Paroissien, who motivated me and collaborated on my thesis a lot. Also, to the head of the department Mr. Sylvain Branchereau and Engineer Mr. Clement Lucas, all of them contributed to my thesis without hesitation.

Finally, I would like to thank to my family, who always supported me in all of my education.

This thesis was developed in the frame of the European Master Course in "Integrated Advanced Ship Design" named "EMSHIP" for "European Education in Advanced Ship Design", Ref.:159652-1-2009-1-BE-ERA MUNDUS-EMMC.

This page is intentionally left blank.

12. REFERENCE

Abbey, T. (n.d.). *Dynamic Design Analysis Method DDAM and Modal Effective Mass.* SAVIAC DDAM analysis.

Abbot, H. L. (1881). *Report Upon Experiments and Investigations to Develop a System of Submarine Mines for Defending the Harbors of the United States.* USA: US Government Printing Office.

Alexander, J. E. (2009). Shock Response Spectrum. *A Primer. Sound and Vibration Magazine, 6-14.*

ANSYS, I. 2. (2009). *ANSYS LS-DYNA User's Guide.* Récupéré sur ANSYS, Inc.: http://orange.engr.ucdavis.edu/Documentation12.1/121/ans_lsd.pdf

Barras, G. (2012). Numerical simulation of underwater explosions using an ALE method. The pulsating bubble phenomena. *Ocean Engineering, Volume 41,* pp. 56-66. France.

Belsheim&O'Hara. (1963). *Interim Design Values for Shock Design of Shipboard Equipment.*

Cho-Chung-Liang&Min-Fang-Yang&Yuh-Shiou-Tai. (2001). *Prediction of shock response for a quadrupod-mast using response spectrum analysis method.* Taiwan.

Cole. (1948). *Underwater Explosions.* Princeton University Press, Princeton.

Costanzo, F. A. (2010). *Underwater Explosion Phenomena and Shock Physics.* Florida USA, Naval Surface Warfare Center Carderock Division, UERD: Naval Surface Warfare Center Carderock Division, UERD: Proceedings of the IMAC-XXVIII.

Demir, E. (2015). *Shock analysis of an antenna structure subjected to underwater explosion.* Ankara: Middle East Technical University, Turkey.

Ding, M. Y. (2011). *Shock Analysis.* ANSYS Inc.

Hollyer, R. S. (1959). *Direct Shock-Wave Damage to Merchant Ships From Non Contact Underwater Explosions.* Norfolk Naval Shipyard.

Hurwitz, M. M. (1981). *The Dynamic Design Analysis Method (DDAM).* David Taylor Naval Ship Research and Development Center.

Irvine, T. (2002). *AN INTRODUCTION TO THE SHOCK RESPONSE SPECTRUM.*

Irvine, T. (2012). SRS ALGORITHM LIMITATIONS FOR A RECTANGULAR BASE INPUT-Revision D.

ISSC. (2006). 16th INTERNATIONAL SHIP AND OFFSHORE STRUCTURES CONGRESS., (pp. 1, pp. 35-38.). Southhampton, UK.

Jiang Tao, Y. W.-l.-y.-l. (2009). *Simulation of resistant shock capability of missile launcher based on DDAM.* Qingdao – China.

Keil, A. (1961). *The response of ships to underwater explosions.* DTIC Document. New York: Armed Services Technical information Agency, United States Of America.

Kim&Koo, W. K.-D. (2015). *Simplified formulas of heave added mass coefficients.* Incheon, Korea.

Koci, J. T. (2011). *Calculation Of a Shock Response Spectrum.* Czech Republic: VSB – Technical University of Ostrava.

Mark, S. W. (1984). *Numerical Analysis of The Elastic Shock Response of Submarine Installed Equipment.* NTIS Rep. AD-A152-564.

McCarthy, J. R. (1995). *Shock Design Criteria For Surface Ships- NAVSEA.* Ship Survivality and Structural Integrity Group. Direction of commander, Naval Sea Systems Command.

Morgan, K. (2015). *Shock & Vibration using ANSYS Mechanical.* ANSYS lnc.

Nastran, N. (2009). *Dynamic Design Analysis Method (DDAM) Handbook version 9.2.* NEI NASTRAN.

Navarro, M. G. (2015). *Rules and methods for dimensioning embarked materials for surface ships when subjected to UNDEX.* Nantes: Institut Catholique d'Arts et Métiers (ICAM).

O'Hara, B. a. (1963). *Interim Design Values for Shock Design of Shipboard Equipment.*

Plesset&Prosperetti. (1977). Bubble dynamics and cavitation. *Annual Review of Fluid Mechanics, 145-185.*

Rayleig, L. (1917). *On the Pressure developed in a Liquid during the Collapse of a Spherical.* Philosophical Magazine.

Reid, W. D. (1996). *The response of surface ships to underwater explosions.* Melbourne Victoria.: DSTO Aeronautical and Maritime Research Laboratory.

Remmers, G. M., O'Hara, G. J., & Cunniff, P. F. (1996). Dynamic Design Analysis Method DDAM. *Shock and Vibration, 3,* 461-476.

Schaller, A. (2008). *SIMULATION DES CHOCS DANS L'INDUSTRIE NAVALE,(seconde partie- calcul des equipements).* ADDL.

SIEMENS. (2004). *Advanced Dynamic Analysis User's Guide.*

Snay, H. (1956). *Hydrodynamics of underwater explosions.* Washinton D.C.: Symposium on Naval Hydrodynamics.

Tsai, S.-C. (2017). *Numerical simulation of surface ship hull beam whipping response due to submitted to underwater explosion.* Nantes: Institut Catholique d'Arts et Métiers (ICAM).

YAO Xiong-liang, Z. Q.-x.-m.-h. (2008). *Numerical simulation of the anti-shock performance of a gear case,.* Harbin 150001, China: Harbin Engineering University.